ORGANIC ELECTROCHEMICAL TRANSISTORS FOR WEARABLE SENSING

YANG ANNENG

PhD

The Hong Kong Polytechnic University

2020

The Hong Kong Polytechnic University

Department of Applied Physics

Organic Electrochemical Transistors for Wearable Sensing

YANG Anneng

A thesis submitted in partial fulfillment of the requirements for the degree of Doctor of Philosophy

August 2019

CERTIFICATE OF ORIGINALITY

I hereby declare that this thesis is my own work and that, to the best of my knowledge and belief, it reproduces no material previously published or written, nor material that has been accepted for the award of any other degree or diploma, except where due acknowledgement has been made in the text.

_____ (Signed)

YANG Anneng (Name of student)

Abstract

Wearable biosensing technologies could serve as a useful tool for personalized healthcare management and have a massive market in the future. However, conventional electrochemical sensors have rarely been used in wearable applications due to relatively high detection limit and low sensitivity. Organic electrochemical transistors (OECTs) have emerged as a versatile sensing platform for different wearable applications due to its intrinsic amplification function and ion-to-electron transducing ability.

In this thesis, the fabrication of a highly sensitive OECT sensor on a flexible fiber is firstly presented. The fiber-based sensor can provide in situ amplification of detection signal with high sensitivity. It shows very stable performance during bending tests, which is critical to applying this device into wearable electronics. The detection limit of the functionalized sensor to the target analyte can be down to 10 nM. The sensor response to the specific analyte is about two orders magnitude higher than that to other interferences, indicating the device's good selectivity. The fiber-based sensor is then woven together with cotton yarns, resulting in a flexible and stretchable fabric device. The fabric device can be integrated into a diaper and remotely operated by using a mobile device with a custom-made app. The fabric device integrated into a diaper is suitable for wearable biosensing because of its light-weight and compactness. Due to the advantages of wearability and high sensitivity, the fabric sensor can offer a unique platform for convenient wearable healthcare monitoring.

Secondly, a quick response OECT senor is thoroughly investigated. The channel dimension of the OECT is finely tuned to realize quick stabilization of the channel

current. The dual gate design of the sensor can eliminate certain interfering species (such as uric acid, ascorbic acid) in body fluids from detection of target analytes. After gate modification, numerous elements in body fluid can be quickly and selectively detected by the sensor. In order to efficiently perform wearable sweat sensing, a sweat absorption layer is assembled onto the sensor, resulting in a quick sampling of body fluids. The device conformably worn on a fingertip can quickly collect enough sweat in several minutes and perform sweat glucose test. The glucose level in sweat can be wirelessly monitored by a portable meter via a mobile phone, which can provide a non-invasive way for quick detection of various physiological signals of human body.

Lastly, a flexible OECT device is fabricated and used for wearable electrocardiogram (ECG) recording. In order to increase the device response speed, the channel length of the device is decreased to about 2 μm. The response time can be as short as tens of microseconds, which is sufficient for ECG signal recording. The channel and gate of the OECT can be mounted on different parts of human body to record ECG signal. By optimizing the distance between the channel and gate of the device, high-quality recording of ECG signal is achieved. The wearable monitoring of ECG signal is further demonstrated. The proposed ECG recording device can be integrated into the wearable electronic system for monitoring multiple clinical signals.

In summary, fabric OECT sensors have been successfully fabricated and used for sensitive and selective detections of target analytes. Wearable and quick detections can be realized by using a dual gate OECT, and its operation mechanism is comprehensively investigated. The short-channel OECT with fast response speed is fabricated and used for ECG recording. By combing the merits of the above sensing techniques, the wearable OECT sensors could revolutionize the current wearable technologies in diagnostics and physiological monitoring.

List of Publications

(1) **Yang, A.**; Li, Y.; Yang, C.; Fu, Y.; Wang, N.; Li, L.; Yan, F. Fabric Organic Electrochemical Transistors for Biosensors. *Adv. Mater.* **2018**, *30*, 201800051.

(2) **Yang, A.**; Yan, F. Flexible/Stretchable Biosensors or Bio-inspired Sensors. Book chapter submitted to *Flexible Bioelectronics*

(3) **Yang, A.**; Yan, F. *et al* Dual gate organic electrochemical transistors for quick response biosensors. In preparation.

(4) Wang, N.; **Yang, A.**; Fu, Y.; Li, Y.; Yan, F. Functionalized Organic Thin Film Transistors for Biosensing. *Acc. Chem. Res.* **2019**, *52*, 277-287.

(5) Fu, Y.; **Yang, A.**; Yan, F. Chemical Substances. In *Seamless Healthcare Monitoring: Advancements in Wearable, Attachable, and Invisible Devices*; Tamura, T., Chen, W., Eds.; Springer International Publishing: Cham, 2018; 335-365.

(6) Chen, L.; Fu, Y.; Wang, N.; **Yang, A.**; Li, Y.; Wu, J.; Ju, H.; Yan, F. Organic Electrochemical Transistors for the Detection of Cell Surface Glycans. *ACS Appl. Mater. Inter.* **2018**, *10*, 18470-18477.

(7) Fu, Y.; Wang, N.; **Yang, A.**; Law, H. K. w.; Li, L.; Yan, F. Highly Sensitive Detection of Protein Biomarkers with Organic Electrochemical Transistors. *Adv. Mater.* **2017**, *29*, 1703787.

Acknowledgements

I am grateful for all the support and guidance I have received over the last three years and for my unforgettable time at PolyU.

First and foremost, I would like to express my sincere gratitude to my chief supervisor, Prof. Feng YAN, who allowed me to join his active group and to explore the most cutting-edge research area in biosensing. Without his broad knowledge and academic insight, my Ph.D study would not go on smoothly. Without his exceptional patience and valuable guidance to my research, I would not finish my thesis successfully.

I would also like to extend my heartfelt gratitude to the technicians and staff in Department of Applied Physics and UMF: Dr. Vincent CHAN for our department instruments training and management; Dr. Terence WONG and Ms. Joyce LAU for guidance and maintenance of the facilities in cleanroom; Dr. Hardy LAO and Dr. Pai WONG for training and maintenance of the instruments in Materials Research Centre; Mr. Lam Two CHAN and Ms. Henrietta HO for chemical ordering and lab safety management; Mr. Vincent LAM for information technology assistance; Miss Cecilia CHAN, Mr Sammy LO, Miss Tiffany WONG, Miss Meijei WONG, and Miss Yonnie CHEUNG for their kind help in handling all the administrative works. It definitely save me much time to focus on the research.

Many thanks to Dr. Helen LAW from HTI and Dr. Mo YANG from BME for their kind help in cell culture. I would also appreciate the collaboration with Prof. Zijian ZHENG and his student, Mr. Shuaichen WANG, for their advice about inkjet printing and device fabrication. I would also like to give a special thanks to Dr. Naixiang WANG, who teached me how to fabricate organic electrochemical

transistors and perform futher characterizations.

I am also grateful to my colleagues in PolyU: Dr. Ying FU, Dr. Haifeng LING, Mr. Jiajun SONG, Mr. Yuanzhe LI, and Dr. Ji YU, with whom we always actively discuss related research hotspots; Miss Gerile OUDENG, who shares her experiences with me on cell culture and biochemical experiments; Dr. Chenxiao YANG and Mr. Yifei TAO for their kind help on fabric device fabrication; Dr. Peng YOU, Dr. Qidong TAI, Dr. Shenghua LIU, Mr. Guanqi TANG, Mr. Chunhin MAK, Mr. Jiupeng CAO, Miss Tianyue Wang, Miss Lizhen CHEN, Mr. Adam TANG, Mr. Sam LIU, Mr. Hokleung LOI and many other research students and postdoc researchers, with whom I spent a memorable and enjoyable time.

Finally, through all this I have had the unconditional and unwavering support of my parents, my wife, and my brother. Sincere thanks to my wife for her care and continuous encouragement. I dedicate this thesis to my beloved family, and I love you forever.

Table of Contents

List of Figures

Chapter 1 Introduction

1.1 Background

The rise of wearable bioelectronics has attracted much attention from different research disciplines due to its vital role in personalized healthcare management, predictive clinical diagnostics, physiological and chronic disease monitoring, and treatment.[1,2] The analytical instruments, such as 12-lead electrocardiograph machine, Sysmex XE-2100 complete blood count machine, and blood specific protein analyzer are usually bulky and not available for personal use, which will accelerate the medial burden of government. Furthermore, the bulky instruments are maintained at a high cost because of their complex structure. In some cases, the test and analysis of the instruments are time-consuming because of their operation at full load. As shown in **Figure** 1.1 and 1.2, the wearable techniques usually use novel portable sensors to detect various physical signals (skin temperature, electrocardiography, pulse, electrooculography, electromyography, electroencephalography, respiratory rate, etc.) of human body and biochemical signals (sodium ion, potassium ion, pH, glucose, uric acid, ascorbic acid, hemoglobin, lactic acid, etc.) of human body fluids to provide some useful clinical information. For physiological and/or clinical investigations,[3-6] body fluids including interstitial fluid, sweat, tear, saliva, urine, etc. contain many key analytes that can be regarded as indicators of human health state.[7-9]

Due to the progress of silicon-based semiconductor and related micro-fabrication techniques, the physical signals produced by organ/tissue electrical activities have been detected by commercial chips and circuits. Therefore, the wearable sensors are firstly devoted to the monitoring of physical signals, such as temperature, pulses, and

respiration rate, due to good signal stability and sensor reliability. Some wearable products, such as apple watch®, Fitbit watch®, iRhythm Ziopatch®, google glass®, Nike+®, etc., have been internationally popularized and successfully used for different physical signal recordings.[10]

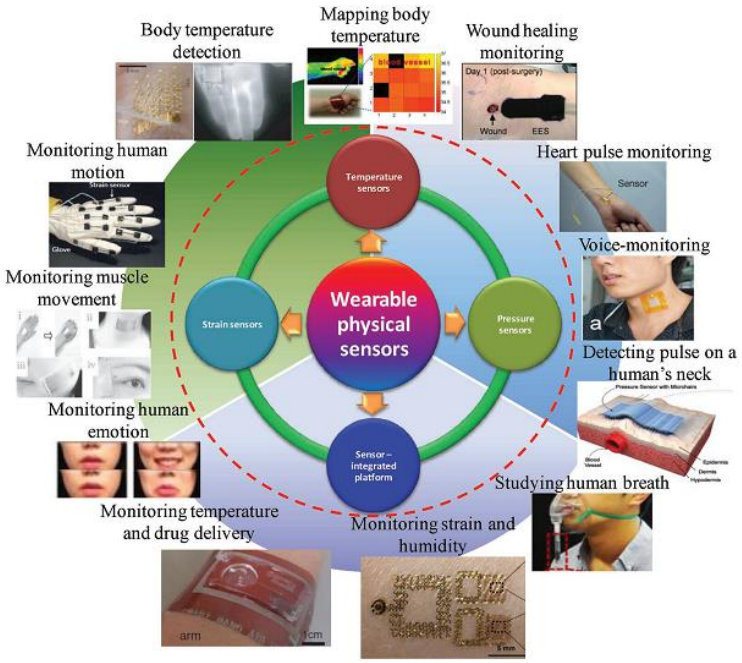

Figure 1.1. The illustration of wearable sensors used for the detection of various human physical signals.

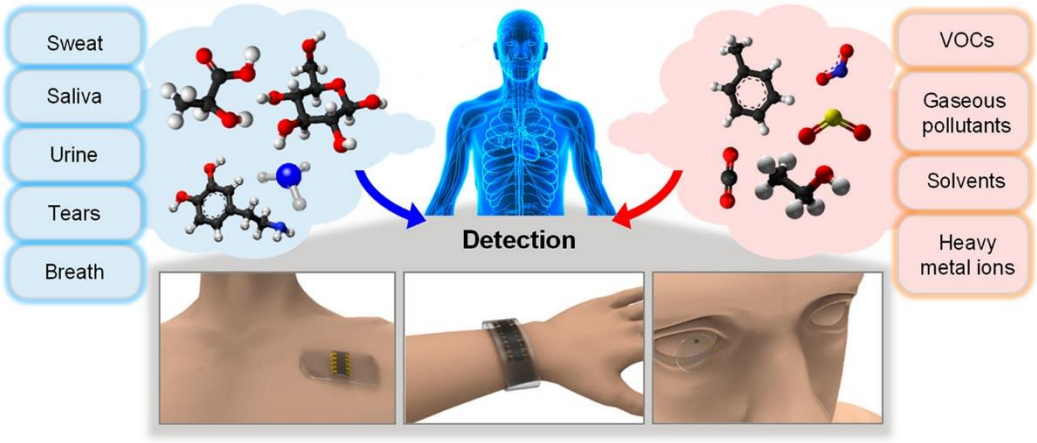

Figure 1.2. The illustration of wearable sensors used for biochemical signal detections of human body fluids.

The conventional electrochemical techniques have been used for wearable biosensing for several decades, in which amperometry and potentiometry are two standard techniques to determine the levels of target analytes in body fluids (Upper parts of **Figure** 1.3). Some biochemical molecules, such as Na^+, K^+, glucose, uric acid, are detected by wearable biosensors, which are mainly based on the above two electrochemical transducing mechanisms.[11,12] Some advances have been achieved recently to boost the development of wearable biosensors and further investigation of various body fluids.[13] The significant efforts have been made to improve the sensitivity and selectivity of wearable sensors. The surface functionalization of the sensor is one of the main directions.[14] The wearability of the sensor has also been improved by optimizing substrate flexibility and integration of wireless detection system.[15,16] The detection limit of amperometric and potentiometric sensors can be down to micromole level during wearable applications.[12] Besides, optical methods are also commonly used in wearable electronics, such as colorimetry and fluorometry (Lower part of **Figure** 1.3).[17,18] With the advancement of fabrication and integration technology, the advanced wearable device tends to be an integrated system of various types of sensors and modules, such as ECG sensor, temperature sensor, pH sensor, glucose sensor, and uric acid sensor together with readout module, wireless transmission module, and visualization module, to realize precise, wireless, and real-time physiological state monitoring of human body.

The portable glucose meter is a classic and vital representative of wearable biosensors, by which glucose level in blood can be invasively detected by puncturing a fingertip and dropping blood to the sensing area.[19,20] However, the trace element in body fluids cannot be well discriminated by the conventional electrochemical sensors and optical sensors. At the same time, the wearable sensors can still find more room to improve their wearability and conformability during wearable

applications without sacrificing their sensitivity and selectivity. Moreover, noninvasive detections of the target analytes in body fluids is also a prevailing trend in wearable technique development because of its painless operation.[12,21,22]

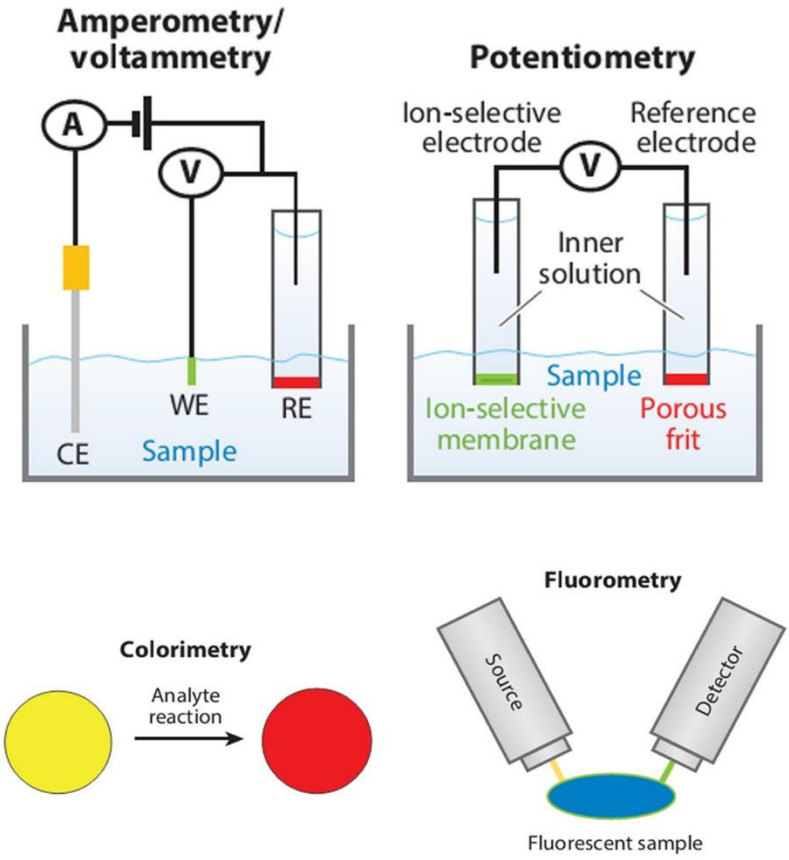

Figure 1.3. Conventional electrochemical techniques used for wearable detections: amperometry/voltammetry, potentiometry, as well as optical methods: colorimetry, and fluorometry.

Recently, organic electrochemical transistor (OECT), one kind of organic thin-film transistors, has been used for different biosensing applications due to its high sensitivity and excellent biocompatibility.[2,23] Since it was discovered by Wrighton *et al* in 1984, OECT is quickly exploited as an outstanding candidate of sensors. As shown in **Figure** 1.4, a typical OECT consists of a gate, a channel (organic semiconductor), and electrolyte which connects the gate and channel and acts as a dielectric layer during OECT operation. The ions in the electrolyte can be expelled

into/out the channel after applying a gate voltage and to dope/de-dope the channel, thus changing the channel conductance and corresponding current that flows through the channel. A subtle change of effective gate voltage can cause a cascade channel current change which can be easily captured by a source meter.

Based on the working mechanism of the as-mentioned OECT, it shows below advantages in sensing: i) *In situ* amplification capability. The OECT can be used for noninvasive detection of trace elements in the electrolyte that cannot be discriminated by conventional detection techniques. ii) Ion-to-electron interface. The interface between the OECT and detected target in the electrolyte makes it an ideal candidate of the biology interfaces for different physiological activity monitoring. iii) Low operation voltage. The device operating under 1 V has no harm to human body, which is useful for *in situ* detections during wearable applications.[24] The wearable techniques integrated with OECT are still rare and will be the focus of this thesis.

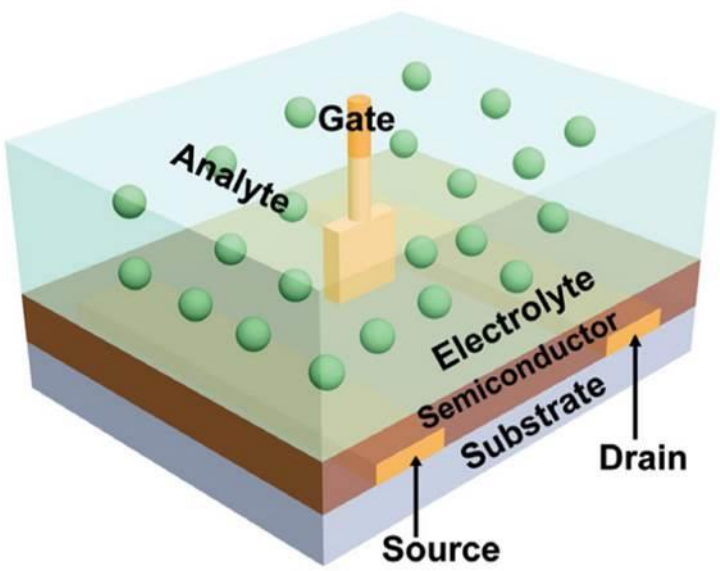

Figure 1.4. Schematic of a typical OECT-based biosensor.

1.2 Objectives of research

The wearable electronics is a multi-disciplinary research project which requires a combination of materials science & engineering, biology, chemistry, and electrical engineering. Since the invention of the first wearable device (eyeglass) in the 13th century, it undergoes substantial progress in its wearability, comfortability, accuracy, sensitivity, efficacy, and multifunctionality. The current techniques enable wearable devices to simultaneously monitor major physical signals, such as skin temperature, pulses, blood oxygenation, as well as some analytes with a high concentration in body fluids, such as glucose in blood, lactic acid, Na^+, and K^+ in sweat. However, a highly sensitive and efficient device used for noninvasive and trace element detections in body fluids is still urgently needed in wearable applications.

The first objective of the thesis is to develop a highly sensitive fiber-based OECT device for wearable biosensing applications. The fiber-based device can be readily integrated into textiles and conforms to different body posture to perform reliable and efficient wearable sensing. The investigation of gate modification strategies paves a better route for highly sensitive sensor design. The second objective of the thesis is to develop a quick response OECT biosensor to obviate the existed issues of long waiting time and slow response speed of OECT sensing. Through the analysis between response time and channel dimension, the study would provide a better understanding during device design and wearable sensing. Furthermore, the dual gate design is utilized in the device fabrication so that the interference effect of different kinds of analytes in body fluids can be substantially decreased during wearable sensing, thus increasing sensor detection selectivity. The last objective of the thesis is to develop a wearable electrocardiograph (ECG) sensor, in which OECT device is regarded as a high gain amplifier to record high-quality ECG signals.

1.3 Outline of thesis

The organization of the thesis is as follows:

Chapter 1: Introduction. The background and evolution of wearable electronics are briefly introduced. Then the OECT-based sensor and its potential in wearable applications are addressed. The objectives and outline of the thesis are further presented.

Chapter 2: Literature review. The techniques used in wearable biosensing are introduced. The three primary wearable sensing techniques are detailed as follows. The conventional electrochemical techniques are firstly detailed. Then optical techniques are briefly addressed. The transistor-based techniques for wearable applications are finally reviewed.

Chapter 3: Fabric OECT for biosensors. Fiber-based OECTs are fabricated, in which multi-layer structure is introduced to improve their bending stability during the fabrication of fiber-based devices. Then they are used for sensitive and selective metabolite detections. By using its conformability and flexibility, the fiber-based device is woven into textiles and integrated into a diaper for wireless and wearable glucose detection in artificial urine.

Chapter 4: Dual gate OECT for quick wearable biosensing. The flexible dual gate OECT sensor is fabricated through photolithographic techniques. In order to realize quick stabilization and response as well as efficient wearable functionalities, the channel dimension, gate modification strategy, sweat collection layer design, mobile meter, and corresponding visualization design are thoroughly investigated. Finally, the wearable detection of sweat glucose levels is demonstrated.

Chapter 5: OECT for highly sensitive ECG recording. The short channel (2 μm) OECT sensor is fabricated and its transient response time can be down to several tens of microseconds which guarantees precise recording of ECG signal. The home-made circuit and the sensor recording site for high-quality ECG monitoring is further investigated

Chapter 6: Conclusions and Perspectives. The summary of the work in the thesis is presented, and further challenges and opportunities are proposed.

Chapter 2 Literature review

2.1 Introduction

The sensor is a kind of analytical device which can be used for sensing one particular physiological parameter. Considering the excellent mechanical properties, flexible sensors are emerging for wearable and conformable applications. Because of their high sensitivity and specificity, electrochemical biosensors have been fully developed for several decades since the first concept of biosensor proposed by Leyland C. Clark in 1962.[25] There are large amounts of electrochemical biosensors for different healthcare applications nowadays, such as glucose sensor, lactate sensor, catecholamines sensor, and uric acid sensor. The fundamental operating principle of a biosensor is based on the reaction of enzyme and/or antibody with target analyte. Recently, flexible biosensors have attracted much attention because of the prosperous future in wearable applications.[26] Normally, an analyte can be detected and analysed by various electrochemical approaches, such as amperometric, potentiometric techniques, impedance method, and conductometry, which exhibit electrical signals at functionalized electrodes and transduce the target analyte concentrations to readable signals (**Figure** 2.1).[14,27] The colorimetric method is also exploited for biosensing applications, in which the active layer would undergo different extent of color change when the transducer was exposed to different concentrations of specific analyte.[28] More recently, the transistor-based platform has become popular in biosensing area as it can achieve higher sensitivity and lower detection limit than that of conventional electrochemical techniques.[29] Because the physical parameters can be monitored by the commercial products, it will not be detailed in this chapter.

Flexible polymers, such as polyethylene terephthalate (PET), polydimethylsiloxane

(PDMS), polyimide (PI), nylon fiber and poly (methyl methacrylate) (PMMA), papers and textile have become popular substrates for the fabrication of various wearable sensors.[30] By using the flexible substrates, different configurations of wearable sensors have been prepared, such as test strip,[12] skin patch/tattoo,[31] textile,[32] etc.

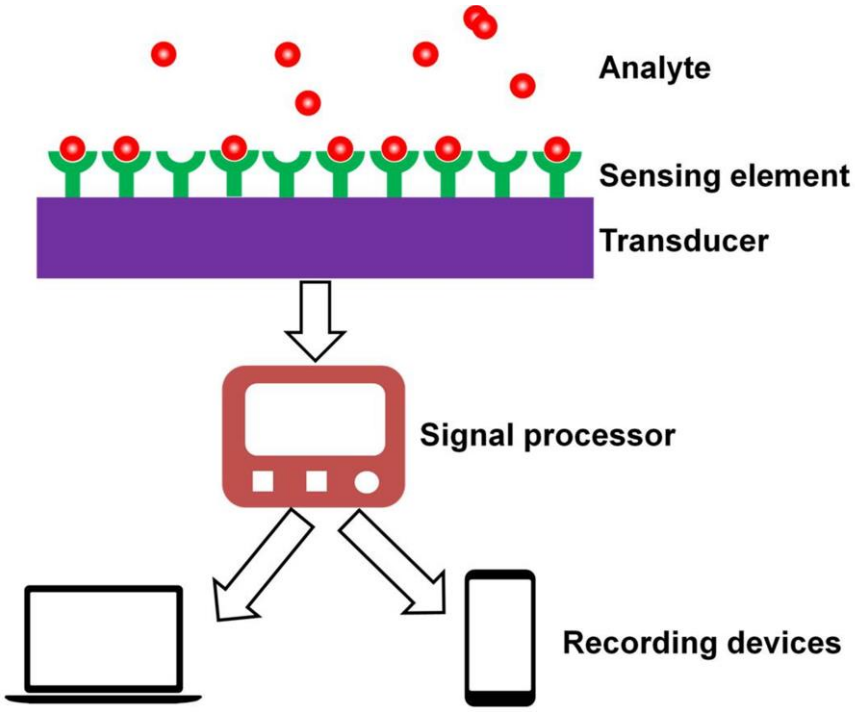

Figure 2.1. Schematic of electrochemical biosensor for wearable electronics.

Non-invasive wearable biosensors have been developed for different sensing scenarios, which can be conveniently used and harmless to patients and athletes. Besides blood, body fluids, such as sweat,[33] tears,[34] and saliva[35] can also provide useful information for physiologically relevant molecules and biomarkers in the human body.[21] The levels of electrolytes (pH, Na^+, K^+, $NH4^+$, Ca^{2+}) and metabolites (glucose, lactate, uric acid, ascorbic acid, urea) can be analyzed by the sensors, which are valuable information for our further healthcare action. Furthermore, the sensors can provide excellent flexibility and conformability during wearable sensing circumstances.

Some reports focusing on different areas of biosensor have been reviewed.[4,14,20,27,29,36-41] Ronkainen *et al.* reviewed enzymatic and affinity electrochemical biosensors preparations and presented some example applications.[14] Turner summarized up to date development of biosensors, such as noninvasive sensors, implantable sensors, and emerging technologies for biosensing applications.[20,27] The introduction of nanotechnologies in biosensors, such as the modification of carbon nanotubes and quantum dots, can efficiently increase the reactivity between sensing element and analyte and enhance transducing efficiency, leading to increased sensitivity of the devices. The wearable applications of biosensors were also reviewed [4,36,37] because they can afford conformability to human skin and provide the possibility of long-term and real-time monitoring of individual health state, such as blood glucose level, ions concentrations, heart rate, etc. Transistor-based biosensors have been reviewed by many publications ranging from materials selection, device preparation and characterization to different biosensing scenarios.[29,39,40] Economou *et al.* summarized different flexible substrates (plastic, paper, and textile, respectively) which can be used for different biosensing applications.[38] However, a comprehensive review of wearable biosensors according to different detection techniques which include conventional electrochemical, colorimetric, optical, and transistor-based detection techniques has not yet been included. In this chapter, the conventional electrochemical techniques for different flexible biosensing applications will be reviewed, and we will focus on two major biosensing techniques: amperometry and potentiometry. Other techniques, such as impedance, conductometry, voltammetry, colorimetric and optical biosensing techniques will also be briefly introduced. Then wearable biosensors that are based on field effect transistor (FET) and OECT will be thoroughly reviewed. The merits of OECT in biosensing applications will be detailed.

2.2 Amperometric/potentiometric wearable biosensors

2.2.1 Introduction

The electrochemical biosensor is considered as one of the most critical wearable biosensors in which amperometric and potentiometric biosensors have been widely used in research and clinical applications as it has simple structure and acceptable detection limit. For the amperometric method, a potential is applied between the working electrode and reference electrode of an electrochemical cell and the current which flows through the working electrode is recorded as an indicator of a specific reaction. The current changes produced by electrochemical redox of working electrode with the target molecules in electrolyte are recorded along time while the constant potential (electrochemical oxidation or reduction peak voltage) is maintained between the working electrode and reference electrode. The amperometric biosensor is commonly used for biosensing applications (both biocatalytic and affinity sensors) because of its simple configuration and relatively low detection limit. The potentiometric biosensor is used to measure the potential change between working electrode and/or reference electrode with negligible current variance. By modifying the working electrode (usually with ion-selective membrane) with biological recognition element (such as enzyme) and other novel materials (such as graphene, carbon nanotube), the target molecules in electrolyte can be transduced to the potential change by enzyme and ion-selective membrane and are further detected by a meter.

Currently, there are two significant methods to modify working electrodes to improve the sensitivity and selectivity of the above-mentioned flexible biosensors. The enzyme is one of the most useful substances to modify the working electrodes and increase the

responsivity and specificity of the devices that are called biocatalytic sensors. Antibody (Ab)/Aptamer is another biomaterial used for the working electrode modification which can bind to the specific molecules (antigen) and cause the readable signal output.

2.2.2 Amperometric biosensors

Amperometric electrochemical biosensors hold a vast potential market in wearable and healthcare products, especially for daily diabetic management because of its simple structure and user-friendly.[21] Nowadays, most commercial invasive blood glucose meters are based on the amperometric technique. The test strip substrates are mostly made by polymer and the flexible test strip can be easily used to collect the blood sample and inserted to the glucose meter for further blood glucose level detection. It is crucial for diabetic diagnosis and further diabetic management because diabetes can cause many complications, such as cardiovascular disease, neuropathy, nephropathy, retinopathy. The diabetic population has reached 422 million in 2014 (for those over 18-year-old) according to World Health Organization (WHO) report, and glucose sensor accounts for about 85% of the total biosensor market (more than US$13 billion market size at an annual turnover).[42] As invasive glucose sensors based on blood assay via finger pricking and a subcutaneous needle can provide more accurate blood sugar level detection, it is still widely used in diabetic management and continuous glucose monitoring.[42]

Different flexible configurations have also been designed to meet different biosensing requirements. Lee *et al.* [33] fabricated a multi-layer flexible biosensor patch and used for sweat glucose detection (**Figure** 2.2(a)). In this patch, silicone is used as the flexible substrate that can well adhere to the skin with excellent conformability. Besides, the glucose patch can be integrated with pH sensors, humidity sensors, and

temperature sensors. In order to increase the sweat rate and sweat collection efficiency, a sweat absorption layer was placed between the skin and patch and a water-proof band was used to adhere the patch on the skin firmly. The authors claimed that this path could be reused multiple times to decrease the fabrication cost. As this patch contains multiple biosensors, the glucose sensor can be dynamically calibrated according to the skin temperature and sweat pH detected by the embedded sensors. So the accuracy of glucose sensors can be increased, which will promote the wearable glucose biosensing toward practical applications. The glucose concentrations measured by the glucose patch range from 10 μM to 1 mM. The working electrode of the flexible biosensor was modified with glucose oxidase, Prussian blue, and nafion, so the device can specifically react with glucose in sweat and work as a glucose sensor. However, the accuracy of this glucose sensor is not confirmed because sweat rate is a crucial factor to influence the glucose concentration in sweat and this influence may lead to an unexpected correlation between sweat glucose level and blood glucose level.

In order to increase the accuracy of sweat biosensors, Chen *et al.* [43] used iontophoresis method to extract interstitial fluid (ISF) from subcutaneous tissue to the skin surface. The glucose in extracted ISF can be detected by the patch adhered to the skin of extracted tissue (**Figure** 2.2(b)). This ultrathin biosensor using PMMA or PI as the substrate could provide good adherence and flexibility. As the glucose level in ISF was much more correlative with blood glucose level than that in sweat, they confirmed that a correlation coefficient of more than 0.9 for glucose level was obtained by this continual glucose sensing technique in comparison with the data from clinical blood detection. As shown in **Figure** 2.3, this flexible biosensor showed good selectivity and sensitivity when the working electrode was carefully modified. Bionic ROSE transfer printing technique was used in this work to transform functional devices from wafer

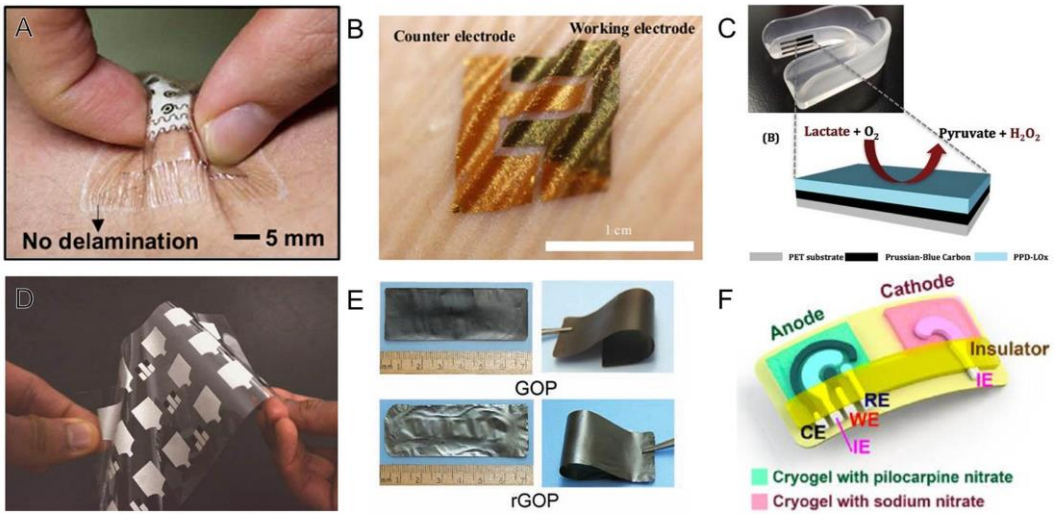

Figure 2.2. The designs of different amperometric flexible biosensors. (a) Flexible sweat patches with multiple biosensing functionalities (glucose, temperature, humidity, and pH). (b) Sweat glucose patch with iontophoresis module. (c) Saliva lactate biosensor mounted on the mouthguard. (d) Sweat glucose sensor integrated with ECG electrode. (e) Free-standing graphene paper based hydrogen peroxide sensor. (f) Flexible alcohol biosensor.

intact. And a paper battery can be used to power the device and realize the signal transmission. It can be regarded as a significant step towards clinical application because it enabled real-time comparison between in vivo blood glucose level and in vitro ISF glucose level.

Besides non-invasive sweat biosensors, flexible tattoo-based amperometric biosensors were used for metabolite composition detections in saliva.[35] Kim *et al.* tried to adhere tattoo-like flexible biosensor on the mouthguard to realize real-time monitoring of lactate levels (**Figure** 2.2(c)). Flexible PET substrate was used in the devices, and the lactate oxidase enzyme and poly(o-phenylenediamine) were modified on the flexible working electrode of the device. Amperometric measurements showed that saliva lactate levels in the region of 0.1-1.0 mM could be detected, which correlates with blood lactate level.[44] The flexible lactate sensor is the first attempt to detect metabolites in saliva, noninvasively. The lactate sensor was also used for perspiration

metabolite detection by Imani *et al.*[11] A shown in **Figure** 2(d), the flexible lactate sensor was fabricated on the thin polyester sheet (only 50 um thickness).

Furthermore, an ECG sensor was also integrated into the lactate sensor to perform multiple signal recordings. The three-electrode configuration was printed as amperometric sensor electrodes, and two bigger outer electrodes were printed as ECG recording electrodes in this design. This enzymatic-based lactate sensor together with ECG recording electrodes can be worn on the chest and perform continual and real-time monitoring of sweat lactate level and ECG signal. On-skin tests confirmed that this hybrid system could measure both physiochemical and electrophysiological signal simultaneously and less cross-talk between these two signals was realized by printing hydrophobic Ecoflex layer to separate the amperometric lactate sensor from the ECG electrodes. The hybrid sensors verified that this flexible lactate sensor showed good selectivity to lactate when compared with the control sensor (Lactate oxidase free sensor). However, other factors such as local sweat pH and skin temperature that may influence the enzyme activity and transducing efficiency of the device have not been studied. So, the reliability of the device needs to be confirmed especially in practical applications. Since the sensor utilized a wireless platform to record and transmit signals to a personal computer, it can be integrated into wearable electronic scenarios. Notably, a button battery can be continuously used for nearly two days according to the power consumption of this wearable device.

Another impressive H_2O_2 sensor reported by Xiao *et al.* is based on a flexible reduced graphene oxide paper (rGOP).[45] Platinum nanoparticles were deposited on the free-standing rGOP to increase the catalytic activity of the film which was also modified with MnO_2 nanowires at the same time (**Figure** 2.2(e)). The amperometric measurement showed that this device had a H_2O_2 linear responsitivity from 2.0 μM to 13.33 mM. Extracellular H_2O_2 secreted by cancer cells was successfully detected by

this device. Although it is a primary result of the flexible H_2O_2 sensor, the flexible sensor is useful in a lab on a chip system for cell metabolites detection.[46,47] Besides common molecules in body fluids, such as glucose and lactate that can be detected by amperometric methods, alcohol can also be analyzed by this approach.[7,48] In this tattoo-based flexible sensor (**Figure** 2.2(f)), alcohol oxidase was used to modify the working electrode and alcohol secreted from sweat can be detected by the amperometric sensor. The iontophoresis method was used to increase the sweat rate which is commonly used in *in situ* sweat detection.[43] The alcohol sensor displayed highly selective and sensitive response to ethanol. Furthermore, the flexible readout circuit was designed to increase the wearability. The Bluetooth wireless transmission platform was utilized to perform real-time data collection and analysis. This flexible alcohol sensor can find some applications in our highways for those driving under the influence or some crime scenes with un-normal alcohol concentration.

Overall, the flexible amperometric biosensor can be used in enzyme-based sensing

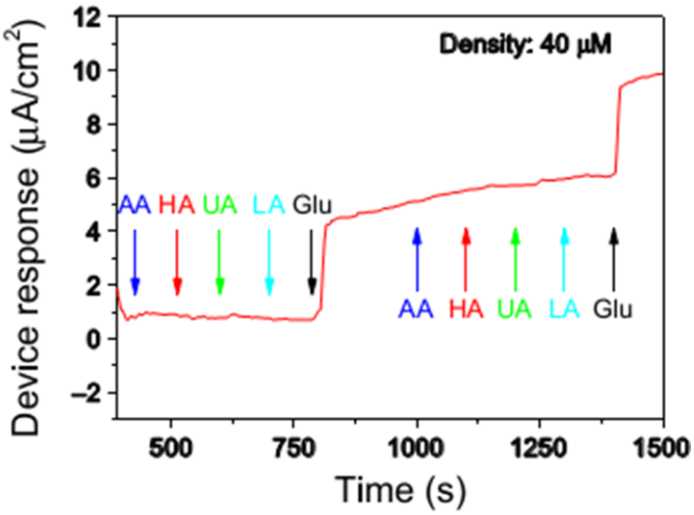

Figure 2.3. The selectivity of sweat glucose sensor patch.

circumstances, such as wearable sweat, saliva, and tear sensor. The detection process is convenient, and the target analyte concentration can be easily converted to a current

signal. There are plenty of flexible biosensors using enzymatic-based working electrodes for different analyte detections.[49] However, enzymes cannot be stored for a long time, and their activity may degrade sharply depending on the local environment. So, further calibration is needed in practical applications.

2.2.3 Potentiometric biosensors

The potentiometric sensor is used to measure the potential difference between the sensing electrode (working electrode) and the reference electrode, which is correlated with the detected ion concentration. So, this method is ideal for charged ion detection. Notably, an ion-selective membrane should be carefully designed to increase the sensor's selectivity. Due to its simple structure and acceptable sensing performance, the potentiometric sensor is widely used for ion and gas detections.

One of the most famous potentiometric sensors should be the "smart wristband" (**Figure** 2.4(a)).[12] The wristband was consist of a flexible sensor array (on the flexible PET film), a flexible printed circuit board and a portable battery. It is a multifunctional flexible biosensor that can detect glucose, lactate, Na^+, K^+ concentrations in sweat, and skin temperature (**Figure** 2.4(b)). The glucose and lactate sensors of wristband utilized the amperometric technique to measure the working electrode current which can be regarded as the indicator of the analyte concentration. The Na^+ and K^+ sensors of wristband utilized the potentiometric technique to measure the ion concentration in sweat. The Na^+ and K^+ selective membranes were designed and coated on the working electrodes to increase the sensors' sensitivity and selectivity. As shown in **Figure** 2.4(c) and (d), the ion sensors showed good sensitivity when different concentrations of Na^+ and K^+ solutions were added. The linear relationship between the potential of working electrode and logarithmic ion concentration can be found in the insets of **Figure** 2.4(c) and (d). Its selectivity of the devices was examined, and the result showed an

acceptable detection range. The response rate is less than several seconds according to **Figure** 2.4(c) and (d), which is rather fast. In order to increase the accuracy of the ion sensors, a temperature sensor was employed to calibrate the glucose and lactate sensors. The wristband can be worn on the forehead (acted as headband) to perform continuous monitoring of sweat components secreted by forehead skin.

Furthermore, a concept called "cloud data" was proposed, and the data collected by

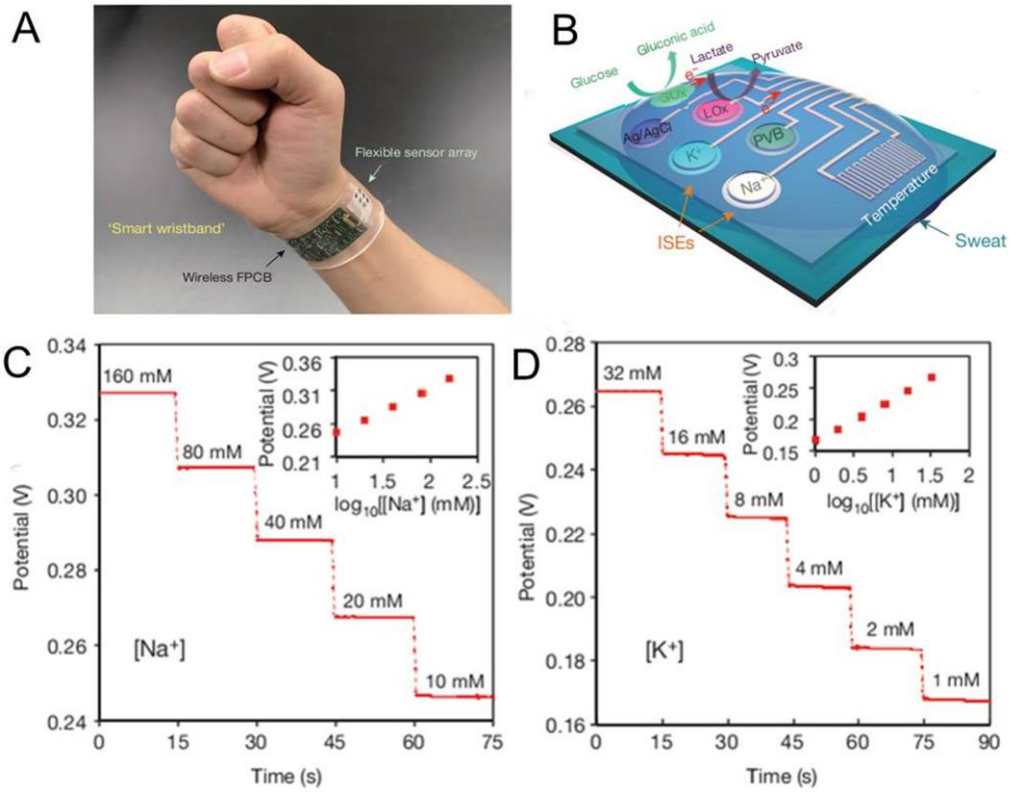

Figure 2.4. The smart wristband for wireless multi-analytes detections. (a) The photo of the flexible wristband. (b) The multifunctional flexible sensor array can be used for different analyte detections. (c)–(d) The potentiometric Na^+ and K^+ sensor can be used for Na^+ and K^+ detection, respectively.

the wearable sensor can be wirelessly uploaded to a cloud server. The massive data sets can be collected through large numbers of volunteer participation. By using data-mining techniques, the collected sensing data can be further analyzed and used to predict the health state of individuals and clinical needs of society.

Rose *et al* fabricated a Na^+ sensor on the flexible PI substrate. [50] As shown in **Figure** 2.5(a), radio-frequency identification (RFID) circuit was integrated into the flexible ion sensor, resulting in a battery-free patch that can be powered up by about 10–20 loops of the coiled antenna under RFID communication through mobile phone. The

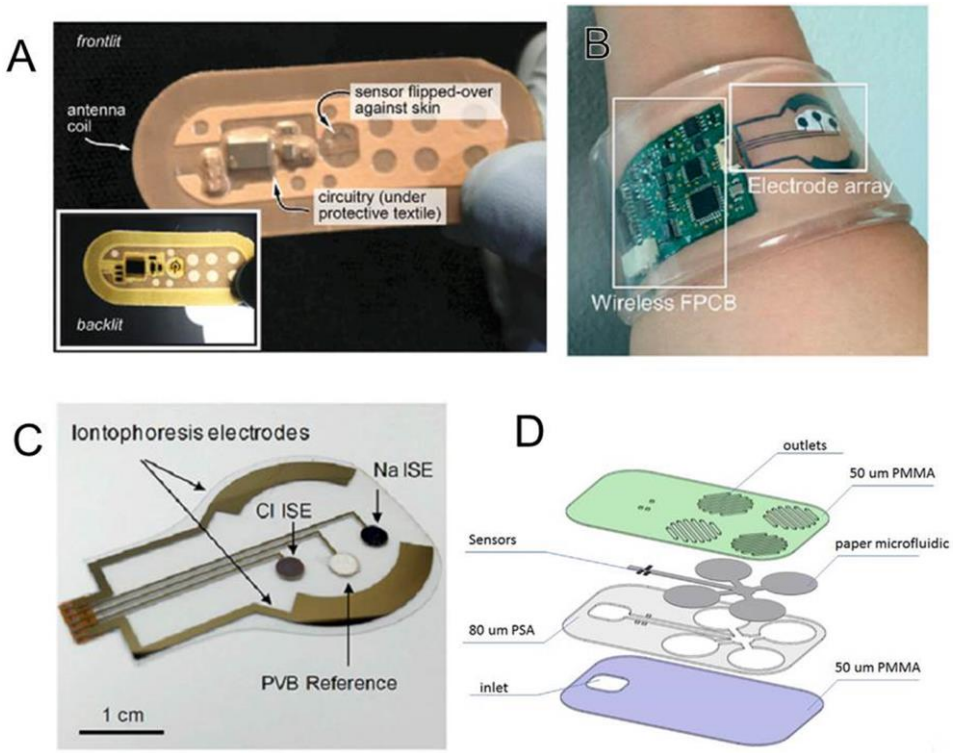

Figure 2.5. The wearable potentiometric biosensors. (a) The wearable Na^+ biosensor with radio-frequency identification function. (b)-(c) Wireless ion sensor integrated with glucose sensor and iontophoresis electrodes. (d) The multi-sensing patch with microfluidic design and wireless readout circuit.

ion concentration in sweat can be detected by the sensor through a mobile phone. In order to increase the detection accuracy and wearability of the flexible sensor, the iontophoresis method was introduced to extract sweat from the skin for robust sensing.[51] The device is wearable and conformable with good design (**Figure** 2.5(b)). The Na^+ and Cl^- can be selectively detected by this wearable sensor. The biosensing electrodes were surrounded by iontophoresis electrodes as they can extract enough sweat extracting for sensing applications (**Figure** 2.5(c)). The detection range of the

ion sensor was from 10 mM to 160 mM. The sensitivities for Na^+ and Cl^- were 63.2 and 55.1 mV per decade of concentration, respectively. By using similar device design, Ca^{2+} concentration and pH of sweat were detected successfully.[52] Another impressive flexible sweat sensor on thin-film PMMA substrate was also used for ion detection. The microfluidic patch and wireless readout circuit were integrated into the sensor, and it can increase both the sampling efficiency and portability of sensor. Potentiometric measurement of Na^+ and pH concentrations, amperometric measurement of lactate concentration, humidity, and temperature sensing were integrated for multi-sensing applications in sweat.

Fiber-based biosensors were designed for wearable applications.[53] The different working electrodes (sensing fibers), such as Na^+, K^+, Ca^{2+}, pH sensing fibers and reference fibers were weaved together with yarn and used for different sweat analyte detections (**Figure** 2.6(a)). As shown in **Figure** 2.6(b), the fabric Na^+ sensor showed good sensitivity and selectivity. The bending and twisting stability was excellent according to the tests. The fabric biosensors integrated into garment were used for continual monitoring of target analytes in sweat during medium exercise. The ion concentrations measured by the fabric biosensor were comparable to that measured by inductively coupled plasma-atomic emission spectrometry. So it would be promising

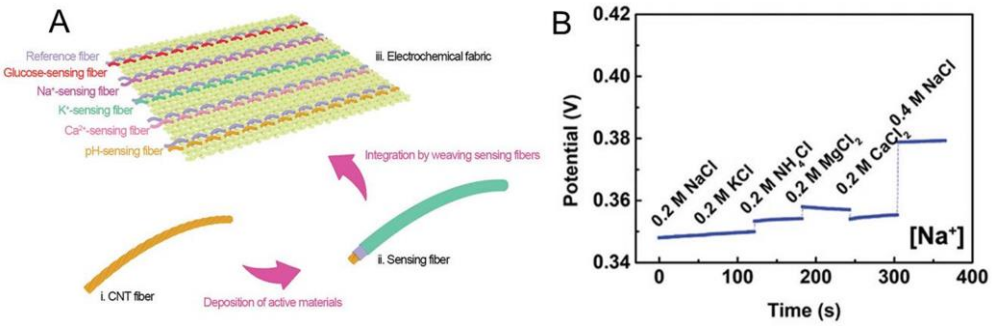

Figure 2.6. The fiber-based potentiometric biosensor. (a) The illustration of multi-sensing fabric biosensor. (b) The Na^+ selectivity of fabric potentiometric sensor.

for wearable electronic applications.

2.2.4 Other conventional wearable biosensors

There are some electrochemical techniques, such as cyclic voltammetry (CV), square wave voltammetry (SWV), differential pulse voltammetry (DPV), and electrochemical impedance spectroscopy (EIS) that can be used to detect target analytes in body fluids. CV measurement is widely used for some preliminary characterization of sensors.[54]

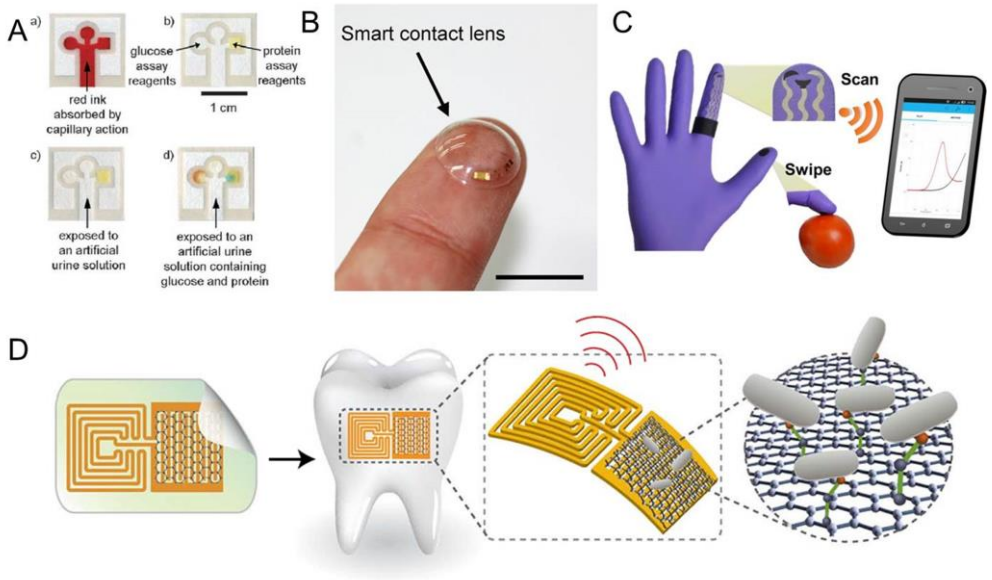

Figure 2.7. Other conventional optical/electrochemical wearable biosensors. (a) Paper-based colorimetric glucose biosensor. (b) Smart contact lenses used for glucose detection in tears. (c) Flexible and stretchable glove biosensor for on-site organophosphorus detection by SWV method. (d) The graphene nanosensor embedded on the tooth enamel was used for bacterial detection in saliva by resistance method.

The colorimetric method can be used to detect the concentration of glucose in urine.[17] A patterned paper was modified with enzymes, iodide, and enzymatic oxidation of iodide, which resulted in a color change from clear to brown. The color change could

be used as an indicator of glucose concentration (**Figure** 2.7(a)). Based on a similar mechanism, protein concentration in urine can be read out from the color change of the test strip. The glucose sensor showed a response to the glucose concentrations ranging from 0 to 500 mM. Although it is cheap and can be used without any other external device (color change can be easily discriminated), its accuracy and response speed still needs to be further optimized.

By using the microfluidic technique, colorimetric biosensor integrated with flexible sweat extracting layer was developed.[55] Smart contact lenses were developed by Prak *et al* and used for real-time and wireless monitoring of glucose concentration in tears.[34] As shown in **Figure** 2.7(b), the lenses were soft, stretchable, and transparent, which are suitable for wearable biosensing. By using SWV techniques, a flexible and stretchable glove-based biosensor was developed to detect organophosphate which is useful in wearable food safety applications.[56] As shown in **Figure** 2.7(c), the glove-based biosensor can well conform according to the finger shape. This "lab-on-a-glove" can be used in the rapid screening of organophosphate in vegetables and fruits. The bacteria graphene nanosensor was used for single bacteria detection.[57] The graphene nanosensor was fabricated on a water-soluble silk substrate and then transferred to the tooth enamel which enabled intimate transfer of graphene to the tooth (**Figure** 2.7(d)). The sensor was modified with antimicrobial peptide and the resistance of the sensor will change when bacteria in saliva were bonded on the sensor. Besides, EIS and DPV are useful methods in biosensing area, but they require much more complicated post processing of the sensing signals and may cause the deviation of the output singals.[58,59]

2.3 Transistor-based wearable biosensors

2.3.1 Introduction

Field-effect transistor (FET) and organic electrochemical transistor (OECT) have been used for biosensing applications.[1,23,26,29,30,39,40,60-65] A good biosensor should have high selectivity to the targeted analyte, high sensitivity, low detection limit, good stability, and fast response speed. [8] Compared with conventional electrochemical biosensing techniques; the transistor-based biosensors can realize in situ amplification of detected signals. So, the high sensitivity and low detection limit can be easily achieved.

The FET-based biosensor has a similar device structure to a traditional FET or a thin film transistor (TFT), which contains three terminals (drain, source, and gate electrodes, respectively), a channel (the connection between source and drain electrode), and a dielectric layer.[66] For the OECT-based biosensor, the solid dielectric layer was replaced with an electrolyte that forms two electric double layers (EDLs) on the surface of the gate and channel. Under a gate bias (ON state), carriers (holes or electrons) are accumulated/depleted in the semiconductor channel, resulting in electrical conduction change between source and drain electrodes. Because the channel conductance is very sensitive to the effective gate bias change, a small voltage applied on the gate can cause a prominent channel current response of the device, which is called transconductance of the transistor.

For biosensing applications, FETs operate in aqueous solutions (electrolytes) because biomolecules are usually dissolved in solutions. When the dielectric layer of a FET is replaced with an electrolyte, the device is also called the electrolyte-gated transistor. The semiconductor channel is non-permeable to the electrolyte, and an EDL can only

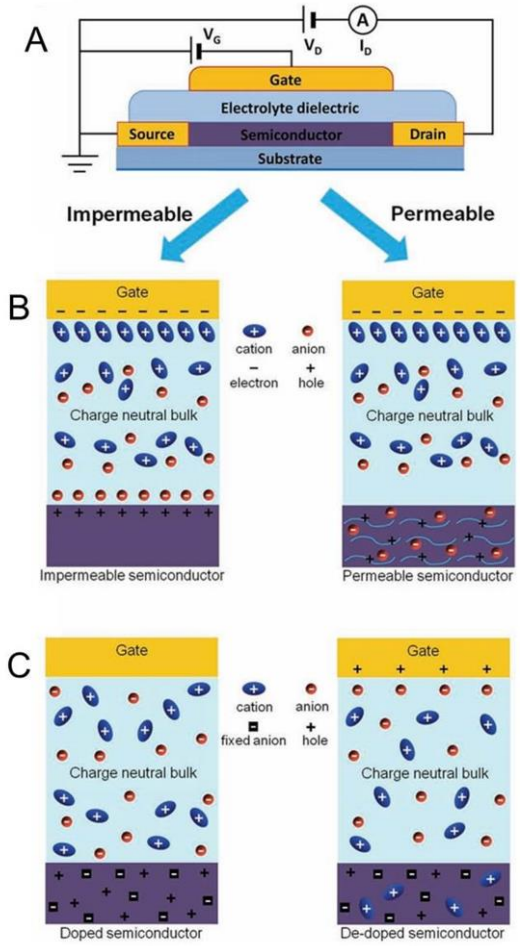

Figure 2.8. The structure of electrolyte gated field effect transistor (left) and electrochemical transistor (right).

be established between the interfaces of gate/electrolyte and electrolyte/channel surface (**Figure** 2.8(a)). For an OECT biosensor, the semiconductor channel is permeable to the electrolyte, and ions can be injected into the whole bulk of the channel to form a sufficient doping/de-doping of the organic semiconductor (**Figure** 2.8(b)), leading to a high bulk capacitance.[60,62] Consequently, the OECT shows a high

transconductance, which is closely related to the sensitivity of a transistor-based biosensor.[23,65] In order to increase the selectivity of the transistor-based biosensor, the gate or channel is modified with biomaterials such as protein, antibody, and enzyme, and the target analytes in electrolyte will specifically react or bind with the biomaterials on the sensor.

Owing to their high sensitivity, transistor-based biosensors have demonstrated their wide applications in different sensing areas, such as glucose, uric acid, ascorbic acid, lactic acid and protein detections in blood, sweat, urine, saliva, tears and other body fluids.[1,29,30,40,61,63]. Flexible transistor-based biosensors can provide non-invasive and continuous monitoring of targeted analytes in body fluids due to their excellent flexibility and conformability, which is useful for both inpatient and individual diagnostics and healthcare management.[67,68,69,70] In this section, wearable FET-based and OECT-based biosensors used for the detection of different biomolecules will be introduced. The wearable applications and point-of-care metabolites monitoring will also be reviewed.

2.3.2 Field-effect transistor biosensors

Flexible FETs can be realized based on inorganic semiconductors due to its outstanding bending and twisting performance, which is useful for further wearable applications. Indium oxide-based flexible FETs were fabricated and used for wearable glucose monitoring.[71] The mobility of the device can reach ~22 $cm^2V^{-1}s^{-1}$ with a high on-off ratio (>10^5) and excellent mechanical robustness. The drain and source electrodes were modified with glucose oxidase, chitosan, and single-wall carbon nanotubes (**Figure** 2.9(a)). As shown in **Figure** 2.9(b) and (c), the device showed excellent flexibility and conformability to the curved surface of human skin or an eyeball. The detection limit of the device can be down to 10 nM with a response time

within several minutes, which can be potentially used in wearable tears glucose detection. Silicone-based FET biosensors have been developed on the tip of a pipette

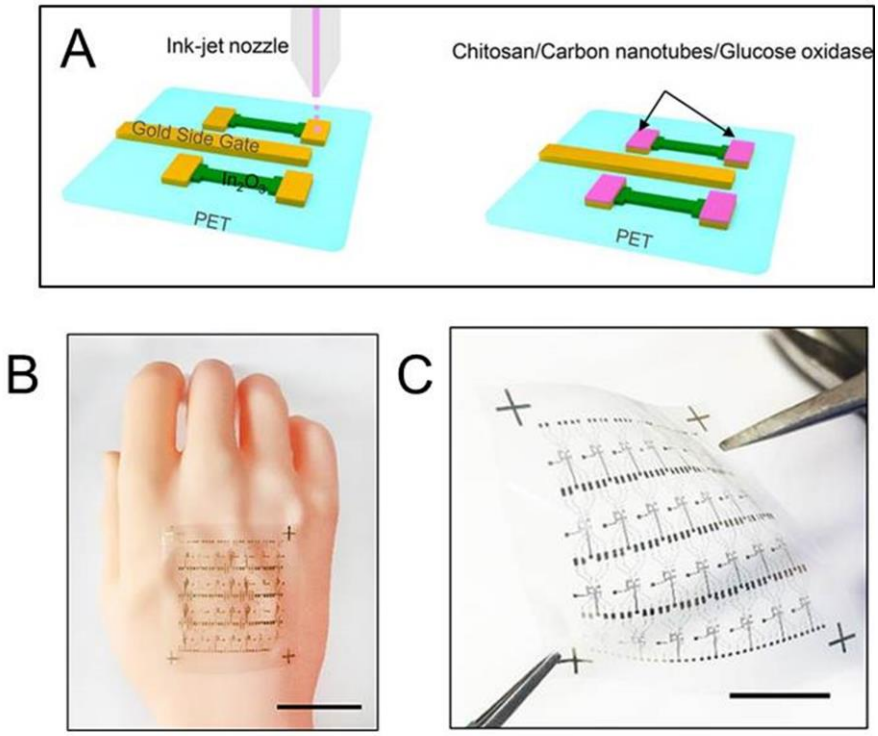

Figure 2.9. The wearable In2O3 nanoribbon FET used for glucose detection with a detection limit down to 10 nM.

for pH and sodium ion detections.[72] This tip-based FET multi-ion sensors can be integrated into the wearable system and used to monitor the ion concentration of human body fluids.

Another novel material, graphene (single layer graphite), has been widely used in FET applications in recent years because it is susceptible to local electric field and charges with high chemical robustness.[68,73-75] Moreover, graphene has very high carrier mobility (up to $2\times10^5 cm^2V^{-1}s^{-1}$), which is more than two orders of magnitude higher than that of the conventional semiconductor silicon.[76] Xiang *et al.* prepared flexible graphene FETs on Kapton substrates by inkjet printing to detect the virus in infectious

organisms (**Figure** 2.10(a)). The antibody was modified on the graphene layer after finishing the printing process to increase the sensitivity and selectivity of the device. As shown in **Figure** 2.10(b), a flexible microfluidic setup was built on the top of the device. The flexible sensor showed a linear response to the target pathogen between 0.1 ug/mL to 100ug/mL with a detection limit down to 0.1 ug/mL (**Figure** 2.10(c)). PET substrates are used in wearable graphene FET fabrications. [68,77,78] A "bioelectronic nose" based on a graphene FET was prepared by Park *et al*,[68] which showed excellent long-term stability and bending durability. Human olfactory receptors were integrated into the device to detect the specific odorant amyl butyrate which mimics the nose function of humans. The detection limit of the "bioelectronic

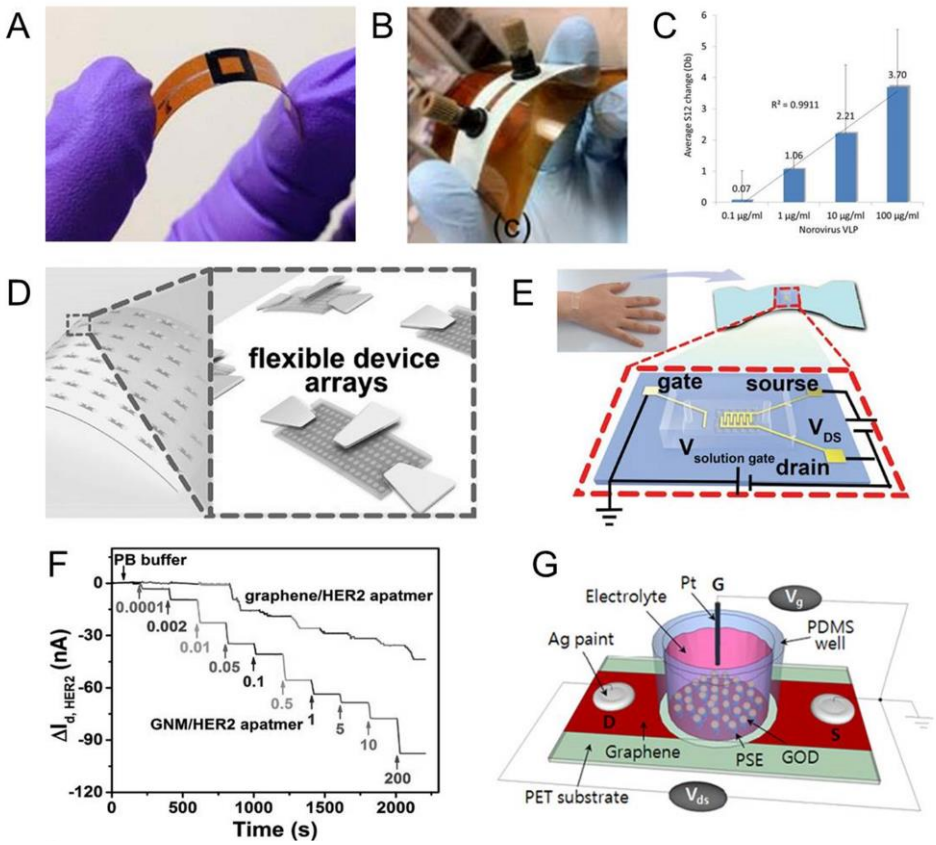

Figure 2.10. The wearable graphene FET fabricated on the PI substrate (a-c), and PET substrate (d-g) substrate, respectively.

nose" to specific odorant molecules can be down to 0.04 fM (Fig. 10(f)).

Graphene nanomesh was also prepared by a chemical vapor deposition method and used to fabricate flexible FETs (**Figure** 2.10(d)). The graphene sensor was modified with an antibody (aptamer) and used to detect human epidermal growth factor receptor 2 which is a cancer marker in cancer diagnostics (**Figure**2. 10(e)). The on-off ratio of the graphene FET is about 1000 at room temperature, and the detection limit of the device can be down to 0.6 $\times 10^{-15}$ M. Besides, the graphene device served as a label-free biosensor used for in vitro detection of human epidermal growth factor receptor 2 secreted by cancer cells. So the flexible biosensor can be developed as the core part of high-performance sensing chips for advanced cancer diagnostic systems.

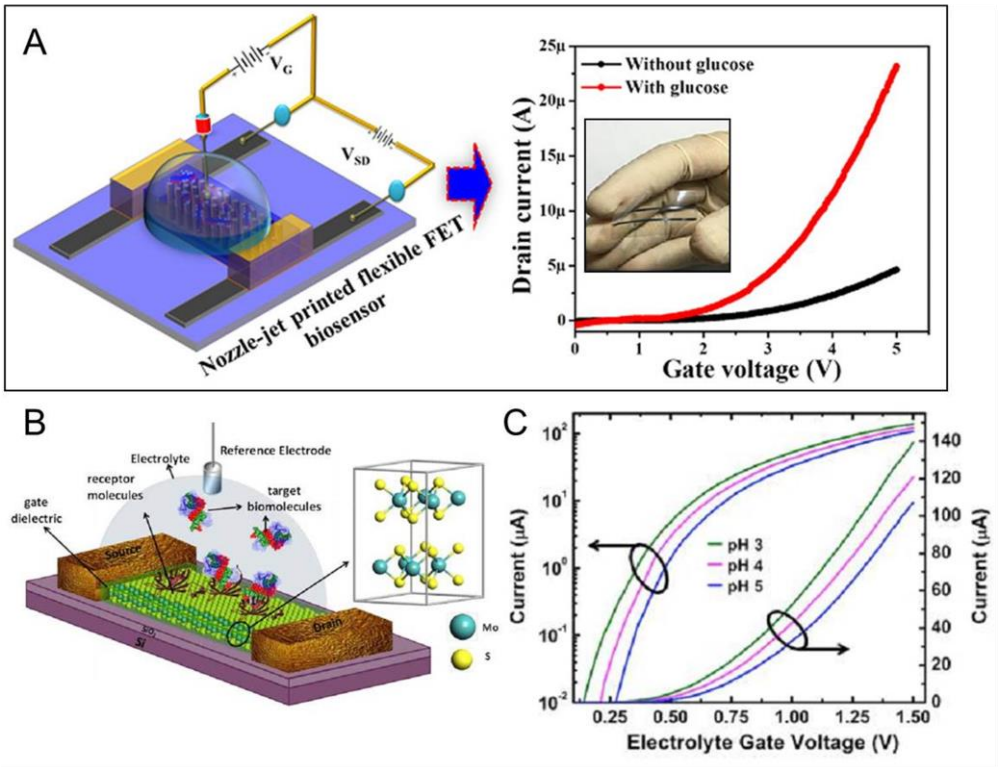

Figure 2.11. The flexible nanorod FETs for high performance glucose detections (a). MoS_2-based FET for protein and pH sensing (b-c).

The graphene FETs have also been developed as a flexible glucose sensor for wearable

applications.[77] As shown in **Figure** 10(f), the device was fabricated on a flexible PET substrate, and glucose oxidase was modified on the graphene channel area. The sensor can be operated in the detection range of 3.3–10.9 mM, which covers the physiological levels of blood glucose.

Zinc oxide nanorods had been prepared and used as channel materials of various FET biosensors for glucose sensing.[79] The nanorods were modified with glucose oxidase and nafion. Owing to the large specific area of nanorods, the enzyme loading capacity of the device can be increased, which is critical to the improvement of the sensing performance. As shown in **Figure** 2.11(a), the FET biosensor exhibited good flexibility and bending stability. A good selectivity was confirmed by calibrating glucose concentration at the addition of different interferences.

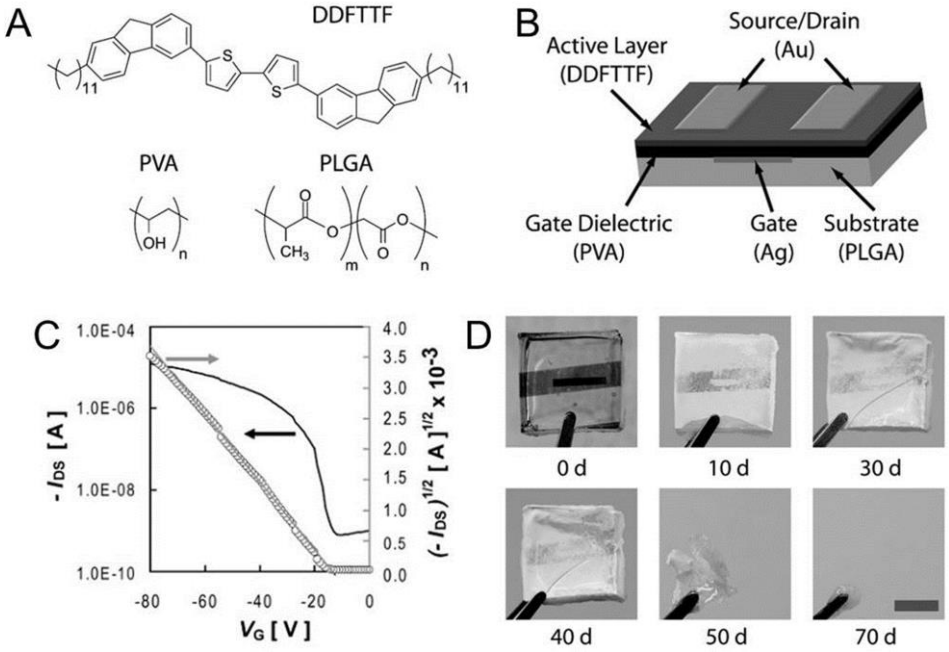

Figure 2.12. The wearable organic FET fabricated on the resorbable substrate.

Recently, two-dimensional materials, such as molybdenum disulfide (MoS_2), tungsten disulfide (WS_2), and molybdenum diselenide ($MoSe_2$), have emerged as promising channel materials of FETs for biosensing applications. Sarkar *et al* fabricated a MoS_2 FET biosensor, which provided rapid, inexpensive, and label-free biomolecular detections (**Figure** 2.11(b) and (c)).[80] The protein detection limit can be down to 10^{-13} M. More importantly, the resorbable FET biosensor can find many plantable and wearable biosensing applications, such as ex vivo and in vivo glucose level monitoring for better diabetic management (**Figure** 12).

2.3.3 Organic electrochemical transistor biosensors

OECT is another type of thin-film transistor that can be used for biosensing because it can be operated in aqueous solutions.[81] Wearable OECTs have been prepared on the flexible substrates and used for continuous and/or non-invasive monitoring of biomolecules and ions in body fluids, such as glucose in blood or tears, lactic acid, Na^+, K^+ in sweat, and specific DNA or protein in serum.[82] Owing to the high sensitivity of the OECTs, a trace amount of analyte in body fluids can be easily identified, which will be useful for early diagnosis of diseases.

As shown in **Figure** 2.13(a), the flexible OECTs were fabricated and used for highly sensitive detection of various biomolecules.[85] The source, drain, and gate electrodes of the device were deposited by using the magnetron sputtering method. PEDOT:PSS was used as the active layer of the channel. The platinum gate electrode of the device was modified with glucose oxidase, graphene oxide, polyaniline, nafion, and graphene to increase the selectivity of the glucose sensor. The flexible device can be perfectly attached to the skin surface and showed good bending stability even after 1000-time bending tests. The detection limit to glucose and uric acid can be down to 30 nM, which is sensitive enough for the detections of the glucose and uric acid levels in

saliva. In order to realize non-invasive detections, saliva samples were collected and measured by using glucose and uric acid sensors (**Figure** 2.13(b) and (c)). So the flexible devices can be used as test strips for noninvasive and wearable glucose detection.

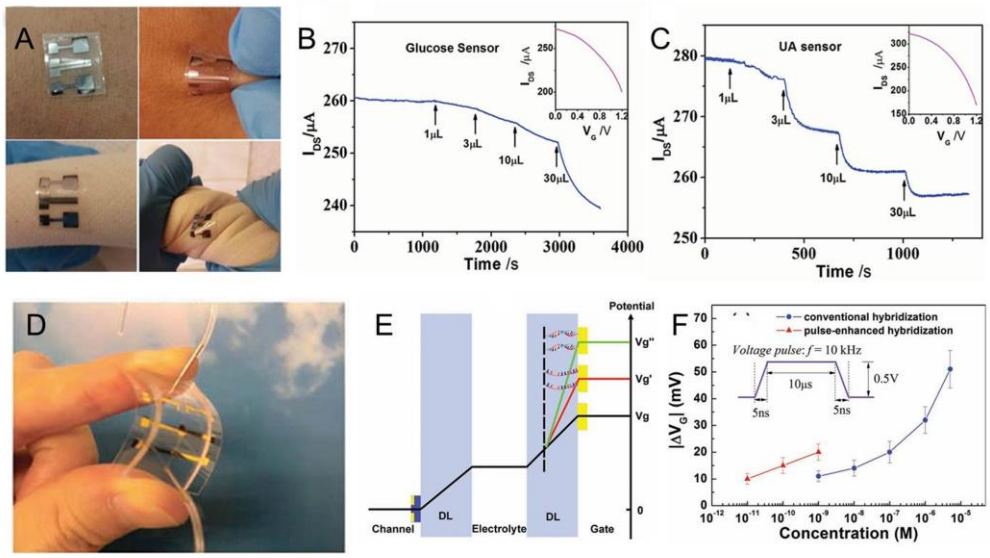

Figure 2.13. The flexible OECT biosensor fabricated on the PET substrates (a-c), and microfluidic platform (d-f) for artificial urine, saliva, and DNA detections.

Flexible DNA sensors integrated with microfluidic systems were investigated (**Figure** 2.13(d)).[86] DNA probes were immobilized on the gate of an OECT and complementary target single-stranded DNA (ssDNA) can specifically bind to the DNA probes. As shown in **Figure** 2.13(e), the effective gate voltage was changed when ssDNA was bonded to the DNA probes and resulted in a right shift of the transfer curve to a positive gate voltage. The flexible DNA sensor can be used for continuous sampling and detection of ssDNA. The detection limit of the DNA sensor was about 1 nM, which can be further decreased to about 10 pM after a voltage pulse was applied on the gate voltage to enhance DNA hybridization (**Figure** 2.13(f)).[87] Highly sensitive protein sensors can be realized based on the similar method.[88,89] By using the sensing technique, the target DNA in body fluids can be detected.

A wearable sweat biosensor for protein (e.g. cortisol) detection has been developed by Parlak *et al.*.[70] The sensor was designed to be a patch that can be readily attached to any part of human body. As shown in **Figure** 2.14(a), the cortisol sensor consisted of top flexible elastomer as the substrate, a PEDOT:PSS channel, three electrodes, a sample reservoir layer to store sweat, a molecularly selective membrane for cortisol screening, and a bottom polydimethylsiloxane layer with laser-patterned microcapillary channel arrays. The molecularly selective membrane can selectively choose cortisol in the sensing region. The microcapillary channel arrays were patterned in the top layer of the sensor, which can promote the sweat extraction to the sensing area of the patch. The device showed good flexibility and can conform on the skin surface (**Figure** 2.14(b)). The sensor was used for cortisol detection in volunteers' sweat. The detection results by this patch were correlated with those obtained by the enzyme-linked immunosorbent assay method, a standard method to determine the

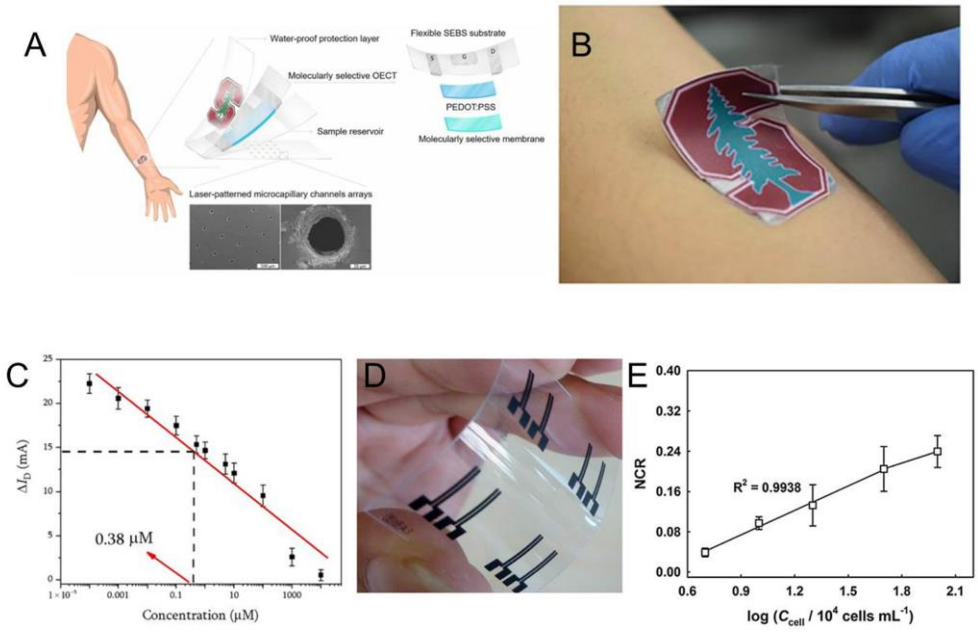

Figure 2.14. The wearable OECT sensor used for sweat cortisol detection (a-c) and bacteria detections (d-e), respectively.

concentration of cortisol (**Figure** 2.14(c)). Although the detection limit of this patch for cortisol was only about 1 uM, it presented a non-enzymatic biosensing technique for wearable detections of various biochemical elements.

Flexible OECTs can be printed layer-by-layer on flexible substrates, which is suitable for mass production.[90] As shown in **Figure** 2.14(d), the OECT biosensor was screen-printed on the PET substrate by using carbon paste and showed good flexibility. The antibody, poly (3-aminophenylboronic acid, 3-ABA), was deposited on the gate electrode of the device for cancer cell identification. The device showed a moderate response to the additions of Hela cells with different concentrations (**Figure** 2.14(e)). This printing technique can be further used for large-scale and inexpensive fabrication of wearable OECTs.[91,92] For different sensing applications, the gates can be further printed with different modification layers.

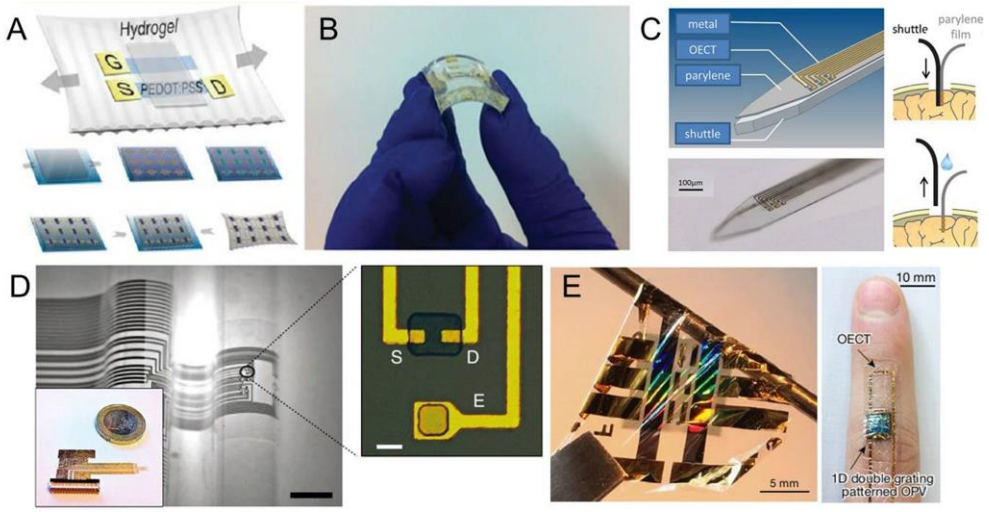

Figure 2.15. The wearable OECT biosensors fabricated on the PDMS (a-b), and parylene substrate (c-e) for different sensing applications.

In order to realize wearable applications, much effort has been devoted to the study of flexible OECTs which show good stretchability and conformability.[93-95] Flexible devices on polydimethylsiloxane substrates can work under stretching status and used

for some bioelectric applications (**Figure** 2.15(a) and (b)). Parylene thin films show good conformability and can be used as substrates of OECTs prepared by the photolithography process. The OECTs on thin parylene films have been used as probes for neural interfaces (**Figure** 2.15(c) and (d)).[96,97] More recently, OECTs were integrated with solar cells and showed a huge potential for self-powered wearable electronics.

Chapter 3 Fabric organic electrochemical transistors for biosensors

3.1 Introduction

Robust, flexible, and wearable electronics have attracted much attention in recent years.[12,93,98,99] Motivated by huge potential markets, several conceptual products as the state-of-the-art technologies are expected to step into our normal life, ranging from curved and foldable Samsung smartphone, wearable Google glass to smart clothing for monitoring real-time body state. Ideal smart clothing should be based on flexible electronics devices woven together with textiles, which are difficult to be achieved by using conventional electronic devices with planar structures. Therefore, electronic devices assembled on flexible fibers, such as fiber-based solar cells,[100] electrochemical supercapacitors,[101] thin-film transistors (TFTs)[102-104] and self-powered energy conversion devices,[105] have evoked the growing interests of researchers. The flexible and lightweight fiber-based devices could be integrated into smart clothes by weaving them with textile fibers to achieve desirable functions.[40]

OTFTs have found a wide range of applications in flexible electronics particularly displays, memories, and sensors.[1,24,82,106-108] OECTs, as one type of OTFTs, can operate in liquid electrolytes with low voltages (less than 1V) and are promising for chemical and biological sensing, such as the detections of ion,[109] glucose,[24,110,111] uric acid (UA),[85] dopamine (DA),[112,113] DNA,[86] bacteria[114] and cells,[115,116] etc. To prepare high-performance fiber-based OECTs, not only the organic channels but also the metal electrodes of the devices should have good bending stability on the surface of thin fibers. The channel regions should be defined by patterning the source and drain

electrodes on the fibers, and the electrode material needs to have high enough conductivity to minimize the voltage drop on a long and thin electrode wire, which has not been tackled in fiber-based transistors reported before.[117,118]

In this chapter, we report the fabrication and functionalization of OECTs on Nylon fibers and the integration of the devices in fabrics. Highly conductive multilayer films with the structure of Cr/Au/PEDOT:PSS were coated on the fibers and used as source/drain electrodes. The devices showed excellent bending stability and were successfully used for various chemical and biological sensing applications with high sensitivity and selectivity. The fiber-based devices were woven together with commercially available cotton fibers using a conventional weaving machine without detectable degradation of device performance after the weaving process. As a potential application, the flexible and stretchable fabric biosensors were integrated into diapers and used to detect the glucose concentrations of artificial urine by a mobile phone. Our results demonstrated the advantage of using fabric devices in wearable electronics.

3.2 Experimental section

3.2.1 Materials

Nylon fibers (0.08mm, 0.15mm, 0.30mm, 0.50mm) were purchased from Nantong Jinda Chemical Fiber Co., Ltd. Glucose oxidase (GOx) (50 kU g^{-1}) was purchased from Aladdin Reagent Database Inc. and stored at -20 ℃ for future use. Uricase (UOx) (>3U mg^{-1}) was purchased from Worthington Biochemical Corporation and stored at -20 ℃. Hydrochloric acid, sodium chloride (NaCl), calcium chloride ($CaCl_2$) and aluminum sulfate ($Al_2(SO_4)_3$) were purchased from Sigma-Aldrich Co. Glucose, Dopamine (DA), Ascorbic acid (AA), Uric acid (UA), Polyaniline (PANI) (5 wt.

%,dispersion in xylene), Phosphate buffered saline (PBS) solution (pH 7.4), poly(3,4-ethylene dioxythiophene):poly(styrene sulfonate) (PEDOT:PSS) aqueous dispersion (Clevios PH500) and Nafion (5%) aqueous solutions were all purchased from Sigma-Aldrich Co. and stored at 4 ℃. Chitosan (CHIT) was purchased from Advanced Technology & Industrial Co., Ltd and used as received. Graphene flakes with an average size of several micrometers and graphene oxide (GO) were both prepared by the chemical methods.[119]

3.2.2 Device fabrication

Figure 3.1(a) demonstrated the fabrication procedure of the OECT fiber sensors. Patterned Cr (~10nm)/Au(~100nm) source and drain electrodes were deposited on Nylon fiber by RF magnetron sputtering. The length of the channel was 0.4 mm. Before dip-coating PEDOT:PSS layer, the surface of the fiber was treated with oxygen plasma for 3 minutes. Then the fiber was coated with PEDOT:PSS layer and transferred to a glove box filled with high purity N_2 for post-annealing at 100 °C for 1 hour. Then parylene layer (~2 μm) was deposited on the surface to serve as an encapsulation layer on the electrodes. The gate electrode (Ti (~10nm)/Pt(~100nm)) of a fiber OECT was fabricated by the similar process mentioned above.

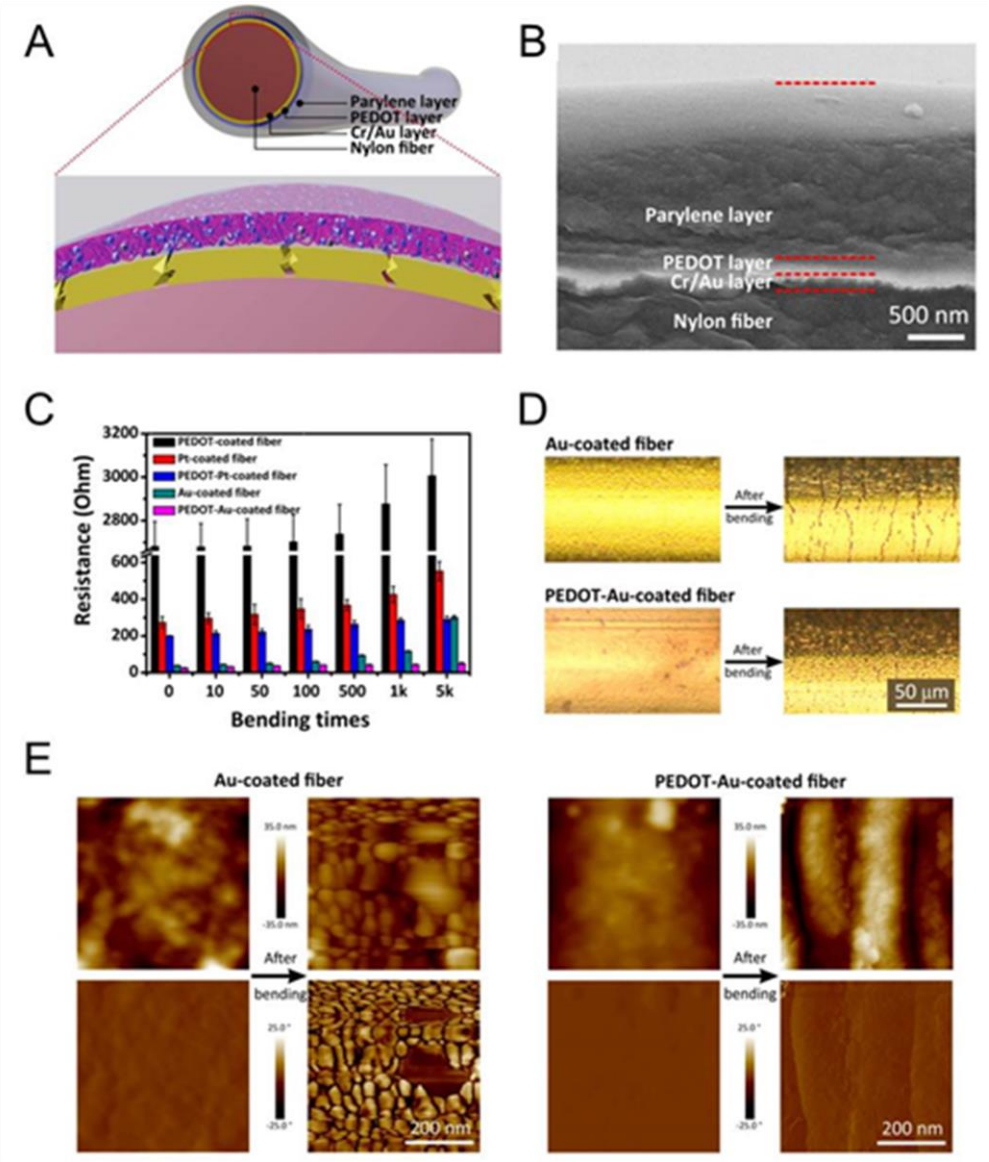

Figure 3.1. (a) The design of core-shell conductive nylon fiber with Cr/Au/PEDOT:PSS/parylene coating. (b) SEM image of the cross-section of a core-shell conductive nylon fiber. (c) Resistance versus bending times of five kinds of conductive fibers, includes PEDOT:PSS, Pt, Pt/PEDOT:PSS, Cr/Au and Cr/Au/PEDOT:PSS -coated fibers; (d) Photos and (e) AFM images of Cr/Au and Cr/Au/PEDOT:PSS -coated fibers before and after 1000 times bending tests, respectively.

To prepare high-performance biological sensors, the gate electrodes of OECTs should be modified with biocompatible polymers, graphene-based nanomaterials, and enzyme. For the preparation of CHIT/GOx/Pt gate electrodes of OECT glucose sensors, the fiber coated with Pt layer was firstly treated with 3 minutes oxygen

plasma to improve the surface hydrophilibility, then immersed into the GOx stock PBS solution (10 mg mL^{-1}) for 2 hours. The Pt fiber coated with the enzyme was dried at 4°C in a refrigerator. Then 10 μL CHIT acetic acid solution (CHIT ~5mg mL^{-1}; acetic acid: 50 mM, pH: 5–6) was drop coated on the surface of the dried GOx/Pt fiber electrodes to immobilize GOx molecules. Before use, the modified fiber gate electrode was washed with PBS to remove the unanchored reagents. For the preparation of OECT UA sensor (fiber gate electrode: UOx-GO/PANI/ nafion-graphene/Pt) and OECT DA sensor (fiber gate electrode: nafion-graphene/Pt), the modification processes were similar to the preparation of glucose sensors.

3.2.3 Device characterization

The measurement system contains two Keithley source meters (Keithley 2400) controlled by a Labview program in a laptop. For the transfer characteristic (I_{DS} vs V_G), V_{DS} was fixed at 0.01V, and the channel current was measured as a function of V_G. For the real-time monitoring of the channel current of a sensor to additions of various analytes in PBS solutions, V_{DS} was fixed at 0.01 V, V_G was fixed at 0.6 V.

Artificial urine (AU) was used to simulate the effect of normal human urine.[120] The AU solution used in our diaper sensor test was 105.5 mM NaCl, 63.7 mM KCl, 36.3 mM NH_4Cl, 3.85 mM $MgSO_4$, 16.95 mM Na_2SO_4, 32.3 mM NaH_2PO_4.[121] The pH of AU was adjusted to be 6.0 by adding the hydrochloric acid solution. The diaper embedded with the glucose-sensitive textile sensor can be used to selectively detect glucose in AU. A remote and real-time test platform controlled by a mobile phone app was established to measure the current response of diaper sensor to the addition of different solution species in our setup. In the test, AU (~20 mL) was firstly added to the diaper to create a solution environment for the sensor. Then glucose dissolved in AU (~10 mL) was added to the diaper to a final concentration of about 3 mM which is

considered to be the abnormal level of glucosuria.[122] Finally, the major interference UA dissolved in AU was added to the diaper to the final concentration of about 1 mM which is at the normal level of UA in human urine.[123] After finishing the test, the data recorded by the mobile phone can be saved for further use.

3.2.4 Design of wireless biosensing system

The overall architecture of our wireless biosensing platform is finely designed and can be divided into three components, which include fiber OECT-based sensor, readout circuit, and user application program. For the design of readout circuit, Arduino Uno R3 board based on Atmel Atmega328 is selected as the microcontroller, with upgraded I/O pins by integrating with high performance 12-bit DAC (MCP4725, with built-in programmable gain amplifier (PGA)) and 16-bit ADC (ADS1115, with built-in voltage follower) modules via I2C communication. The circuit board is powered by four 1.5 V alkaline batteries. The wireless transmission of data between the circuit board and mobile phone is realized using Bluetooth and customized mobile app with a user-friendly interface. For the consideration of privacy, collected data is saved in the internal storage of the phone for future data analysis.

3.3 Fabrication of highly durable and flexible fiber-based OECT

For a fiber-based OECT, long electrode wires that can conduct current from the channel, which should have the conductance much higher than that of the channel. Although some conductive polymers show conductivities up to ~10^3 S/m,[124] metals, like silver, copper, and gold, exhibit the conductivities of ~10^7 S/m that are four orders of magnitude higher than that of the former.[125] So gold electrodes were used

in our devices as source and drain electrodes to meet the high conductivity

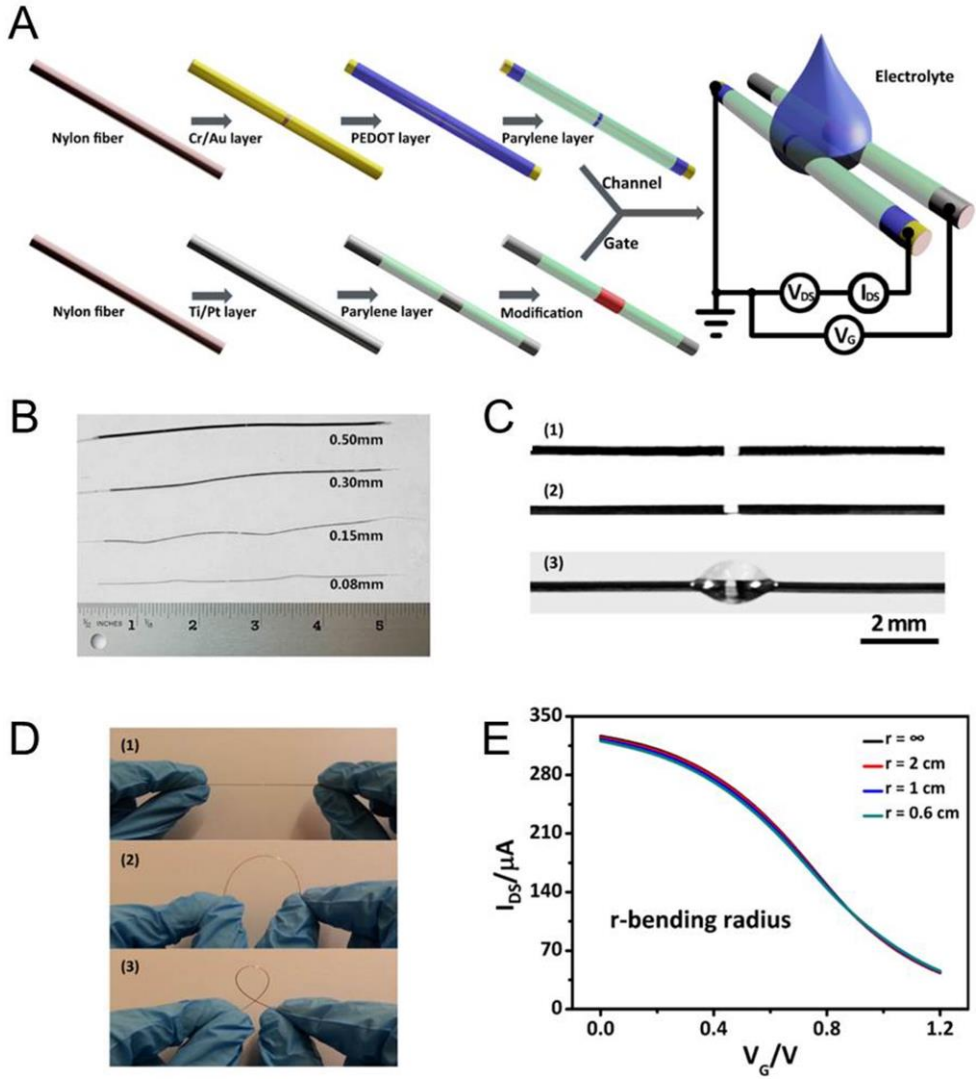

Figure 3.2 (a) The fabrication process of functionalized fiber-based channel and gate for an OECT. (b) Photo of fiber-based devices with different diameters: 0.08mm, 0.15mm, 0.30mm and 0.50mm. (c) Photos of a fiber channel before and after coating a PEDOT:PSS layer and hydrophilic property on its surface. (d) Photo of a fiber device with different bending statues. (e) Transfer characteristics of a fiber-based OECT with different bending radius. Fiber diameter is 0.30 mm and V_{ds} = 0.01V.

requirement. To improve the bending stability of the gold electrodes, we prepared Cr/Au/PEDOT:PSS multilayer films on nylon fibers, where Cr is used as an adhesion layer for Au on the nylon surface. **Figure** 3.1**(**a) shows the design of a nylon fiber

that is coated with a Cr/Au (thicknesses: 10nm/100nm) layer and a highly conductive PEDOT:PSS layer (thickness: ~100nm) prepared by magnetron sputtering and dip coating, respectively. PEDOT:PSS aqueous dispersion was mixed with DMSO and glycerin (both with a volume ratio of 5%) to improve the conductivity of PEDOT:PSS layers.[126] In addition, (3-Glycidyloxypropyl) trimethoxysilane (GOPS) cross-linker was added to the aqueous dispersion with a volume ratio of 1% to improve the stability of PEDOT:PSS. Then a layer of parylene of 2 μm was coated on the surface by vacuum deposition to passivate the conductive layer. **Figure** 3.1**(**b) shows a scanning electron microscopy (SEM) image of the cross-section of a fiber with a clear demonstration of each layer on the nylon surface.

Figure 3.1**(**c) shows the resistances of three nylon fibers (diameter: 0.3cm) coated with Cr/Au, Cr/Au/PEDOT:PSS and PEDOT:PSS layers, respectively, before and after the bending tests for up to 5000 times. It is reasonable to find that the coating of PEDOT:PSS on the surface can decrease the resistance of the Nylon/Cr/Au fiber from 39 to 26 Ω/cm. The resistance of the Cr/Au/PEDOT:PSS fiber is two orders of magnitude lower than that of a fiber with one layer of PEDOT:PSS only. Notably, the average resistance of the fibers coated with Cr/Au increase from 39 to 301 Ω/cm during the bending tests while the resistance of the multilayer coating of Cr/Au/PEDOT:PSS shows a much smaller increase (from 26 to 51 Ω/cm). The PEDOT:PSS layer shows very little relative change in its resistance during bending tests, which is consistent with our results reported before.[24] To better understand the effect, we observed the surface of the fibers under optical microscopy and atomic force microscopy (AFM). As shown in **Figure** 3.1**(**d) and (e), we can find that Cr/Au films in both composite fibers crack after the bending tests. Consequently, the resistance of the fiber with Cr/Au increase. However, in the sample with Cr/Au/PEDOT:PSS multilayer film, the PEDOT:PSS layer coated on the surface of

Au can connect the separated Au fractions and lead to a more stable resistance of the fiber. A similar strategy was applied on the gate electrode with a Ti/Pt layer, where Ti is used as an adhesion layer for Pt on Nylon. After coating a thin layer of PEDOT:PSS film on Ti/Pt, the bending stability of the wire is dramatically improved, as shown in **Figure** 3.1(c). Although many papers reported micro-patterning of metal electrodes to improve their stability in flexible and stretchable electronics, it is rather challenging to pattern the electrodes on thin fibers.[127] Therefore, the deposition of metal/PEDOT:PSS multilayer films can be a very convenient approach to prepare highly stable and flexible electrodes for fiber-based devices.

Figure 3.2**(**a) shows the fabrication process of an OECT on a flexible Nylon fiber. Cr/Au source and drain electrodes were deposited on a Nylon fiber by magnetron sputtering with a narrow tape protected on the channel region. The channel length was controlled to be 0.4 mm, and the channel width was equal to πD, where D is the diameter of the fiber. Then a thin PEDOT:PSS layer was coated on the surface of the whole fiber, including the channel region and the electrodes, by dip coating. To encapsulate the source and drain electrodes, a thin layer of parylene (~2μm) was then deposited on the fiber surface except for the channel region. Gate electrode on another Nylon fiber was prepared with the same process. Since the gate electrode of an OCET does not need high conductivity,[1] we find that a fiber coated with Ti/Pt is good enough for the gate. We used Pt layer as the gate of the device because Pt has high electrochemical activity and can be used for various types of biosensors. A Ti/Pt (thicknesses: 10nm/100nm) layer is deposited on the Nylon fiber by magnetron sputtering followed by the coating of a parylene layer on the surface except for the region of the gate electrode. **Figure** 3.2(b) and (c) show fiber devices with different diameters, which are hydrophilic on their surfaces. The devices are flexible, lightweight and show excellent stability in bending tests, as demonstrated in **Figure**

3.2**(**d).[128,129] Then the devices were characterized in PBS solutions. The transfer characteristic (I_{DS} vs V_G) of an OECT with a diameter of 0.3 mm is presented in **Figure** 3.2**(**e), which shows very stable performance at different bending radius.

The channel current of a fiber-based OECT (p-channel) is given by:[82]

$$\begin{aligned} I_{DS} &= \frac{2\pi D}{L}\mu_p C_i (V_p - V_G^{eff} + \frac{V_{DS}}{2})V_{DS} \quad (\text{when } |V_{DS}| << |V_p - V_G^{eff}|) \\ V_p &= qp_0 t / C_i \\ V_G^{eff} &= V_G + V_{offset} \end{aligned} \quad , \qquad (3.1)$$

where I_{DS} is the channel current, V_G the gate voltage, L the channel length, q electron charge; μ_p the hole mobility, p_0 the initial hole density in the active layer, t the thickness of the conducting layer, V_p and $V_G{}^{eff}$ are the pinch-off voltage and the effective gate voltage, respectively; V_{offset} is an offset voltage due to potential drops at interfaces; C_i is the effective gate capacitance per unit area of the channel. To obtain stable device performance shown in **Figure** 3.2**(**e), the hole mobility and gate capacitance should be unchanged at different bending radius.

Since the temperature of our surrounding environment changes with time, biosensors may show error signals in wearable applications if the devices are temperature sensitive.[130,131] The fiber-based OECT was characterized in a PBS solution at temperatures from 0 to 80 °C, which corresponds to the suitable temperature range for biological environments[132] (**Figure** 3.3)**.** The transfer curve of the device shifts slightly to a higher gate voltage with the increase of temperature, which can be attributed to the increased pinch-off voltage V_p of the device. Considering more holes can be activated to the conductive states at a higher temperature, it is reasonable to find the increase of pinch-off voltage with the increase of temperature.[133] Notably, the transfer curve has little change in the shape and shifts for only about 80 mV in

the temperature range between 0 and 80 °C, which can be easily calibrated in the data analysis of practical applications.

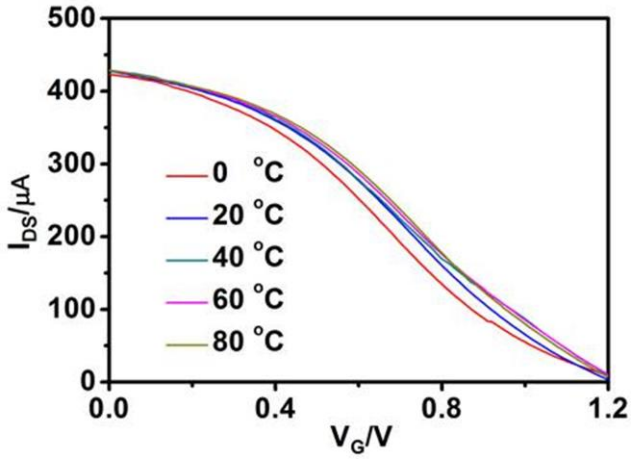

Figure 3.3. Transfer characteristic (I_{DS} *vs.* V_G) of a fiber-based OECT measured at different temperatures (from 0 to 80 °C). The V_{DS} is 0.01 V.

3.4 Routes to highly sensitive and selective OECT biosensor

Figure 3.4**(**a) shows the sensing mechanism of a fiber-based OECT used as a biosensor. The gate voltage is applied to the two electric double layers (EDLs) on the surfaces of channel and gate, respectively. The interaction of the analyte with the gate or channel will change the potential drop at an EDL and lead to the change of the effective gate voltage V_G^{eff}.[82,86] In this chapter, we only demonstrate the detection of analytes (i.e. glucose, UA, and DA) that have interactions with gate electrodes. A similar effect can be observed if an analyte has an interaction with the channel of an OECT.

First, the fiber-based OECTs are used as glucose sensors by modifying the Pt gate electrodes with the composite of enzyme glucose oxidase (GOx), chitosan (CHIT)

and graphene flakes on their surfaces.[111] **Figure** 3.4**(**b) shows the responses of a fiber-based glucose sensor (diameter: 0.3mm) to different glucose concentrations in a

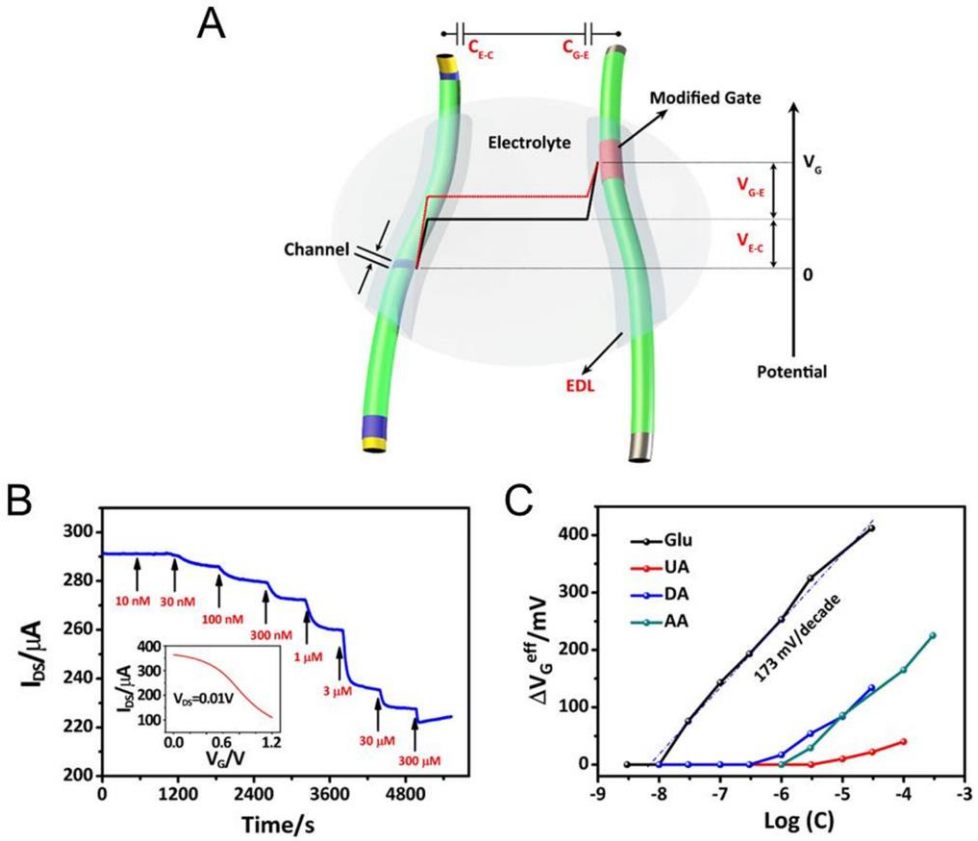

Figure 3.4. (a) Schematic of a fiber based OECT operated in an electrolyte with potential drops across two electric double layers (EDL). (b) Current responses and (c) the corresponding effective gate voltage changes of a fiber-based OECT to the additions of glucose (Glu) with different concentrations. Major interferences including uric acid (UA), dopamine (DA) and ascorbic acid (AA) were tested with the same device. V_{DS} and V_G were fixed at 0.01V and 0.6V, respectively. Inset: Transfer curve (I_{ds} versus V_G) of the OECT measured in PBS solution.

PBS solution. The channel current of the device decreases with the increase of glucose concentration and shows a detection limit as low as 30 nM. As shown in **Figure** 3.4**(**c), the sensor demonstrates a linear response of ΔV_G^{eff} (173 mV/decade) to the consecutive additions of glucose in a wide concentration range (*C*) from 30 nM, which covers the physiological glucose levels in human body fluids, such as

saliva, and thus holds great potential for no-invasive glucose sensing applications.[111] The glucose sensors were prepared on fibers with different diameters (D = 0.08mm, 0.15mm and 0.50mm). It is reasonable to find that all devices showed similar

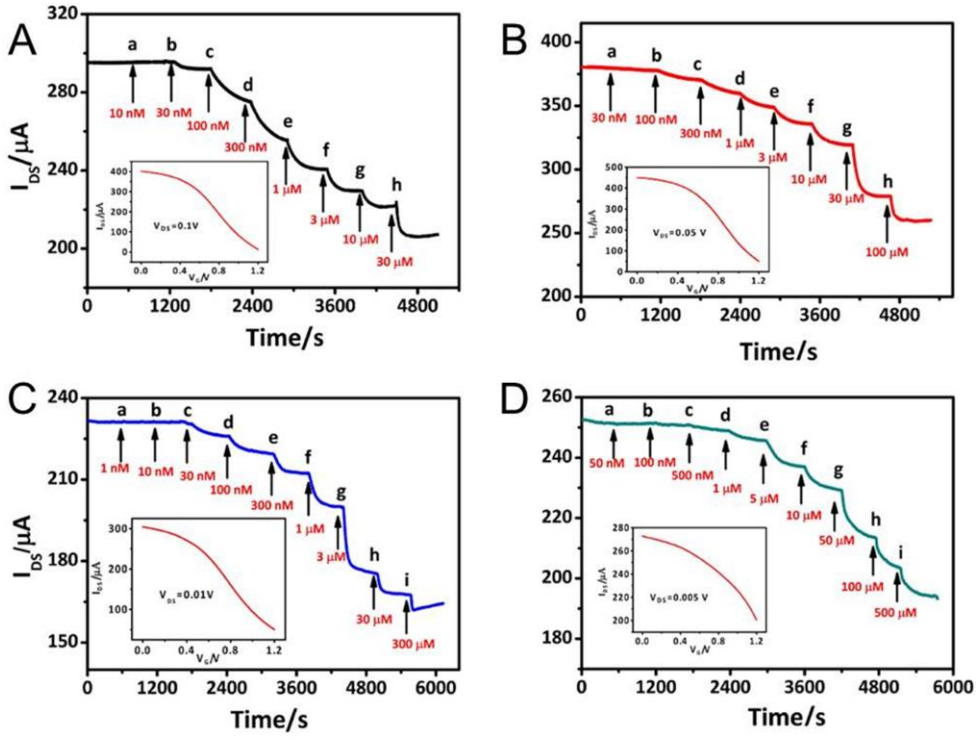

Figure 3.5. Current responses of OECT glucose sensors assembled on fibers with diameters of (a) 0.08 mm; (b) 0.15 mm; (c) 0.30 mm, (d) 0.50 mm. The inset of each figure shows the transfer curve of the corresponding device. To maintain similar channel current, V_{DS} presented in the insets increases with the decrease of fiber diameter.

detection limits to glucose concentrations (**Figure** 3.5).

Selectivity is another essential parameter for biosensors in practical applications. In practical applications, the error signals caused by biological interferences in human body, such as UA, DA, and ascorbic acid (AA), should be much lower than the effective sensing signals. As shown in **Figure** 3.4**(**c), the detection limit to glucose is nearly two orders of magnitude lower than that to the three interferences and the

device response (ΔV_G^{eff}) to glucose is much higher than those to the interferences. Besides the effect of the enzyme GOx on the selectivity of the device, the modified polymer CHIT on the fiber gate electrode actually served as an effective blocking layer for interferences.[134] The negatively charged CHIT layer in PBS could repel the interferences in anionic states, such as UA and AA, due to the electrostatic force.

Based on similar multilayer modification strategies on gate electrodes, fiber-based OECTs could also be used for many different types of biosensors. A fiber-based OECT is used for high-performance UA detection. To simultaneously improve the sensitivity and selectivity of the device, the gate electrode was functionalized with a multilayer of Nafion-graphene / polyaniline (PANI) / uricase-graphene oxide (UOx-GO). **Figure** 3.6(a) and (b) shows the performance of a fiber-based OECT for UA sensing. The detection limit to UA is about 30 nM, which is similar to that of a planar device reported before.[85] In addition, the device demonstrated a stable linear response to UA (91 mV/decade) in the concentration range from 30 nM to 300 μM. The modified Nafion-graphene/PANI double layers could effectively block the interferences and thus significantly reduce the error signals. The detection limit to UA is about two orders of magnitude lower than its biological interferences, including AA, DA, and glucose. Similarly, highly sensitive and selective DA sensors can be realized by modifying the Pt gate electrodes with Nafion/graphene on the surface. Graphene flakes can induce the electrochemical reaction of dopamine on the gate.[112,113] As shown in **Figure** 3.6(c) and (d)**,** the detection limit of the fiber device to DA is about 10 nM and a good selectivity is demonstrated. Therefore, OECTs fabricated on flexible fibers are a very promising platform for various biological sensing.

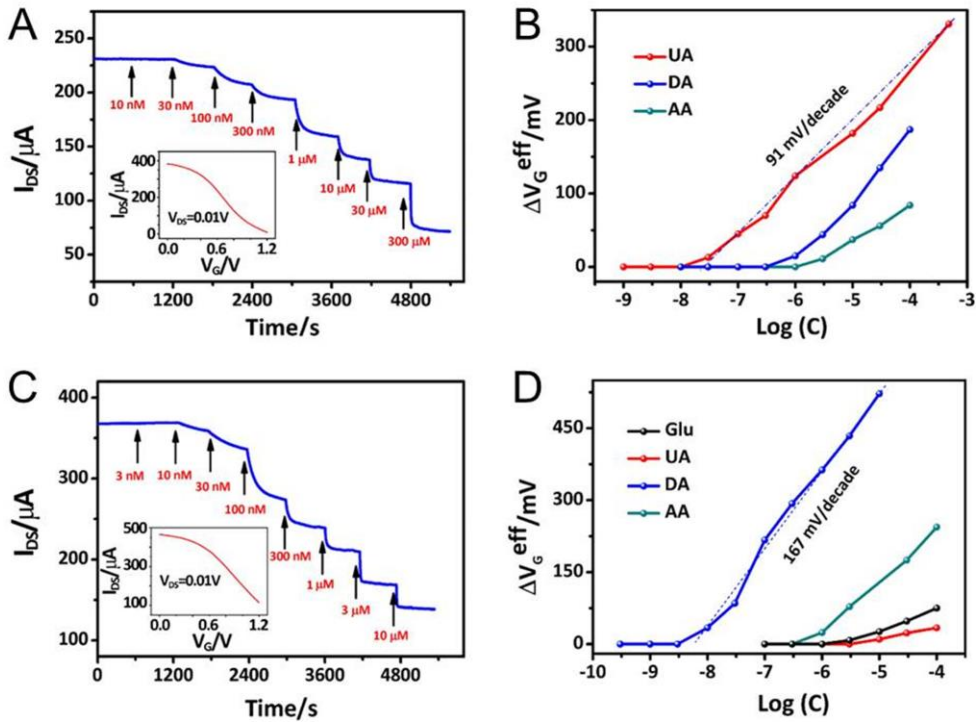

Figure 3.6. Flexible fiber-based OECTs used as a versatile sensing platform for the detection of uric acid (UA) and dopamine (DA) sensing. (a) Current responses and (b) corresponding effective gate voltage changes of a fiber-based OECT UA sensor with a UOx/PANI/Nafion-graphene/Pt fiber gate electrode to additions of UA with different concentrations. (c) Current responses and (d) corresponding effective gate voltage changes of the fiber-based OECT DA sensor with Nafion-graphene/Pt fiber gate electrode. The V_{DS} and V_G are equal to 0.01 V and 0.6 V, respectively.

3.5 Integration of fabric biosensors and its wearable application

Due to the excellent flexibility and bending stability of the fiber-based OECTs, we attempted to weave the devices with cotton yarns by using a typical weaving machine (**Figure** 3.7). We used the fiber devices as both warp and weft in the weaving process, as shown in **Figure** 3.8**(**a). The fabric devices will be rubbed by yarns very frequently during weaving process especially when they are used as warp,

which will inevitably degrade the device performance.[40] To protect the devices during the weaving process, we wrapped a layer of water-soluble polyvinyl alcohol (PVA) yarns on the surface (**Figure** 3.8**(**b)), which can be easily dissolved by water after weaving. **Figure** 3.8(c) shows a 10 cm×10 cm fabric woven with two OECT sensors. The prepared fabric is extremely flexible, stretchable and fully recoverable after several hundred times of stretch.

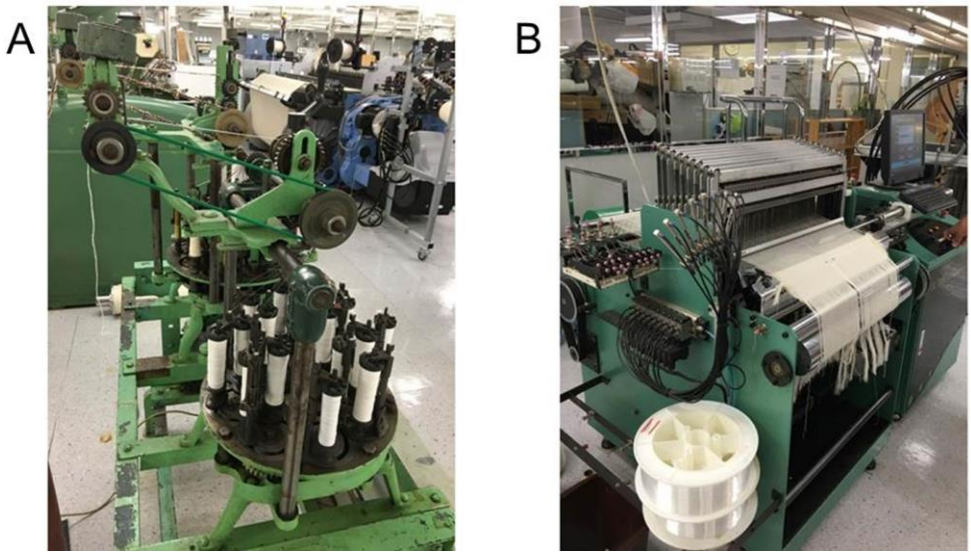

Figure 3.7. (a) Picture of the braiding machine used to wrap up OECTs fiber device with PVA yarns. (b) Picture of e CCI tech automatic dobby sampling loom system used to weave the integrated fabrics.

Figure 3.8**(**d) shows the device performance of an OECT before and after the weaving process. The two transfer curves of the device can be hardly discriminated, indicating that the device performance is very stable during the weaving process. The fabrics embedded with fiber-based OECT sensors were successfully used for the analysis of glucose levels in a PBS solution. The fabric device was placed in a PBS solution with additions of glucose of different concentrations. The channel current decreases with the increase of glucose concentration and an obvious current response can be observed at the concentration of 30 nM (**Figure** 3.8**(**e)), which is similar to the detection limit of the fiber-based device before weaving. Notably, the fabric

glucose sensor shows a fast response to the addition of glucose, indicating that the aqueous solution can diffuse into the fabric very quickly.

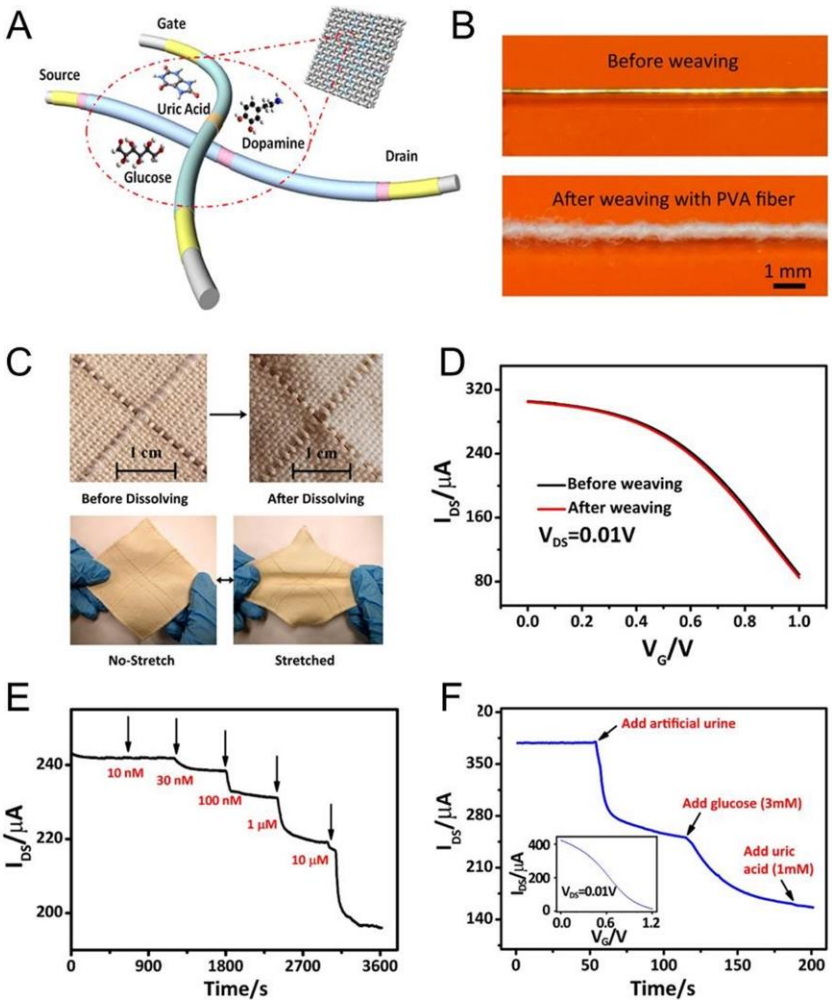

Figure 3.8. (a) Design of flexible fabric OECT sensors by weaving fiber-based devices with cotton yarns. (b) Photos of a fiber before and after weaving with PVA protecting layer. (c) Fabric devices before and after the removal of PVA protecting layer on fibers. (d) Transfer curve of an OECT glucose sensor before and after the weaving process. (e) Current responses of a fabric glucose sensor to additions of glucose with different concentrations. (f) Current responses of fabric glucose sensor integrated in a diaper to the additions of artificial urine, 3mM glucose solution and 1mM uric acid solution.

To demonstrate its practical application, we integrated a fabric OECT into a diaper and used it to detect artificial urine absorbed by the diaper (**Figure** 3.9(a)).[121] Due to

the flexibility and lightweight, the fabric OECT was hardly conceived in the diaper

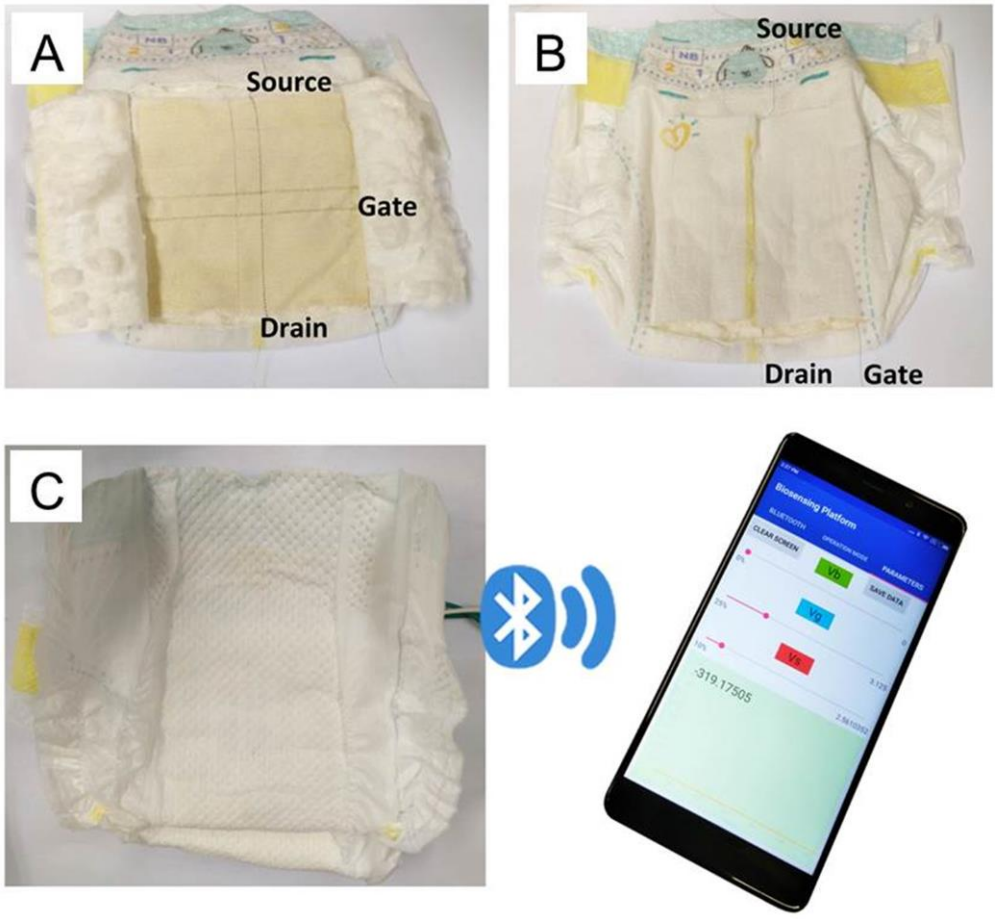

Figure 3.9. Images of a fabric OECT glucose sensor with functionalized gate electrodes assembled into a kid's diaper for glucose detection. (a) The picture of a typical kid diaper and the textile-based OECT glucose sensor (9 cm X 9 cm) (b) The diaper with the embedded textile sensor and three connective wires. (c) The illustration of fabric glucose sensor controlled by a mobile phone through bluetooth.

(**Figure** 3.9(b)). The device was characterized and controlled by a mobile phone via a Bluetooth-integrated circuitry. The signals from the fabric OECT can be conveniently recorded by the mobile. As shown in **Figure** 3.8**(**e), the device showed very stable performance before we added artificial urine. The channel current showed an obvious response when 20 mL artificial urine was dropped on the diaper, indicating that the gate voltage was applied on the channel via the solution in the

diaper. Then 10 mL glucose solution was added on the diaper, which induced a noticeable decrease of the channel current of the device. The average glucose concentration in the diaper is estimated to be 3 mM, which is the threshold value for glucosuria.[122] So the urine of diabetes patients can be conveniently monitored by using the fabric OECT glucose sensor. To show the selectivity of the device, we also added 1mM uric acid in artificial urine, which is a reasonable level in human urine.[123] We can find that the addition of uric acid did not result in an apparent response of the device. So interferences in urine will not influence the signal from the glucose sensor.

Considering the practical measurement conditions, we bent and stretched the diaper for many times during measurements and little influence on the device performance can be observed, indicating that the relative movements of the fibers in the diaper will not change the device performance. According to the device physics of OECTs, the performance of an OECT can be influenced by the double-layer and volumetric capacitances on its gate and channel, respectively, as well as the ionic conductance of the liquid between the gate and the channel.[133,135] Here, the ionic conductance of the artificial urine (ion concentrations > 100 mM) is high enough if we compared it with our recent work on the effect of ion strength.[126] Thus, stable device performance relies on the contact of the liquid with gate and channel regions. In the fabric device, because all fibers are hydrophilic, the liquid can be absorbed by the fabric due to a capillary effect and has full coverage on the OCET fibers, which is the primary reason for the stable performance of the fabric OECT even when relative movements of the fibers occur. On the contrary, a planar OCET integrated into a diaper cannot show stable performance during bending tests. For the planar device, the liquid can flow on its surface and may change the contact area on the channel and gate. On the other hand flowing liquid may induce a streaming potential between gate and

channel.[136] Consequently, the device performance of the planar OCET becomes unstable during bending tests. Therefore, the fabric OCETs show a distinct advantage over planar devices in the analysis of dynamic aqueous solutions. Obviously, the fabric sensors can be conveniently used in the analysis of body fluids, like sweat, saliva, urine, and tears, in wearable electronic systems.

3.6 Summary

In summary, robust and flexible fiber-based OECT biosensors are fabricated on nylon fibers. By introducing a Cr/Au/PEDOT:PSS core-shell structure for the source and drain electrodes, the devices show excellent bending stability and are woven as both warp and weft by using a typical weaving machine with no change in the device performance before and after the weaving process. The fabric devices are flexible and stretchable and successfully used to detect the glucose level of artificial urine contained in a diaper. We notice that the fabric device is particularly suitable for wearable applications because aqueous solutions like body fluids can be absorbed by the fabric due to capillary action, which leads to stable performance of OECTs at different bending status. This work opens a window of using fiber-based OECTs in the analysis of body fluids via remote control and paves a way of integrating the multifunctional devices into a cutting-edge noninvasive wearable electronic system.

Chapter 4 Dual gate organic electrochemical transistors for wearable bioelectronics

4.1 Introduction

Wearable sensors have been widely used for monitoring of physical signals (heart rate, respiration rate, skin temperature, etc.) and biochemical/chemical elements (glucose, lactate, sodium ion, potassium ion, etc.).[11,12,33,51,137] They can provide real-time monitoring of personal health state as well as physical fitness of athletes.[138] Currently, most commercially available wearable products have been popularly used for physical signal monitoring. Although some chemical/biochemical sensing applications have been reported, the wearable sensor still needs long waiting time to reach test stabilization and get test result.[3] Furthermore, the design of wearable sensors is complicated, and sensitivity and selectivity of the sensor are barely satisfied.[34]

OECTs have gained much attention in wearable sensing technologies due to their intrinsic signal amplification ability and good interface between conductor and biology.[23] A typical OECT consists of an organic semiconductor channel, which can be gated through electrolyte solution via a gate voltage.[81] The ions in solution are pushed in/out the entire volume of the channel under the gate potential to dope/de-dope the channel, thereby modulating the channel conductivity. Therefore, the OECT can serve as an ion-to-electron converter with high gain at relatively low voltage (less than 1 V). The OECT has been widely used for different highly sensitive sensing applications, including physical signal sensing,[95,97] chemical,[83,85] ions,[109] cell barrier,[115,116] protein,[89] DNA,[86,139] and RNA sensing.[140]

The merits of high sensitivity and low detection limit of the OECT sensors can guarantee its superior biosensing performance in personalized and wearable healthcare management to decrease the cost and resource utilization of current centralized diagnostics.[24,141] The detection limit of the OECT senor to glucose can be down to 30 nM, and non-invasive detection of glucose level in the saliva was realized.[85] The fabric OECT device is also developed and used for wearable glucose detection in artificial urine. The trace element, cortisol, a hormone of human body, can be efficiently detected by wearable OECT senor integrated with microcapillary PDMS well and molecularly selective nanoporous membrane.[70] The drawbacks of the OECT sensors used in current wearable applications are their long stabilization time and instability of the channel current after gating with gate voltage which could decrease the sensors detection accuracy and wearability.

Measurement of sweat composition is a useful way to monitor the chemical and biological signals which can be used as an indicator of individual health state. Glucose is an essential component in sweat which is correlated with blood glucose level .[8] By using a wearable sensor, the glucose level of the diabetics can be noninvasively monitored and managed, thus maintaining a better life quality than those with daily fingertip prick and blood collection. Furthermore, the real-time and non-invasive monitoring of glucose levels can provide predictive healthcare and help to manage the patient health status.[142] Currently, sweating is usually induced under medium physical exercise or iontophoresis, and the induced sweat is collected and further detected by different wearable sensors.[12,43] It is a grand challenge to realize wearable sweat detection in sedentary environment through a safe way due to low sweating rate and inefficient sweat collection strategies.

Here, we present a wearable OECT-based biosensor that can realize quick stabilization of response signal and quick detection of target analyte at high

sensitivity. We found that the stabilization time of the channel current under certain gate voltage can be tuned by varying the channel dimensions. The dual gate configuration is utilized in the design of the sensor to increase sensor selectivity. After performing gate modification, the sensor is used for quick glucose detection with high sensitivity and selectivity. The efficient sweat collection strategy is reported by integrating super hydrophilic textile and thin PDMS well with the OECT device. The resulting sweat biosensor worn on a fingertip can collect enough sweat in several minutes for sweat analysis due to the super hydrophilicity of the textile. The glucose level in sweat can be real-time and wirelessly detected and analyzed by a mobile meter though the custom-made app on a mobile device. Therefore, the advantages of the dual gate OECT in quick and wearable sweat glucose detection can make it possible to use the device for versatile wearable applications in the future.

4.2 Experimental section

4.2.1 Materials

The flexible PET film (thickness: 0.2 mm) was obtained from Servtek Materials Technology (Guangzhou) Co., Ltd. Dimethyl sulfoxide, glycerin, and dodecylbenzenesulfonic acid (DBSA) were all purchased from Sigma-Aldrich, Inc. and used as received. Lactic acid, urea, and ascorbic acid were purchased from J&K Scientific (Hong Kong) Ltd. AZ5214 and SU-8 2002 photoresists were purchased from MicroChem Corp. and kept away from direct light. Silicone elastomer kit (Sylgard 184) was purchased from Dow Corning, and the base elastomer and curing agent were mixed with a weight ratio of 10:1 and cured at 70 ^{o}C for 2 to 3 hours to form a solid PDMS for further use.

4.2.2 OECT device fabrication

A typical OECT microfabrication process included the deposition of metal, PEDOT:PSS, and insulation layer, through multi-layer photolithography. PET film was annealed at 120 ^{o}C for 1 hour to promote polymer chain reorganization and decrease its deformation during further fabrication process. Then, the film was thoroughly washed by sonication with acetone, deionized water, and isopropyl alcohol, receptively, followed by blow-drying with high purity nitrogen. AZ5214 photoresist was coated on the film and exposed under ultraviolet by using Karl Suss MA6 Mask aligner. The exposed film was developed in AZ 300K developer to define the pattern of metal pads, interconnects, and source/drain contacts of the OECT. Then Cr (~10 nm)/Au (~100 nm) electrodes were deposited on the defined pattern of the film by RF magnet sputtering and lift-off in acetone. The dual Pt gate electrodes (~90 nm) were patterned and deposited through a similar process. The channel area was then patterned through another photolithography process. The PEDOT:PSS aqueous solution supplemented with 5% dimethyl sulfoxide, 5% glycerin, and 0.25% DBSA, was coated on the patterned channel area of the film and annealed at 110 ^{o}C for 20 minutes to form a thin PEDOT:PSS layer. The PEDOT:PSS pattern was subsequently defined through further lift-off process. Finally, the device was packed with SU-8 2002 negative photoresist through photolithography process to expose the channel and dual gate area.

4.2.3 Gates modification strategies

The inner and outer gates of the OECT device were modified with functional polymers and functional polymers/enzyme, respectively, to fabricate the highly sensitive biosensor as previously.[83] The details were as follows: The two gates were

first coated with one thin layer of nafion (5 mg/mL) to block interference of most negative molecules. Then polyaniline solution (10 mg/mL) was cast on the nafion-coated gates to increase the specific area of the gate electrodes to promote enzyme loading. The outer gate (enzymatic gate) of the device was coated with glucose oxidase (10 mg/mL) in PBS solution and dried in the humidified environment at 4 ^{o}C. The inner gate (control gate) of the same device was coated with PBS solution and dried in the humidified environment at 4 ^{o}C. Finally, the enzyme on the gate was immobilized by drop casting chitosan acetic solution (5 mg/mL; acetic acid: 50 mM). The modified device was stored in a humidified environment at 4 ^{o}C for further use. Before sensing measurements, the device was rinsed with PBS solution to remove the unanchored enzyme.

4.2.4 Sweat absorption layer design and device assembly

The sweat absorption layer consisted of a two-layer structure, one superhydrophilic textile layer, and one thin PDMS well layer. The superhydrophilic textile was purchased from CoolMax®. As shown in **Figure** 4.1(a), the textile was finely tailored to fit the area of the channel and two gates (about 0.5 cm^2) and adhered to it by sealing the textile edge. Then the thin PDMS well with microfluidic channel was bond with the textile to form the sweat absorption layer (area: ~1.5 cm^2). Finally, it is bonded to the OECT device by using the inherent adherence of PDMS. The as-prepared device was stored in 4 ^{o}C for further wearable applications.

4.2.5 Device characterization

The OECT devices with different channel length (10 μm, 30 μm, 60 μm, and 100 μm) were fabricated and checked under a Leica microscope (DM1750M). The ratio of width to length of the channel was fixed at 4 for all devices. The PEDOT:PSS film

thickness can be adjusted by changing the spin speed during the PEDOT spin coating process or changing the formulation of the PDDOT:PSS solution. The measurements of transfer curve and real-time channel current response (certain gate voltage) were performed by two source meters (Keithley 2400) controlled through a Labview program in a laptop. For the measurement of transfer curve of a device, drain-source voltage (V_{DS}) was fixed at 0.05 V, and the channel current was measured with the sweeping of gate voltage (V_G) from 0 to 1 V. For the real-time channel current response measurement, PBS solution was added on the channel area of the devices with different channel dimensions. For the glucose level measurements, the channel current response of the dual gate OECT device was first measured under control gate voltage during the addition of PBS with certain concentration of glucose solution, and then the gate voltage was switched to the enzymatic gate after the stabilization of the channel current. The current change was recorded after switching gate voltage from the control gate to the enzymatic gate and converted into effective gate voltage change (V_G^{eff}). The V_G^{eff} can be regarded as the indicator of a particular concentration of glucose solution. By using this method, different concentrations of glucose solution can be measured as a function of V_G^{eff}. The interferences, lactic acid, urea, and ascorbic acid are also added in PBS solution during channel current response measurement to confirm the selectivity of the dual gate device.

4.2.6 Mobile meter design and wearable measurements

The portable meter consisted of four main modules: central microprocessor, analog to digital circuits (ADC), digital to analog circuits (DAC), and Bluetooth module. The integrated device connected to the portable meter was worn on the fingertip or forearm to perform wearable sweat glucose detection. The channel current response of the device on the skin was monitored by the custom app on a mobile device.

4.3 Response time *vs* channel dimension

Figure 4.1(a) shows the basic illustration of a dual gate OECT based on PEDOT:PSS, one widely used p-type organic semiconductor,[143] which can be gated by the outer gate and inner gate through electrolyte to realize the de-doping process.[126] A voltage (V_D) is applied between the drain and source electrodes (channel) on which PEDOT:PSS film is spin-coated and the channel current (I_D) of the OECT is monitored. Two same voltages (V_{G1} and V_{G2}) are applied on the two platinum gates, respectively. Two switches connected to the two gates are switched off during the initial state. Then the

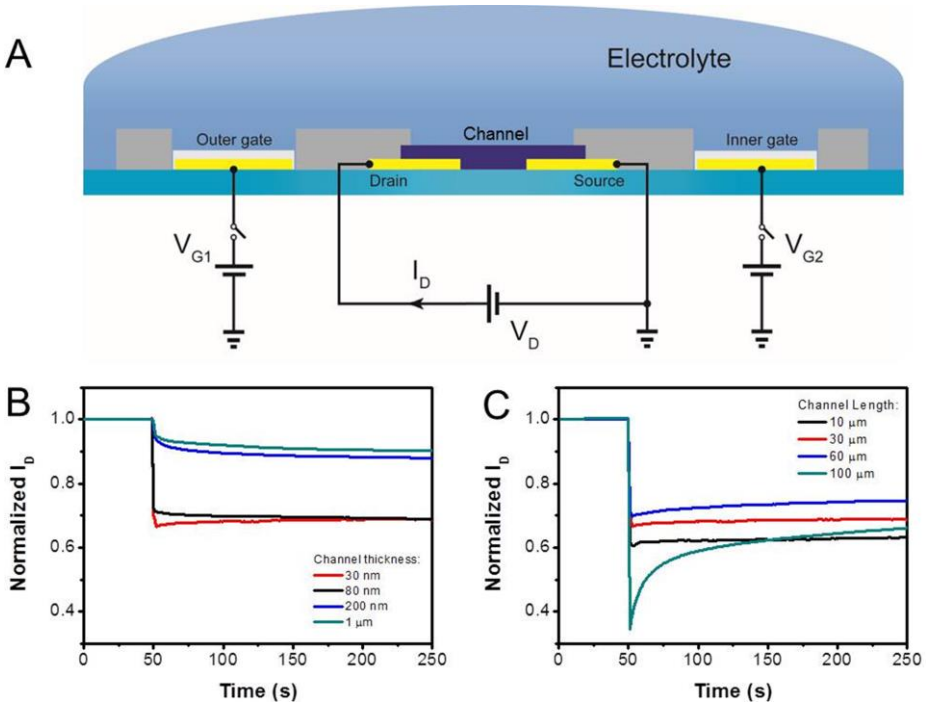

Figure 4.1. (a) The illustration of a dual gate OECT, showing the source, drain, two gates electrodes, and electrolyte. The effect of the channel thickness (b) and channel length (c) of OECT on the stabilization time of the channel current of OECT after adding PBS solution (the first dropping point of the curves) For Figure b, the devices have a channel length (L) 30 mm and channel width (W) of 60 mm. For Figure c, the channel thickness is fixed at 30 nm. The V_D (drain voltage) and V_G (gate voltage) are fixed at 0.05 V and 0.3 V, respectively.

inner gate voltage is turned on and electrolyte is dripped on the device to cover the sensing area of the device. The cations in electrolyte are injected into the entire volume of the channel which can compensate the counter ions (PSS^-) in the PEDOT:PSS film and de-dope it, therefore decreasing the conductivity of the channel. In further biosensing experiment, the outer gate voltage is turned on and the inner gate voltage is turned off after the channel current gets stable. The channel current change after the gate voltage switching can be regarded as an indicator of a specific analyte level if the two gates are further modified with the functional polymers and corresponding enzyme. Details of the dual gate OECT advantages will be discussed later in this chapter.

To study the effect of channel dimensions on the stabilization of channel current of devices after applying a gate voltage of 0.3 V, we choose four types of channel thickness: 30 nm, 80 nm, 200 nm, and 1 μm, respectively. The channel length for the above four kinds of devices is 30 μm and only one Pt gate is used during the characterization of the channel current response time to their dimension. The profile curves of PEDOT:PSS film at different fabrications conditions are shown in **Figure** 4.2. It is noteworthy that the PEDOT:PSS films behave the coffee ring effect and this phenomenon is more prominent for thicker film because more solute needs to be deposited on the channel. Therefore, the thickness stated in the previous context is an estimative thickness at different spinning speed (6000 rpm, 1500 rpm * 2, 500 rpm * 2, and drop cast). The two response behaviors of the channel current for four kinds of devices can be observed in **Figure** 4.1(b). The gradual current decay for thicker channel devices and the spike-and-recovery channel current for thinner channel device are presented after applying gate voltage of 0.3 V. This is consistent with the previous report, and transient behavior of channel current can be determined by:[133]

$$I(t, V_G) = I_D(V_G) + \Delta I_D \left(1 - f\frac{\tau_e}{\tau_i}\right) \exp(-\frac{t}{\tau_i}) \qquad (4.1)$$

I_D is the channel current at steady-state and fixed gate voltage (V_G) and $\Delta I_D = I_D (V_G = 0) - I_D (V_G)$. f is geometric factor (it can be considered as ½ when $V_G >> V_D$). τ_e and τ_i are electronic and ionic transit time, respectively, where $\tau_e = L^2/\mu V_D$ (L is channel length, μ is the mobility of PEDOT:PSS film), $\tau_i = C_d \bullet R_s$ (Cd is the device capacitance, and Rs is the resistance of electrolyte). According to **Equation** 4.1, the transient channel current response to the applied voltage (V_G = 0.3 V) can be a spike-and-recovery curve ($f\tau_e > \tau_i$) or be a monotonic decay curve ($f\tau_e < \tau_i$). The electronic transit time can be considered as a constant in this circumstance. The ionic transit time is proportional to the capacitance of the device. According to the capacitance equation: $C = \varepsilon_0 \bullet A/d$, the capacitance of channel increases with the increase of the film thickness since the area of the film increase substantially due to its thickness increase and porous structure. The geometric factor (f) is approximately ½ due to $V_G >> V_D$ (V_G = 0.3 V, V_D = 0.05 V, respectively). We can find that the transient response of channel current shows a monotonic decay at a thinner thickness of the channel (30 nm). With the increase of the channel thickness, the transient response of channel current transforms from monotonic decay to spike-and-recovery behavior. As shown in **Figure** 4.1(b), the monotonic decay behaviors of the device with the channel thickness of 200 nm and 1 μm show longer waiting time to reach a relatively stable state than that with channel thickness of 80 nm as well as the spike-and-recovery curve behavior of device with channel thickness of 30 nm. It can also be found that the device with the thinnest channel can quickly reach stable state after applying the gate voltage. It is also useful for quickly ion exchange of porous channel during volumetric doping and de-doping process.

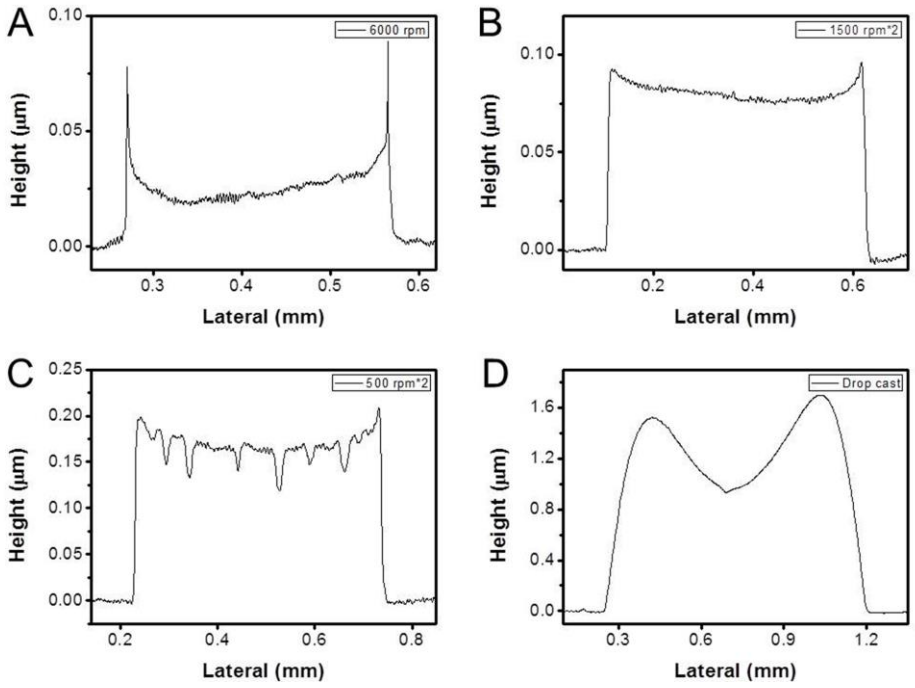

Figure 4.2. The profiles of PEDOT with different thickness: (a) 30 nm, (b) 80 nm, (c) 180 nm, and (d) 1 μm.

Four types of channel length (10 μm, 30 μm, 60 μm, and 100 μm) are chosen to further check their effects on the stabilization of the channel current. The channel thickness for all devices is 30 nm since it can realize a quick response and stabilization of the channel current of a device. As shown in **Figure** 4.1(c), the spike-and-recovery response of channel current is observed in all kinds of devices. According to equation: $\tau_e = L^2/\mu V_D$, τ_e increases with the increase of the channel length, thus enabling much more significant spikes and longer stabilization time of the channel current response. It is consistent with **Equation** 4.1 that a larger τ_e can induce a more significant spike-and-recovery response and therefore a longer stabilization time of the channel current after applying the gate voltage of 0.3 V. We can find that the stabilization time of the devices with the channel length of 10 μm and 30 μm is quite similar. So, an OECT device with 30 μm channel length is enough for quick stabilization of channel current and used for quick detection. The smaller channel length of the device, the

higher precision of the fabrication technique is required. In order to achieve the best cost-effective fabrication of the OECT device, the 30 μm of channel length and the 30 nm of channel thickness are chosen for further device fabrication unless otherwise stated.

4.4 Dual gate OECT for quick detection

As shown in **Figure** 4.3(a), the transfer curves of a dual gate device gated by its inner gate and its outer gate are nearly overlapped. It indicates that the uniformity of two gates of the device is successfully realized. The gate uniformity can guarantee less interference introduction from the device and its high accuracy by using the dual gate biosensing method. The good gate uniformity can be further confirmed by the current response of a dual gate OECT in **Figure** 4.3(b). The current change of the channel is negligible after switching gate voltage from the inner gate to the outer gate (as shown by the red arrow in **Figure** 4.3(b)).

As mentioned above, the selectivity is a critical factor of wearable biosensor because its target analytes exist in the complex environment of human body fluids.[8] The dual gate device with Pt gate electrodes is sensitive to H_2O_2 according to the anode reaction occurred on the gate:[85]

$$H_2O_2 \xrightarrow{Pt} 2H^+ + O_2 + 2e \qquad (4.2)$$

The glucose oxidase on the gate can catalyze glucose conversion into gluconolactone and is reduced in the process. Theurther redox reaction reactivates the reduced enzyme and produces hydrogen peroxide. The above redox reactions are cycled and produce more hydrogen peroxide when enough glucose exists in the solution. The produced hydrogen peroxide is catalyzed by the Pt gate electrode and oxidized into oxygen

(**Equation** 4.2), thus inducing electron transfer into the gate electrode and subsequently affecting the channel current. Glucose can be sensed according to the above reaction mechanism, and its concentration is proportional to the production of hydrogen peroxide during enzymatic redox reaction and corresponding channel current change.[82]

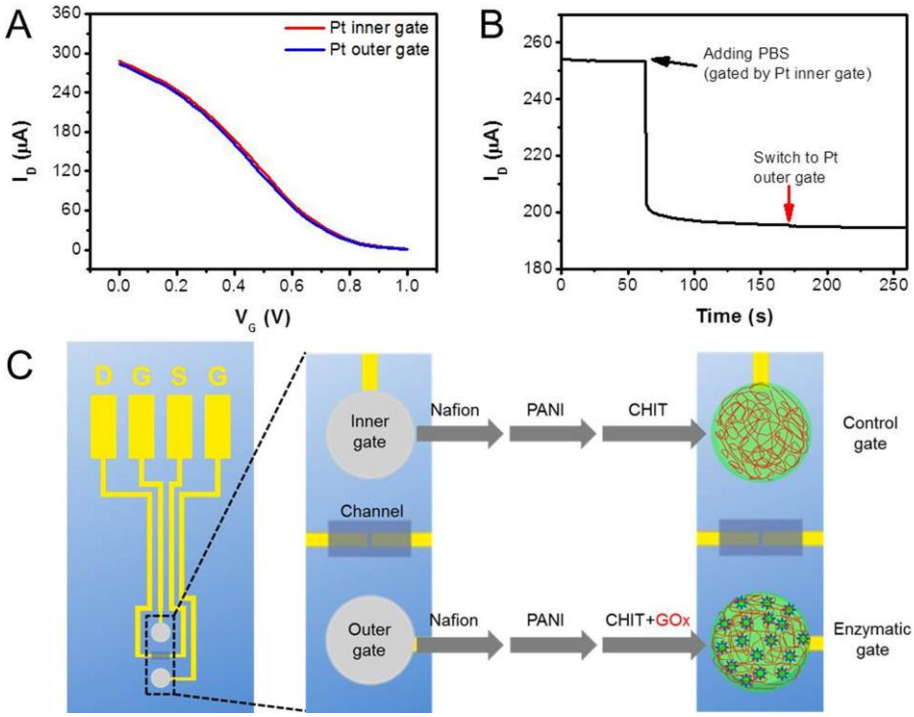

Figure 4.3.(a) Transfer characteristics of a dual-gate OECT gated by the Pt inner gate, Pt outer gate, and a Pt wire, respectively. (b) Current response of a dual-gate OECT after adding PBS solution and switching to Pt outer gate. (c) The dual-gate design of OECT and its dual-gate modification strategies used for a quick glucose detection. Polyaniline, chitosan, and glucose oxidase are abbreviated as PANI, CHIT, and GOx, respectively. Channel dimensions: W = 120 mm, L = 30 mm, and d = 30 nm. V_D = 0.05 V and V_G = 0.3 V.

During the wearable applications, the flexible biosensors can be used for sensing different analytes, such as glucose, lactic acid, and uric acid in sweat, which can provide useful information for our physiological state. However, the Pt gates of the

device can react with other analytes, like ascorbic acid, lactic acid, and uric acid, which are commonly found in the sweat.[85] The target analyte should be distinguished with minimal interference from other analytes in the analyte solution. In order to achieve specific sensing of one specific analyte, the selectivity of the wearable biosensor must be realized to perform effective biosensing in the complex body fluids. As stated previously,[83] the enzyme modification is carried out on the one gate electrode to realize highly selective detection of an OECT biosensor. The detailed procedure for dual gate modification can be found in the experiment part and **Figure** 4.3(c). Notably, the nafion film cast on the two gates of a dual gate OECT can block most negative species and larger molecules access to the surface of the Pt gates in the analyte solution. The chitosan film deposited on the two gates can provide anchors for glucose oxidase on the enzymatic gate to realize its long-term and reliable catalytic activity. Moreover, the glucose oxidase mixed with nano-materials, such as graphene, and carbon nanotube can substantially increase the catalytic activity of the anchored enzyme to increase the sensitivity of the dual gate OECT device. The control gate (without enzyme modification) of the dual gate OECT can be used to decrease the interference from other analytes in the electrolyte.

4.5 Dual gate OECT for selective and sensitive biosensing

As shown in **Figure** 4.4, the various interferences (ethanol, ascorbic acid, urea, uric acid, and lactic acid) are introduced in PBS solution to check the selectivity of the dual gate glucose sensor. We can find that the negligible channel current response is observed after adding a physiological level of interferences and switching the gate voltage to the enzymatic gate. It confirms that the selectivity of the device is successfully realized by multilayer modification strategies.

After modification to the gates, the dual gate glucose devices are used to perform calibration test, in which different concentrations of glucose in PBS solution are added on the channel and gates area of the device and the channel current change (ΔI_D) is recorded and converted to effective change of gate voltage (ΔV_g^{eff}) during the gate voltage (0.3 V) switching from the control gate to the enzymatic gate. As shown in **Figure** 4.5 and 4.6, calibration curves of glucose ranging from 1 nM to 100 μM are characterized in PBS solution. The current response of the channel shows a

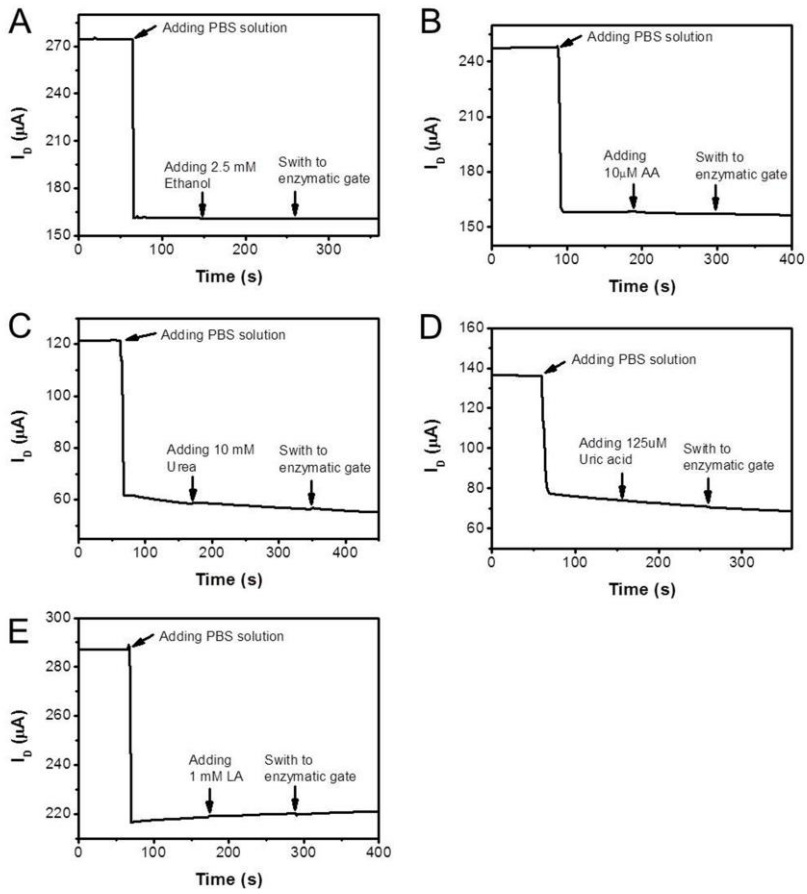

Figure 4.4. The channel current response of dual gate OECTs (glucose biosensor) to the additions of physiological level of interferences (Ethanol, AA, Urea, UA, and LA).

spike-and-recovery behavior as expected in all the calibration curves. It is consistent with the previous current response shown in **Figure** 4.1**(**c) that thin channel OECT behaves a capacitive current. We can find that the channel current can quickly reach stabilization (less than 40 s) after adding PBS solution (black arrow in **Figure** 4.5(a)). The control test (no addition of glucose in the PBS solution) shows that there is no

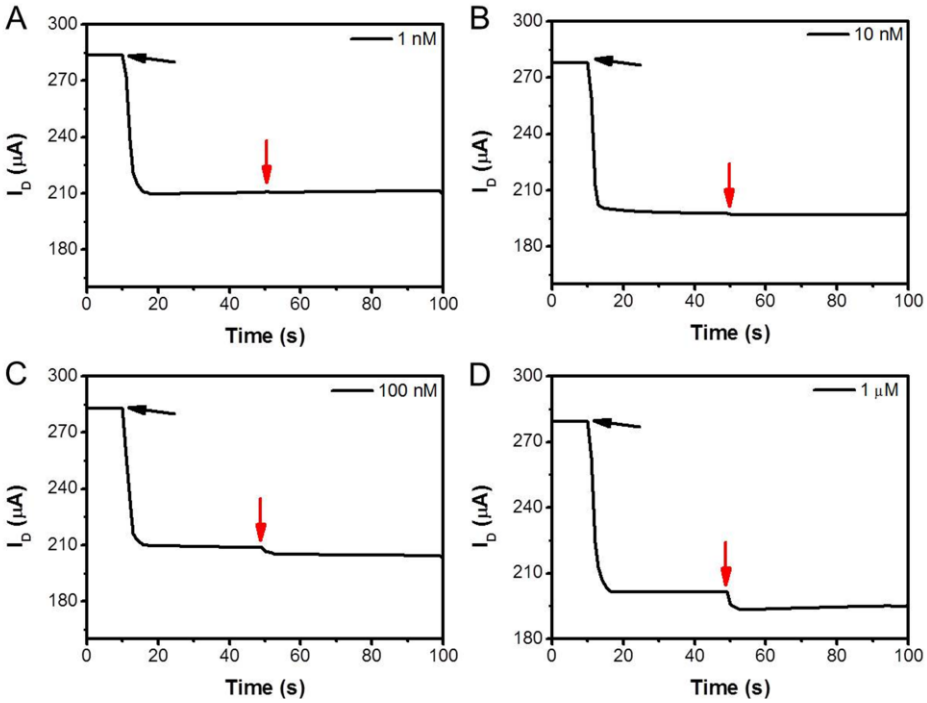

Figure 4.5. The channel current response curves of the dual-gate OECT for glucose detections ranging from 1 nM to 1 μM. The black arrows show the addition of glucose solution (gated through the control gate) and red arrows show the gate voltage switching from the control gate to the enzymatic gate.

current response after switching to the enzymatic gate (red arrow in **Figure** 4.5(a)). The dual gate OECT begins to show an obvious response after addition of 100 nM glucose solution (**Figure** 4.5(d)). The channel current quickly drops and reaches stabilization after switching gate voltage to the enzymatic gate (red arrow in **Figure** 4.5(d)). Due to the dual gate design, our device can realize the quick stabilization of channel current and quick response to the addition of target analyte solution. It solves the long waiting time of traditional single gate OECT detection technique before it

reaches stabilization (it usually takes about several hundreds of seconds). [83,85] The merits of the quick stabilization and response of the device make it possible for wearable applications, such as quick detection and real-time monitoring of physiological and biochemical parameters. Also, the current response increases with the increase of glucose concentration and reaches saturation if glucose concentration is more than 100 μM (**Figure** 4.5 and 4.6). According to **Figure** 4.6(d), the detection limit of the dual gate glucose sensor can be down to 100 nM with a sensitivity of 20.69 mV/decade.

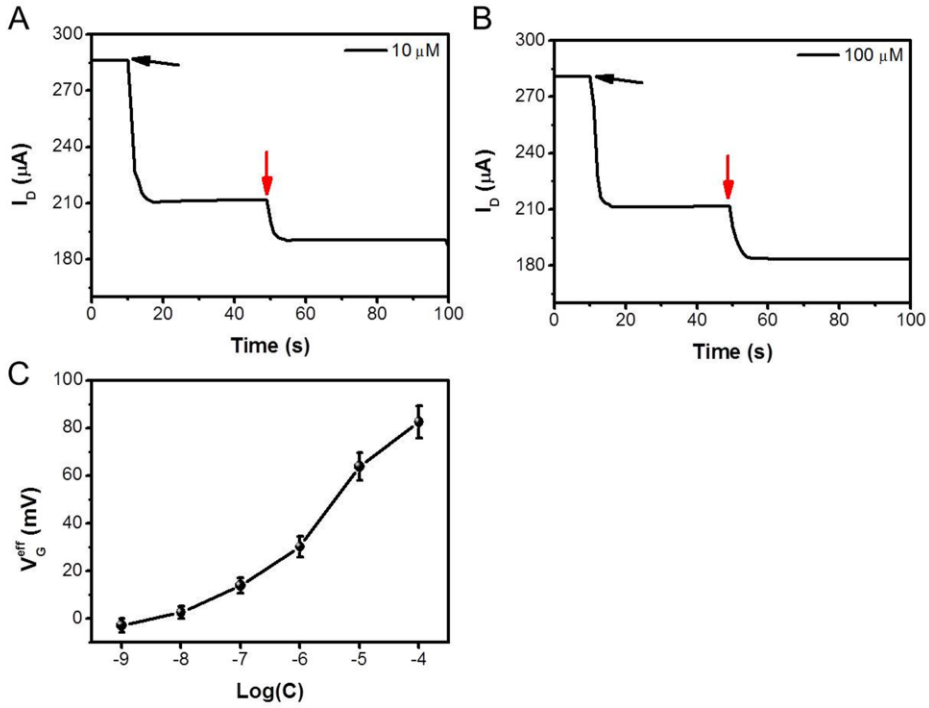

Figure 4.6. (a)-(b) The channel current response curves of the dual-gate OECT for glucose detections ranging from 10 μM to 100 μM. The black arrows show the addition of glucose solution (gated through the control gate) and red arrows show the gate voltage switching from the control gate to the enzymatic gate. (c) The effective gate voltage changes of the dual gate OECT to the additions of different glucose concentrations.

4.6 Wearable sweat biosensing of flexible dual gate OECT

The dual gate device can be worn on the wrist or fingertip as a wearable product and used for biochemical detection of sweat. However, the sweating rate is relatively slow if no external stimulus is applied to human subjects. Considering an average healthy

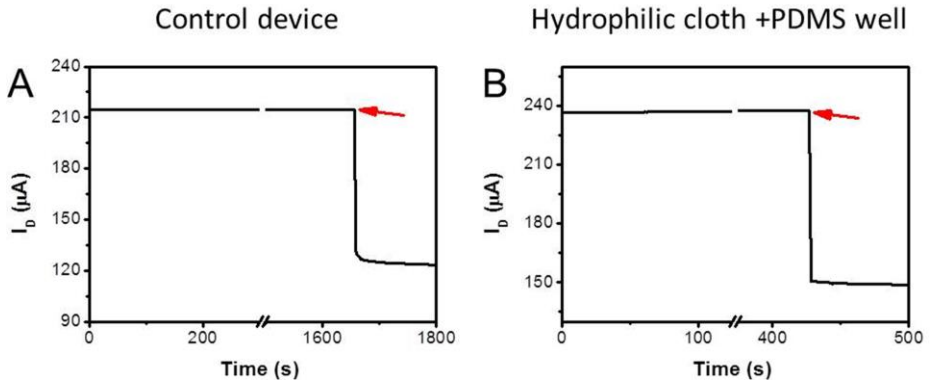

Figure 4.7. The on-body response time of the channel current of a bare dual gate device (a) and dual gate device integrated with sweat capture structure (b) to the secretion of sweat from human skin surface. The red arrows show that enough sweat has been captured by the superhydrophilic cloth in the PDMS well.

human, sweating rate ranges from 1 to 100 nL/min per gland according to their physical state with a density of ~200 glands/cm^2.[9,70] The area of channel and its adjacent two gates of a device is about 10 mm^2 and it can only collect 20~2000 nL sweat per minute when the device adheres on the surface of human skin. The collected sweat is insufficient to fully cover the gate and channel area of the device within dozens of minutes of collection time if a human is in a stationary state (more than half an hour, as shown in **Figure** 4.7(a)). In order to realize in situ efficient sweat collection and further biosensing applications, a sweat-absorbent layer should be developed to decrease the waiting time. As shown in **Figure** 4.8(a), the thin white textile is

superhydrophilic, and the other three kinds of commercial textile behave weak sweat absorption according to their contact angle against artificial sweat. The area of the channel and adjacent gates of the device is covered by the superhydrophilic textile. The remaining part of the device is covered by one thin PDMS well against skin surface. (**Figure** 4.8(b))

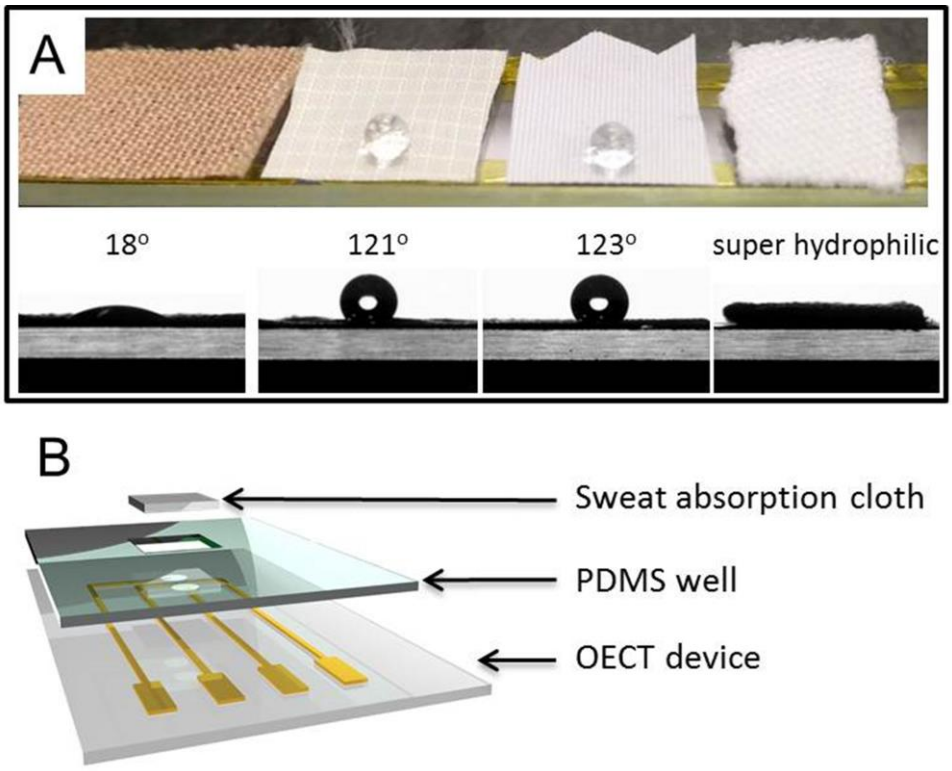

Figure 4.8. (a) The photos and contact angles of four different kinds of commercial cloth. (b) The design of sweat capture structure by combining sweat absorption layer integrated with PDMS collection well to the dual gate biosensor.

As shown in **Figure** 4.7(b), the device with the sweat-absorption layer can quickly collect enough sweat on the textile and begin to perform biosensing (less than 10 minutes). The superhydrophilic textile can quickly absorb secreted sweat by nearby glands and form sweat connection between the channel and gates underneath. Furthermore, the hydrophilic PDMS layer can repel the secreted sweat to its well through the microfluidic channel, which can accelerate the sweat collection into the

superhydrophilic textile. The integrated device can well conform to the curved skin and allows quick and selective detection of a panel of metabolites in human perspiration (**Figure** 4.9(a)). The flexible substrate integrated with the PDMS layer can guarantee stable skin-sensor contact. The integrated superhydrophilic textile avoids the direct contact of human skin with the channel and modified gates of the devices and decreases the disturbance introduced by the friction between the sensor

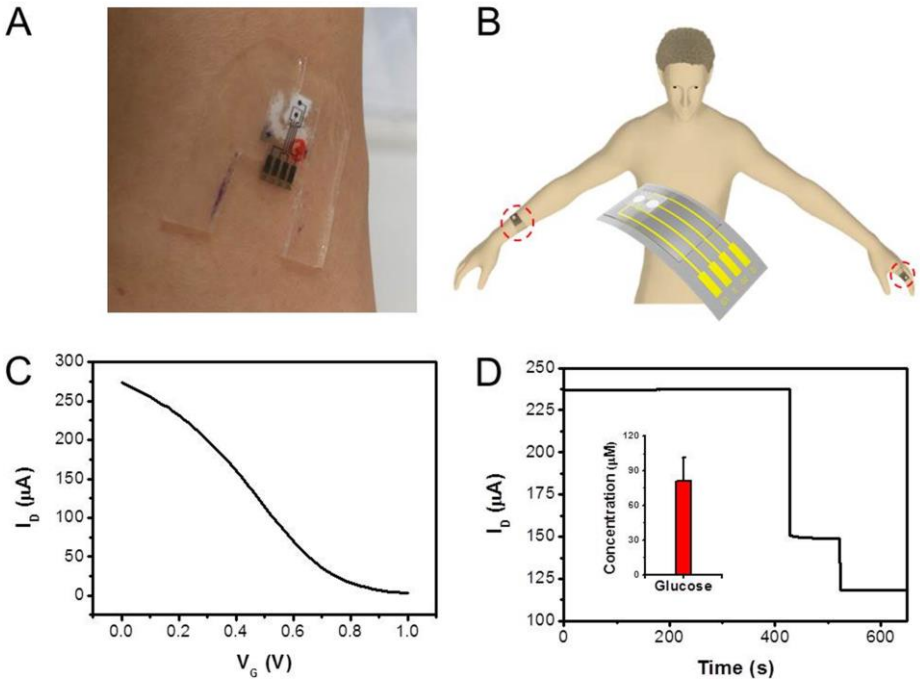

Figure 4.9. (a) The photo of an integrated dual gate device worn on a subject wrist, performing efficient sweat collection, quick and wireless detection of metabolites in human body fluids. (b) Schematic of the integrated dual gate biosensor which can be worn on the different parts of human body. The transfer curve (c) and on-body channel current response (b) of an integrated dual gate biosensor worn on the fingertip to the secretion of sweat. Inset: The deviation of sweat glucose concentration during three repeated tests.

and curved skin.

The portable meter that integrated with a microprocessor, control circuit, readout circuit, power management module, and wireless transmission module is connected to

the sensor through flexible cable and powered by a rechargeable lithium-ion battery (battery capacity: 340 mAh) at low power consumption (**Figure** 4.10). The meter can be remotely controlled by mobile phone and enable sensing data collected from the sensor transmission to the custom app with visualized interface and data logging. As shown in **Figure** 4.11, the portable meter can perform both transfer curve characterization and channel current response characterization, and the test results are hardly discriminated with those got from Keithley 2400 source meters. The accuracy and reliability of the portable meter guarantee its further integration with the dual gate OECTs.

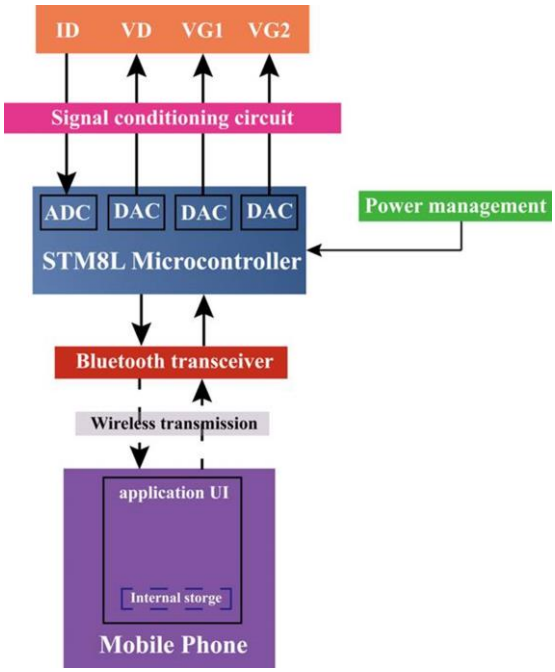

Figure 4.10. Block diagram of wearable biosensing platform.

As shown in **Figure** 4.9(b), the wearable device can be worn on the various parts of the body, such as forearm, fingertip, forehead, chest, and abdomen. The portable meter connected to the sensor can be readily put in an armband or pocket. The real-time current response of the device worn on a volunteer's fingertip is monitored by the

mobile meter and visualized on the mobile phone for the detection of sweat glucose (**Figure** 4.9(d)). It can be found that the gate voltage is not applied on the channel of the sensor in the first seven minutes as there is not enough sweat in the PDMS well to connect its channel and gates. At the time of about 420 s, the channel current decreases sharply because the superhydrophilic textile in the PDMS well has collected enough sweat and established its solution connection. Due to the novel device design, the channel current quickly reaches stabilization in a short period of time after the sharp decrease. The channel current undergoes another minor decrease after switching the gate voltage to the enzymatic gate, which can be regarded as the indicator of sweat glucose. The glucose concentration of the volunteer is about 77 μM according to its ΔV_g^{eff} (**Figure** 4.9(c)) and the calibration curve, which is in the range of healthy person sweat. As shown in the inset of **Figure** 4.9(d), the deviation of averaged glucose concentration is a little significant during the repeated test which may due to the variance of sweating rate. The wearable device can be used for sensing different metabolites, such as glucose, lactate acid, and uric acid in different human body fluids.

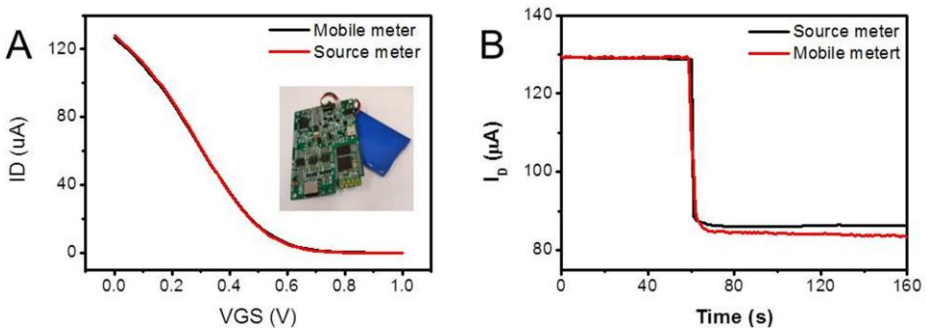

Figure 4.11. Transfer characterization (a) and channel current responses (b) of a dual gate OECT by the commercial source meters and the portable meter.

4.7 Summary

In summary, the dual gate OECT sensors enabling quick response and detection is successfully devised and used for in situ metabolite detections in human sweat. By finely tuning the dimension of the OECT channel, the channel current of the sensors can quickly reach stabilization after applying a gate voltage via electrolyte. The selectivity of the sensors to the target analytes can be increased by using the dual gate design. The dual gate biosensors can be used for selectively and sensitively detection of the target analyte in body fluids by further gates modification process. The glucose calibration curves are obtained with the detection limit of 100 nM and the detection sensitivity of 20.69 mV/decade. We can find that the dual gate sensors integrated with the sweat absorption layer and thin PDMS well can promote sweat collection during wearable applications and decrease the sensor standby time, which is particularly important in real-time detection of metabolites in body fluids. Furthermore, the integrated sensor connected to the portable meters and mobile phone enables in situ real-time and quick detection of glucose levels in sweat. By using a sensor array, the wearable and multiplex detections of human metabolites can be easily implemented in the future. The sensor array also paves the way for developing an efficient wearable system by using the quick response OECT sensor together with the fluid absorption structure and wireless module in quick and in situ analysis of metabolites in body fluids to facilitate noninvasive and personalized healthcare management and ongoing physiological and clinical investigations.

Chapter 5 Organic electrochemical transistors for ECG recording

5.1 Introduction

Wearable bioelectronics has already been emerging as a critical technique for personal healthcare systems.[1,3,10] Electrophysiological activities have been recorded with low impedance electrodes and are further processed by conditioning circuits, such as noise filters and integrated amplifiers, to obtain high-quality signals.[2,95,144] Among the electrophysiological activities, ECG signals can provide valuable information in the detection of heart-related diseases, such as arrhythmias, ischemia, and elderly heart failure.[4,11,145,146] Currently, clinical ECG signals are acquired through a 12-lead ECG recorder. The instrument is usually used for centralized measurement under the operation of experienced specialists. It is also too bulky and complicated for personal use.[148] The portable and wearable ECG devices are urgently needed in practical applications. Their long-term and wearable ECG monitoring can enhance predictive diagnostics and its potential in telehealth management.[144] At the same time, heart malfunction treatment can be provided by implanted pacemakers to extend precious rescue time during individual ECG monitoring.[147] Although some wearable ECG products, such as Zio® by iRhythm Technologies and Apple Watch® Series 4 by Apple Inc, have been used for wireless monitoring of ECG signals, the signal-to-noise ratio (SNR) and accuracy of the recorded signal still need to be increased.

The Ag/AgCl electrode is the standard electrode for high-quality ECG signal recording because of its properties of low impedance and non-polarization.[11] In order to establish good contact between human skin and recording electrodes, the ion gel,

one kind of solid electrolyte, is used to perform reliable cutaneous ECG monitoring.[148,149] Some reports presented advanced ECG recording techniques that can be used for the long term and wearable monitoring of electrophysiological activities. Pani *et al* presented a textile electrode which can be used for wearable ECG monitoring. The PEDOT:PSS-based textile electrode is biocompatible to human skin, thus decreasing its allergic reaction when performing long-term tests. The acquired ECG signal quality (according to QRS detectability, broadband noise) is comparable to that recorded by the Ag/AgCl electrode. Due to the side effect of commercial ECG patches with ion gel to human skin and its high adhesion on exceptionally fragile neonatal, some efforts have been done to develop dry electrode to realize gel-free and/or less sticky ECG sensor.[144,148] The ECG sensor tends to be integrated with other physical and/or biochemical sensors to perform multiplex sensing applications.[5,144]. By monitoring multiplex signals, such as skin temperature, breath rate, ECG signal, glucose level, etc., the device can provide more accurate healthcare management. [12,33,138] However, the two-electrode configuration is popularly exploited in the most ECG recording devices. The characteristic noise from the ambient environment compounded with a low amplitude of ECG signals poses doubts for high-quality signal recording.

Recently, organic electrochemical transistors (OECT) are emerging as an outstanding tissue-electronics interface due to its ion-to-electron transducing and good biocompatibility.[23,24] Furthermore, intrinsic amplification abilities of the OECTs make them possible for weak signal capture.[97,135,150-152] The electrophysiological signals of human body can be transduced into electrical signals and accurately recorded by the OECT device. PEDOT:PSS is commonly used in the fabrication of the OECT device (gate electrode and channel), which provides a good interface between the electrode and skin and decreases the influence introduced from motion artifact.[153,154] Campana

et al firstly demonstrated the OECT ability in ECG monitoring although high noise is observed in the recorded signal.[95] After that, different OECT configurations were further developed and used for ECG recordings.[145,146,155-158] The ultra-flexible and self-powered device was developed and used for cardiac signal recording, and a high signal-to-noise ratio was achieved due to the absence of power-line interference and high gain of the OECT device.[145] However, the wearable ECG applications of the OECT devices are rarely reported.

In this chapter, a flexible OECT device with a short channel is fabricated and used for wearable ECG signal monitoring. The response time of the device can be substantially decreased to tens of microseconds. The high-quality ECG signal can be achieved by optimizing the distance between the channel and the gate of the device on a skin surface. The wearable ECG sensor is finally demonstrated, and a prototype of the portable meter is designed for wearable ECG signal monitoring.

5.2 Experimental section

5.2.1 Materials and reagents

Highly conductive PEDOT:PSS (Clevios PH 1000) was purchased from Heraeus Ltd. and filtered through a nylon filter (pore size: 0.43 μm) before use. The flexible PEN film (thickness: 0.05 mm) was obtained from Teijin Limited. The other materials and reagents can be found in Section 4.2.1

5.2.2 OECT device fabrication

A short-channel OECT was fabricated through a microfabrication technique, which includes the deposition and patterning of metal electrodes, PEDOT:PSS, and

insulation encapsulation layers. The similar process in Section 4.2.2 can be referred during short channel OECT fabrication.

5.2.3 Device characterization

The transfer and output characteristics were tested with two similar source meters. The ion gel was used as solid electrolyte during tests. The thin PDMS layer was assembled onto the OECT device, so it can conformably adhere to the skin. The gate part and channel part of the device were placed on the different sites of human body to perform ECG monitoring. The on-body transient channel current response of the OECT was also investigated by applying a train of gate pulse voltages and response

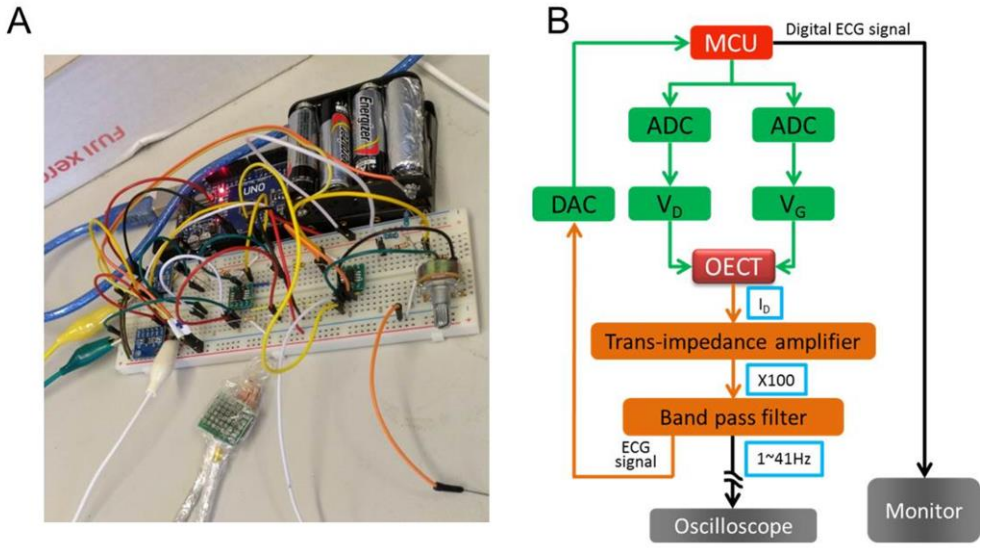

Figure 5.1. (a) The prototype of the portable meter for ECG monitoring. (b) The block diagram of portable meter design.

time of the channel current was recorded. For ECG recording, the transient channel current induced by cardiac potential through the gate electrode was first sent to a preamplifier (Stanford Research Systems, SR570) and then captured by an oscilloscope (Tektronix TDS2000C). The recorded signal was filtered through

bandpass filters (2-40 Hz).

5.2.4 Prototype design of portable monitoring platform

The prototype of the portable meter was shown in **Figure 5.1**(a). The flow chart that was shown in **Figure 5.1**(b) illustrated the working mechanism of the portable meter. The microprocessor can output V_D and V_G through built-in ADC modules to functionalize the device. The channel current of the device was sent to a trans-impedance amplifier and a bandpass filter, and was then transformed to readable signal by DAC of the microprocessor. The digital signal bringing ECG information was transmitted to a visualization device through the microprocessor.

5.3 Short channel OECT electrical performance

As illustrated in **Figure** 5.2(a), the channel and gate of the OECT were fabricated simultaneously. In order to guarantee its flexibility and conformability, the device was fabricated on the thin and flexible PEN substrate. A thick layer of PEDOT:PSS gel was coated on the skin to improve the contact between the gate electrode and human skin. The microphotograph of the channel of the device is shown in **Figure** 5.2(b). The channel length and width of the device are about 2.5 μm and 7.0 μm, respectively. The channel is shorter than that reported by our group, thus increasing its response speed. The gate area is much larger than the channel (more than 1000 times) so that effective gating of the device can be achieved. The short channel device is then tested in PBS solution which is similar to the electrolyte of human body. According to the transfer curve for V_D=0.05V, the ON/OFF ratio of the device is more than 100, and the corresponding max transconductance is 0.26 mS at V_D=0.48V (**Figure** 5.2(c)). The leakage current is more than three orders of magnitude lower that the channel current during the transfer test. The output curves clearly show that the device is operated in

the depletion mode and firstly works in the linear regime and then reaches saturation

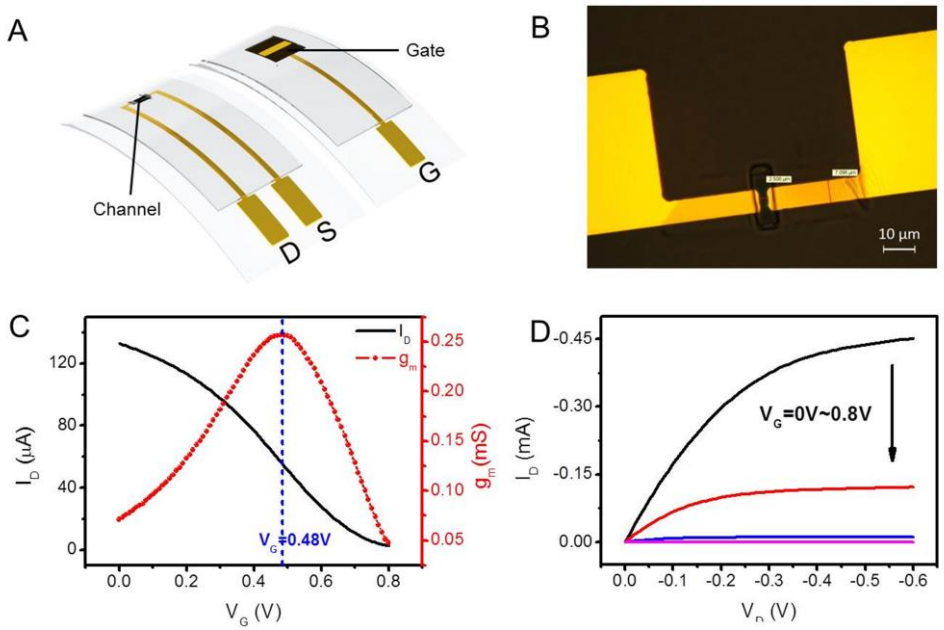

Figure 5.2. (a) The illustration of a short channel OECT with channel length of about 2 μm. (b) Micrograph of channel part of the short channel OECT. (c) Transfer and output curves of the short channel OECT characterized in PBS solution.

regime with the increase of V_D.

Figure 5.3(a) shows the comparison of the transfer curves tested in ion gel by PEDOT:PSS-based electrode and Ag/AgCl electrode. We can find a horizontally left shift if we perform the transfer test by using Ag/AgCl electrode. This may be due to the intrinsic potential difference between the PEDOT:PSS-based gate electrode and the Ag/AgCl electrode. In order to confirm whether the response speed of the device can meet the requirement of ECG signal recording, the transient properties of the device are further characterized and shown in **Figure** 5.3(b)-(d). The electric pulses are applied on the channel through the gate electrode, and the channel current response is recorded accordingly. As shown in **Figure** 5.3(b), the 0.8 V pulse voltage is applied to turn off the device and long-term pulse applying (more than two hours) do not

substantially degrade the performance of the device (**Figure** 5.3(b) only shows a small portion of recording). The response times of on-to-off (τ_{ON}) and off-to-on (τ_{OFF}) which can be estimated through **Figure** 5.3(c)-(d) are about 60 μs and 100 μs, respectively. We can find that τ_{ON} is only half of τ_{OFF} due to the difference in the doping and

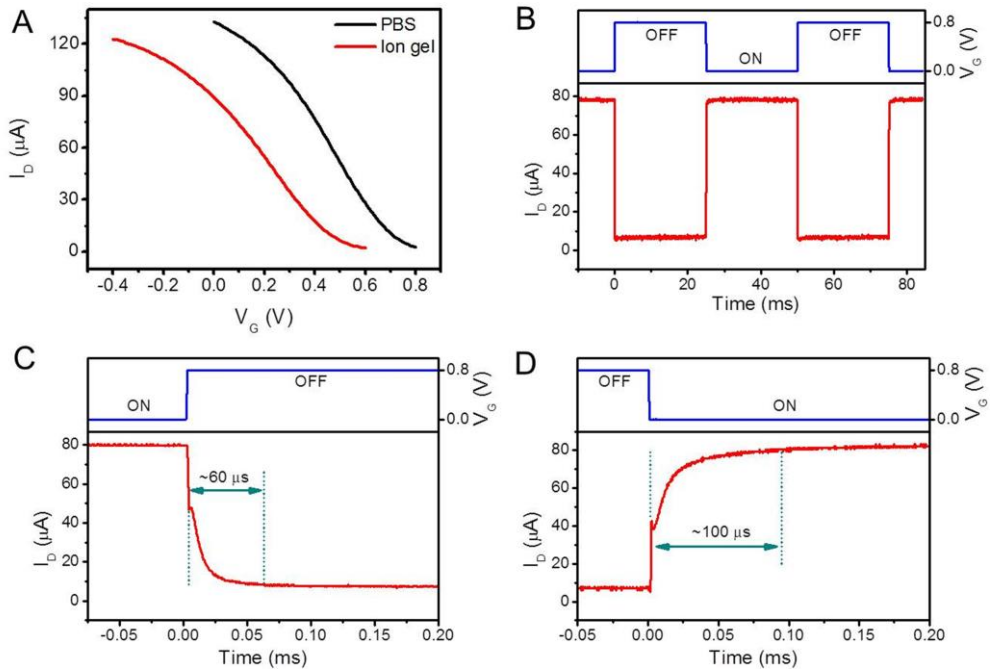

Figure 5.3. (a) Transfer curves of short channel OECT gated by PEDOT and Ag/AgCl gate electrodes. (b)-(d) The transient channel current response of short channel OECT.

de-doping process of the device which is consistent with previous reports about ion diffusion.[159,160] Furthermore, due to the short channel effect, the response time of the device is much shorter than those of previously reported OECT used in electrophysiological signal monitoring.[95,97] So, our device can be employed for recording ECG signals.

5.4 ECG signal quality *vs* recording sites

The ECG signals stem from the muscular tissue of a heart, where pacemaker cells can

spontaneously induce an influx of Ca^{2+} and further cause cell depolarization. This signal quickly spread to the whole heart area, thus causing rhythmic expansion and contraction, which is called the cardiac cycle. The macroscopic ion flux wave during the cardiac cycle leads to the tiny change of skin potential ranging from a millivolt to a few hundred microvolts. Due to its property of potential wave, the ECG signal can be

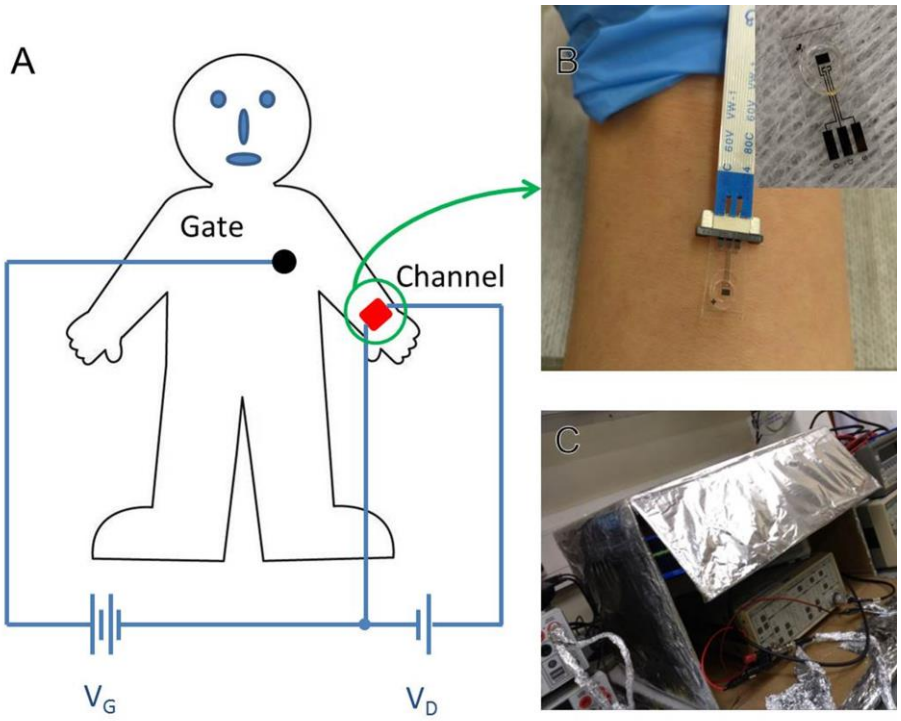

Figure 5.4. (a) The illustration of OECT device placing on human body for ECG recording. (b) The magnified picture of the device adhered on the forearm. (c) The external instruments under shielding for ECG signal capture.

recorded by a potentiometer through the low impedance electrodes.[161,162] In order to demonstrate its ECG recording capabilities, the channel, and gate of the device was adhered on the forearm and heart area, respectively (**Figure** 5.4(a)). A safe gate voltage of 0.3 V was applied on the gate electrode of the device to realize its maximum transconductance and V_D=0.05 V is applied on the channel of the device through drain electrode. The digital photo of the channel part of the device adhering on the volunteer's forearm is shown in Figure 5.4(b), and the channel current is transmitted

to the external device through a cable. The sticky PDMS well is integrated on the top of the channel (inset of **Figure** 5.4(b)) to increase the contact of the device with skin. Due to the interference of ambient noise caused by AC power supply and other sources of radiofrequency, the volunteer and external device was shielded with a metal foil (**Figure** 5.4(c)) and its signal quality can be improved in comparison with the signal recorded in ambient environment.

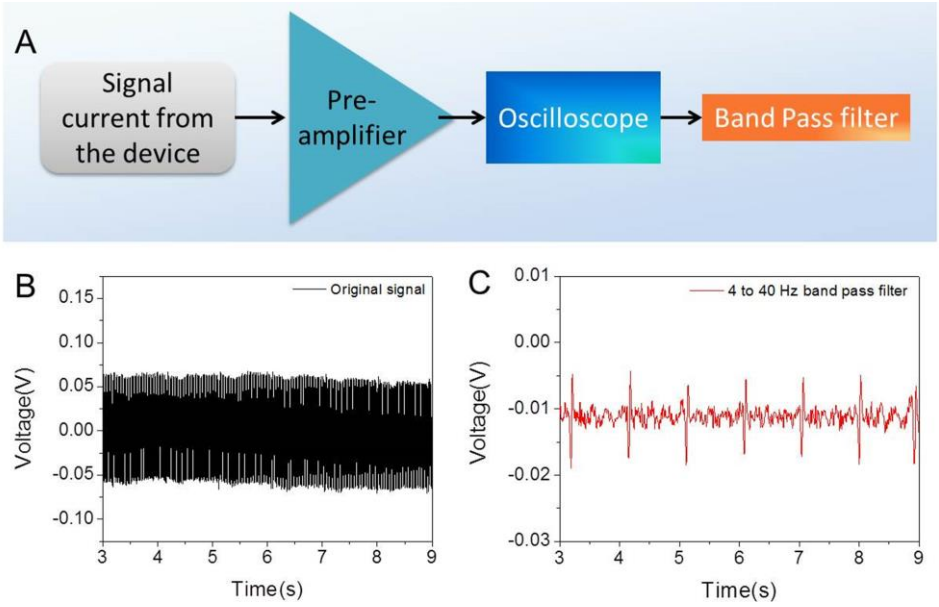

Figure 5.5. (a) The flow chart demonstration of ECG wave processing. The original signal (b) and filtered signal (c) of captured ECG waves.

As shown in **Figure** 5.5(a), the recorded channel current bringing the ECG signal during an ECG test is first passed to the preamplifier to convert the transient current to a readable and amplified voltage signal. The readable signal then can be recorded directly through an oscilloscope. However, the recorded signal still brings large amounts of noise (**Figure** 5.5(b)). According to the frequency spectrum of the recorded signal, the most significant noise comes from the AC power supply. So, the recorded signal is sent to a bandpass filter (4-40 Hz) to remove the interference of the AC power supply. Although the signal begins to show the periodic pulse after passing through the bandpass filter (**Figure** 5.5(c)), the noise is still too large to show the

characteristic peaks of a typical ECG wave.

The recording site of the channel part of the device is adjusted to study its effect on the recording quality of the ECG signal. As shown in **Figure** 5.6(a)-(c), the recorded signals with different distances between channel and gate (60cm, 30 cm, and 10 cm) are presented. We can find that the signal-to-noise ratio (SNR) of the ECG signal increases from 12 to 30 with the distance decrease from 60 cm to 10cm (**Figure** 5.6(d)). However, its P and T peaks get weak when the distance decreased to 10 cm. The amplitude of the potential caused by the cardiac cycle decays when ECG signal

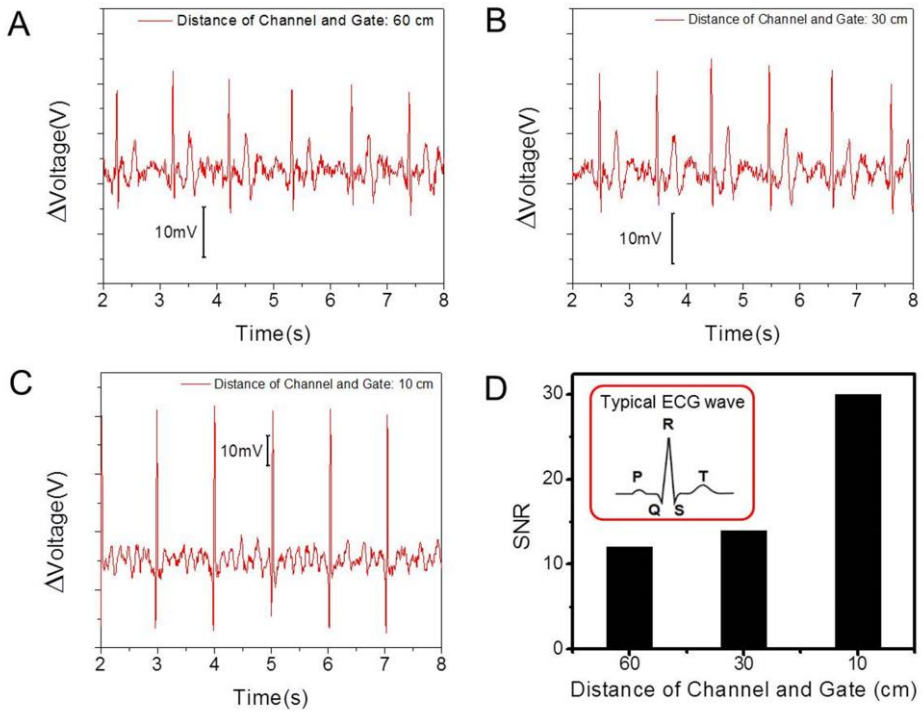

Figure 5.6. (a)-(c) The effects of placing sites of the device channel to ECG signal quality. (d) The histogram of SNR to distances between channel and gate.

spreads from heart to limbs. If we further decrease the distance between the gate and channel, the ECG signal disappears, indicating that the device has a distance too close to discriminate the underneath signal. Also, both the channel and gate are placed on

the heart area, which may cause signal cross-talk between the channel and gate of the device. According to the inset of Figure 5.6(d), the P, QRS, and T peaks are well duplicated in **Figure** 5.6(b), and its SNR can meet the requirements of functional ECG recording. So, our device can realize ECG monitoring with a high recording quality and peak detectability.

5.5 Portable meter for wearable ECG monitoring

The external recording instruments, such as preamplifier and oscilloscope, are usually bulky and not suitable for wearable use. We demonstrate a portable meter using for ECG monitoring (**Figure** 5.1(a)). The portable meter can be worn as an armlet. The real-time ECG monitoring can be realized by using the portable meter and short channel OECT. The portable meter can be further integrated and miniaturized to a small PCB board. After being filtered with a digital filter, the ECG wave can be recorded by using the portable meter (**Figure** 5.7(a)). After applying a two-stage low pass filter (<45Hz), the ECG wave can be observed in **Figure** 5.7(b). The QRS and T peaks can be extracted from the recorded signal. We can find that

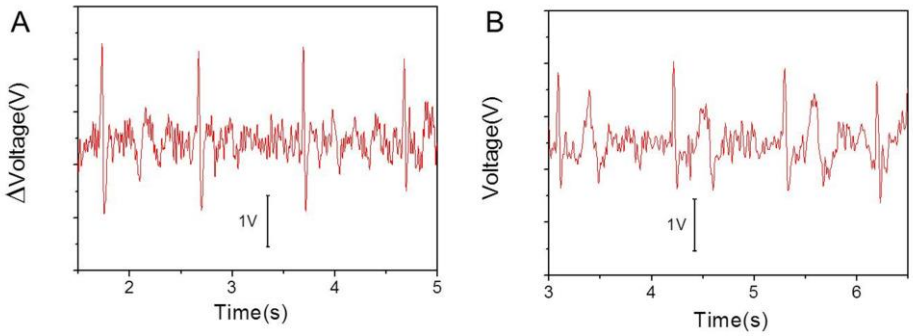

Figure 5.7. The portable meter used for ECG signal monitoring under no filter condition (a) and two-stage low pass filter condition (b). The red lines show ECG traces processed with digital band pass filter.

after using further digital band pass filter, some noise can be removed, and the characteristic peaks of the ECG wave are clearly recognized.

5.6 Summary

In summary, the short channel OECT is successfully prepared by microfabrication technique and used for high quality ECG signal monitoring. The channel length of the device is down to about 2 μm. The ON/OFF ratio of the device is more than 100. The response time (τ_{ON}) is as short as 60 μs. The device is sufficiently fast to record the fine structure of different ECG waves and provide accurate information for clinical diagnostics. The recorded ECG signal quality is closely related to the recording site of the channel and gate of the device. When the distance between the channel and gate of the device is about 30 cm, the best ECG signal can be recorded. The excellent SNR and clearly characteristic peaks of the recorded ECG signal can be simultaneously achieved. Finally, a prototype of the portable meter used in wearable ECG monitoring is demonstrated, which may provide a new concept for wearable healthcare system design.

Chapter 6 Conclusions and perspectives

6.1 Conclusions

In this thesis, different wearable sensors employing the OECT platform, such as glucose sensor, uric acid sensor, ECG sensor, are systemically studied. Two kinds of device substrate, flexible film and flexible fiber, are used for device fabrication to increase its flexibility, conformability, and wearability during wearable sensing. The gate functionalization strategies and channel dimensions are thoroughly investigated to increase sensor sensitivity, selectivity, and response speed. The above device fabrication techniques can be easily integrated and used in quick and highly sensitive diagnostics, especially in some emergencies, which will lead to a promising trend in wearable bioelectronics.

Firstly, the fiber-based OECT device is fabricated and used for biosensing. The multilayer design enables its excellent bending stability after even thousands of bending tests. The gate electrode of the device is modified with the functional polymers, nanomaterials, and specific enzyme, so its sensitivity and selectivity are markedly improved. The fiber-based glucose, dopamine, and uric sensors are successfully fabricated by the above modification method, and outstanding sensing performance is achieved. Their detection limit to the specific analyte can be down to 10 nM with good selectivity (two orders of magnitude higher than interferences). Due to its good flexibility and conformability, the fiber-based glucose sensor is woven with textiles and forms a fabric sensor. The fabric sensor can be regarded as a wearable patch and used for noninvasively glucose detection. The wearable urine glucose detection by using the fabric glucose sensor integrated into a diaper is demonstrated.

In order to solve the issues of long waiting time and instability during the OECT detection, the dimension of the channel is finely optimized to realize its quick stabilization and detection. The dual gate OECT configuration is proposed to increase its sensing selectivity. The proposed technique can realize quick detection of glucose and total detection can be finished within 1 minute. The underlying mechanism of quick detection is analyzed. The sensitivity of the device can be down to 100 nM. The noninvasive detection of sweat glucose is efficiently realized by integrating the OECT senor with a superhydrophilic textile and microfluidic PDMS well. The on-body wearable detection of sweat glucose can be achieved within several minutes, which significantly reduced waiting time during wearable sweat detections. The techniques utilized here combined with optimum design of the device would shed light on the further development of noninvasive wearable biosensors.

The flexible OECT is also exploited to perform ECG signal monitoring. The short-channel OECT device with the channel length of about 2 μm is fabricated and its transient time (τ_{ON}) is as low as 60 μs, which can guarantee accurately recording of fine ECG waves. The high-quality ECG signal recording (the characteristic peaks of a typical ECG wave) can be realized by placing the channel part and gate part closely enough (not less than 10 cm), and the potential recording mechanism is analyzed in detail. The wearable monitoring of the ECG signal with good SNR is demonstrated. This monitoring technique could be further developed for better electrophysiological signal recording and management.

6.2 Perspectives

As mentioned above, the OECTs have been proven to be a promising platform for different biochemical and physical signal detections in versatile scenarios due to its

abilities of intrinsic amplification and ion-to-electron modulating. Furthermore, the biocompatibility of organic semiconductor employed in the OECT guarantees an excellent interface between biological tissue and the OECT device, which could shed light on the long term, nonirritating, and reliable healthcare monitoring in implanted and/or wearable applications. As discussed in the thesis, the device configuration, operation mechanism, fabrication process, and gate/channel functionalization strategies all play crucial roles in the performance of the OECTs and are the major concerns in further developing highly sensitive and wearable biochemical or electrophysiological OECT sensors.

The gate or channel functionalization is essential to highly sensitive and selective OECT biosensors. The biochemical elements can be detected on the gate electrodes or organic semiconductor layer due to the potential drop at the interface between the electrolyte and the gate/channel. The modification strategies can substantially influence device performance. The sensitivity and selectivity can be improved by different functionalization strategies on the gate or channel of the device. However, the majority of the current biosensors are enzyme-based and its strict storage environment and short shelf time are far from satisfaction. So, the gate/channel functionalization strategies should be further developed to increase the device shelf life and air stability without sacrificing its sensitivity and selectivity.

The device configurations, such as fabric device, quick response device, short channel device, can meet different sensing requirements, such as quick response, high transient property as well as outstanding flexibility, conformability, and wearability, in various detection situations. The different device configurations should be exploited according to their particular applications. The interaction between the analytes and gate/channel can facilitate the understanding of the working mechanism of the device. Some models that illustrated the redox and

doping/de-doping process during ion movement into/out from the organic semiconductor layer and encountering of modified gate/channel with biosensing elements. However, the underlying reactions at the micro-interface between the channel/gate and target analytes are yet to be deeply investigated. The advanced techniques used in OECT studies will promote the better understanding and design of high-performance OECT device.

Although the wearable applications are presented in the thesis, the single analyte/signal is detected in each application, and its integration is needed to meet the requirements of practical application. The future efforts should be devoted to the miniaturization and integration of the wearable devices and external meter to realize multiplex detections and inexpensive production of the devices. We can find that the wearable application of the OECT device is an interdisciplinary project which requires the joint efforts of the material scientist, chemist, engineer, biologist, and clinician. It can be anticipated that the wearable bioelectronics employing the OECT platform will advance to a higher level under the mutual efforts of various research areas in the near future.

References

[1] T. Someya, Z. Bao, and G. G. Malliaras, The rise of plastic bioelectronics. *Nature* **2016**,540 (7633), 379

[2] J. Rivnay, R. M. Owens, and G. G. Malliaras, The Rise of Organic Bioelectronics. *Chem. Mater.* **2014**,26 (1), 679

[3] J. Dunn, R. Runge, and M. Snyder, Wearables and the medical revolution. *Personalized Medicine* **2018**,0 (0), 429

[4] M. Ha, S. Lim, and H. Ko, Wearable and flexible sensors for user-interactive health-monitoring devices. *J. Mater. Chem. B* **2018**,6 (24), 4043

[5] D.-H. Kim, N. Lu, R. Ma, Y.-S. Kim, R.-H. Kim, S. Wang, J. Wu, S. M. Won, H. Tao, A. Islam, K. J. Yu, T.-i. Kim, R. Chowdhury, M. Ying, L. Xu, M. Li, H.-J. Chung, H. Keum, M. McCormick, P. Liu, Y.-W. Zhang, F. G. Omenetto, Y. Huang, T. Coleman, and J. A. Rogers, Epidermal Electronics. *Science* **2011**,333 (6044), 838

[6] D.-H. Kim, N. Lu, R. Ghaffari, Y.-S. Kim, S. P. Lee, L. Xu, J. Wu, R.-H. Kim, J. Song, Z. Liu, J. Viventi, B. de Graff, B. Elolampi, M. Mansour, M. J. Slepian, S. Hwang, J. D. Moss, S.-M. Won, Y. Huang, B. Litt, and J. A. Rogers, Materials for multifunctional balloon catheters with capabilities in cardiac electrophysiological mapping and ablation therapy. *Nature Materials* **2011**,10, 316

[7] A. S. Campbell, J. Kim, and J. Wang, Wearable electrochemical alcohol biosensors. *Curr. Opin. Electroche.* **2018**,10, 126

[8] M. Bariya, H. Y. Y. Nyein, and A. Javey, Wearable sweat sensors. *Nat. Electron.* **2018**,1 (3), 160

[9] A. J. Bandodkar, W. J. Jeang, R. Ghaffari, and J. A. Rogers, Wearable Sensors

for Biochemical Sweat Analysis. *Annu Rev Anal Chem (Palo Alto Calif)* **2019**,12 (1), 1

[10] T. T. Quang and L. Nae-Eung, Flexible and Stretchable Physical Sensor Integrated Platforms for Wearable Human-Activity Monitoring and Personal Healthcare. *Adv. Mater.* **2016**,28 (22), 4338

[11] S. Imani, A. J. Bandodkar, A. M. V. Mohan, R. Kumar, S. Yu, J. Wang, and P. P. Mercier, A wearable chemical–electrophysiological hybrid biosensing system for real-time health and fitness monitoring. *Nat. Commun.* **2016**,7, 11650

[12] W. Gao, S. Emaminejad, H. Y. Y. Nyein, S. Challa, K. Chen, A. Peck, H. M. Fahad, H. Ota, H. Shiraki, D. Kiriya, D. H. Lien, G. A. Brooks, R. W. Davis, and A. Javey, Fully integrated wearable sensor arrays for multiplexed in situ perspiration analysis. *Nature* **2016**,529 (7587), 509

[13] H. Lee, T. K. Choi, Y. B. Lee, H. R. Cho, R. Ghaffari, L. Wang, H. J. Choi, T. D. Chung, N. Lu, T. Hyeon, S. H. Choi, and D.-H. Kim, A graphene-based electrochemical device with thermoresponsive microneedles for diabetes monitoring and therapy. *Nat. Nanotechnol.* **2016**,11, 566

[14] N. J. Ronkainen, H. B. Halsall, and W. R. Heineman, Electrochemical biosensors. *Chem. Soc. Rev.* **2010**,39 (5), 1747

[15] J. Kim, M. Lee, H. J. Shim, R. Ghaffari, H. R. Cho, D. Son, Y. H. Jung, M. Soh, C. Choi, S. Jung, K. Chu, D. Jeon, S.-T. Lee, J. H. Kim, S. H. Choi, T. Hyeon, and D.-H. Kim, Stretchable silicon nanoribbon electronics for skin prosthesis. *Nat. Commun.* **2014**,5, 5747

[16] X. Huang, Y. Liu, K. Chen, W.-J. Shin, C.-J. Lu, G.-W. Kong, D. Patnaik, S.-H. Lee, J. F. Cortes, and J. A. Rogers, Stretchable, Wireless Sensors and Functional Substrates for Epidermal Characterization of Sweat. *Small* **2014**,10 (15), 3083

[17] A. W. Martinez, S. T. Phillips, M. J. Butte, and G. M. Whitesides, Patterned

Paper as a Platform for Inexpensive, Low-Volume, Portable Bioassays. *Angew. Chem. Int. Ed.* **2007**,46 (8), 1318

[18] Y. Khan, D. Han, A. Pierre, J. Ting, X. Wang, C. M. Lochner, G. Bovo, N. Yaacobi-Gross, C. Newsome, R. Wilson, and A. C. Arias, A flexible organic reflectance oximeter array. *Proc. Nat. Acad. Sc.* **2018**,115 (47), E11015

[19] J. Wang, Electrochemical Glucose Biosensors. *Chem. Rev.* **2008**,108 (2), 814

[20] A. P. F. Turner, Biosensors: sense and sensibility. *Chem. Soc. Rev.* **2013**,42 (8), 3184

[21] A. J. Bandodkar and J. Wang, Non-invasive wearable electrochemical sensors: a review. *Trends Biotechnol.* **2014**,32 (7), 363

[22] H. U. Chung, B. H. Kim, J. Y. Lee, J. Lee, Z. Xie, E. M. Ibler, K. Lee, A. Banks, J. Y. Jeong, J. Kim, C. Ogle, D. Grande, Y. Yu, H. Jang, P. Assem, D. Ryu, J. W. Kwak, M. Namkoong, J. B. Park, Y. Lee, D. H. Kim, A. Ryu, J. Jeong, K. You, B. Ji, Z. Liu, Q. Huo, X. Feng, Y. Deng, Y. Xu, K.-I. Jang, J. Kim, Y. Zhang, R. Ghaffari, C. M. Rand, M. Schau, A. Hamvas, D. E. Weese-Mayer, Y. Huang, S. M. Lee, C. H. Lee, N. R. Shanbhag, A. S. Paller, S. Xu, and J. A. Rogers, Binodal, wireless epidermal electronic systems with in-sensor analytics for neonatal intensive care. *Science* **2019**,363 (6430), eaau0780

[23] J. Rivnay, S. Inal, A. Salleo, R. M. Owens, M. Berggren, and G. G. Malliaras, Organic electrochemical transistors. *Nat. Rev. Mater.* **2018**,3, 17086

[24] P. Lin and F. Yan, Organic thin-film transistors for chemical and biological sensing. *Adv. Mater.* **2012**,24 (1), 34

[25] L. C. Clark and C. Lyons, Electrode systems for continuous monitoring in cardiovascular surgery. *Ann. N.Y. Acad. Sci.* **1962**,102 (1), 29

[26] S.-T. Han, H. Peng, Q. Sun, S. Venkatesh, K.-S. Chung, S. C. Lau, Y. Zhou, and V. A. L. Roy, An Overview of the Development of Flexible Sensors. *Adv. Mater.* **2017**,29 (33), 1700375

[27] A. Turner, Biosensors: then and now. *Trends Biotechnol.* **2013**,31 (3), 119

[28] J. Choi, D. Kang, S. Han, S. B. Kim, and J. A. Rogers, Thin, Soft, Skin-Mounted Microfluidic Networks with Capillary Bursting Valves for Chrono-Sampling of Sweat. *Adv. Healthc. Mater.* **2017**,6 (5), 1601355

[29] J. T. Mabeck and G. G. Malliaras, Chemical and biological sensors based on organic thin-film transistors. *Analytical and Bioanalytical Chemistry* **2006**,384 (2), 343

[30] S. Wang, T. Chinnasamy, M. A. Lifson, F. Inci, and U. Demirci, Flexible Substrate-Based Devices for Point-of-Care Diagnostics. *Trends Biotechnol.* **2016**,34 (11), 909

[31] A. J. Bandodkar, W. Jia, and J. Wang, Tattoo-Based Wearable Electrochemical Devices: A Review. *Electroanalysis* **2015**,27 (3), 562

[32] M. Papaiordanidou, S. Takamatsu, S. Rezaei-Mazinani, T. Lonjaret, A. Martin, and E. Ismailova, Cutaneous Recording and Stimulation of Muscles Using Organic Electronic Textiles. *Adv. Healthc. Mater.* **2016**,5 (16), 2001

[33] H. Lee, C. Song, Y. S. Hong, M. S. Kim, H. R. Cho, T. Kang, K. Shin, S. H. Choi, T. Hyeon, and D.-H. Kim, Wearable/disposable sweat-based glucose monitoring device with multistage transdermal drug delivery module. *Sci. Adv.* **2017**,3 (3), e1601314

[34] J. Park, J. Kim, S.-Y. Kim, W. H. Cheong, J. Jang, Y.-G. Park, K. Na, Y.-T. Kim, J. H. Heo, C. Y. Lee, J. H. Lee, F. Bien, and J.-U. Park, Soft, smart contact lenses with integrations of wireless circuits, glucose sensors, and displays. *Sci. Adv.* **2018**,4 (1), eaap9841

[35] J. Kim, G. Valdes-Ramirez, A. J. Bandodkar, W. Jia, A. G. Martinez, J. Ramirez, P. Mercier, and J. Wang, Non-invasive mouthguard biosensor for continuous salivary monitoring of metabolites. *Analyst* **2014**,139 (7), 1632

[36] J. R. Windmiller and J. Wang, Wearable Electrochemical Sensors and

Biosensors: A Review. *Electroanalysis* **2013**,25 (1), 29

[37] W. Zeng, L. Shu, Q. Li, S. Chen, F. Wang, and X. M. Tao, Fiber‐Based Wearable Electronics: A Review of Materials, Fabrication, Devices, and Applications. *Adv. Mater.* **2014**,26 (31), 5310

[38] A. Economou, C. Kokkinos, and M. Prodromidis, Flexible plastic, paper and textile lab-on-a chip platforms for electrochemical biosensing. *Lab on a Chip* **2018**,18 (13), 1812

[39] M. Magliulo, K. Manoli, E. Macchia, G. Palazzo, and L. Torsi, Tailoring Functional Interlayers in Organic Field-Effect Transistor Biosensors. *Adv. Mater.* **2015**,27 (46), 7528

[40] C. Liao, M. Zhang, M. Y. Yao, T. Hua, L. Li, and F. Yan, Flexible Organic Electronics in Biology: Materials and Devices. *Adv. Mater.* **2015**,27 (46), 7493

[41] B. R. Eggins, *Chemical sensors and biosensors*. (John Wiley & Sons, 2008).

[42] R. Gifford, Continuous Glucose Monitoring: 40 Years, What We′ve Learned and What's Next. *ChemPhysChem* **2013**,14 (10), 2032

[43] Y. Chen, S. Lu, S. Zhang, Y. Li, Z. Qu, Y. Chen, B. Lu, X. Wang, and X. Feng, Skin-like biosensor system via electrochemical channels for noninvasive blood glucose monitoring. *Sci. Adv.* **2017**,3 (12), e1701629

[44] J. L. Chicharro, A. Lucia, M. Perez, A. F. Vaquero, and R. Urena, Saliva composition and exercise. *Sports medicine (Auckland, N.Z.)* **1998**,26 (1), 17

[45] F. Xiao, Y. Li, X. Zan, K. Liao, R. Xu, and H. Duan, Growth of Metal–Metal Oxide Nanostructures on Freestanding Graphene Paper for Flexible Biosensors. *Adv. Funct. Mater.* **2012**,22 (12), 2487

[46] K. D. Kıranşan and E. Topçu, Free-standing and Flexible MoS2/rGO Paper Electrode for Amperometric Detection of Folic Acid. *Electroanalysis* **2018**,30 (5), 810

[47] Y. Zhao, D. Huo, J. Bao, M. Yang, M. Chen, J. Hou, H. Fa, and C. Hou,

Biosensor based on 3D graphene-supported Fe3O4 quantum dots as biomimetic enzyme for in situ detection of H2O2 released from living cells. *Sens. Actuators B Chem.* **2017**,244, 1037

[48] J. Kim, I. Jeerapan, S. Imani, T. N. Cho, A. Bandodkar, S. Cinti, P. P. Mercier, and J. Wang, Noninvasive Alcohol Monitoring Using a Wearable Tattoo-Based Iontophoretic-Biosensing System. *ACS Sensors* **2016**,1 (8), 1011

[49] D. Pradhan, F. Niroui, and K. T. Leung, High-Performance, Flexible Enzymatic Glucose Biosensor Based on ZnO Nanowires Supported on a Gold-Coated Polyester Substrate. *ACS Appl. Mater. Inter.* **2010**,2 (8), 2409

[50] D. P. Rose, M. E. Ratterman, D. K. Griffin, L. Hou, N. Kelley-Loughnane, R. R. Naik, J. A. Hagen, I. Papautsky, and J. C. Heikenfeld, Adhesive RFID Sensor Patch for Monitoring of Sweat Electrolytes. *IEEE Trans. Biomed. Eng.* **2015**,62 (6), 1457

[51] S. Emaminejad, W. Gao, E. Wu, Z. A. Davies, H. Yin Yin Nyein, S. Challa, S. P. Ryan, H. M. Fahad, K. Chen, Z. Shahpar, S. Talebi, C. Milla, A. Javey, and R. W. Davis, Autonomous sweat extraction and analysis applied to cystic fibrosis and glucose monitoring using a fully integrated wearable platform. *Proc. Nat. Acad. Sc.* **2017**,114 (18), 4625

[52] H. Y. Y. Nyein, W. Gao, Z. Shahpar, S. Emaminejad, S. Challa, K. Chen, H. M. Fahad, L.-C. Tai, H. Ota, R. W. Davis, and A. Javey, A Wearable Electrochemical Platform for Noninvasive Simultaneous Monitoring of Ca2+ and pH. *ACS Nano* **2016**,10 (7), 7216

[53] L. Wang, L. Wang, Y. Zhang, J. Pan, S. Li, X. Sun, B. Zhang, and H. Peng, Weaving Sensing Fibers into Electrochemical Fabric for Real-Time Health Monitoring. *Adv. Funct. Mater.* **2018**,28 (42), 1804456

[54] J. R. Windmiller, A. J. Bandodkar, G. Vald és-Ram írez, S. Parkhomovsky, A. G. Martinez, and J. Wang, Electrochemical sensing based on printable temporary

transfer tattoos. *Chem. Commun.* **2012**,48 (54), 6794

[55] A. Koh, D. Kang, Y. Xue, S. Lee, R. M. Pielak, J. Kim, T. Hwang, S. Min, A. Banks, P. Bastien, M. C. Manco, L. Wang, K. R. Ammann, K.-I. Jang, P. Won, S. Han, R. Ghaffari, U. Paik, M. J. Slepian, G. Balooch, Y. Huang, and J. A. Rogers, A soft, wearable microfluidic device for the capture, storage, and colorimetric sensing of sweat. *Sci. Transl. Med.* **2016**,8 (366), 366ra165

[56] R. K. Mishra, L. J. Hubble, A. Mart ń, R. Kumar, A. Barfidokht, J. Kim, M. M. Musameh, I. L. Kyratzis, and J. Wang, Wearable Flexible and Stretchable Glove Biosensor for On-Site Detection of Organophosphorus Chemical Threats. *ACS Sensors* **2017**,2 (4), 553

[57] M. S. Mannoor, H. Tao, J. D. Clayton, A. Sengupta, D. L. Kaplan, R. R. Naik, N. Verma, F. G. Omenetto, and M. C. McAlpine, Graphene-based wireless bacteria detection on tooth enamel. *Nat. Commun.* **2012**,3, 763

[58] X. Liu, P. A. Duckworth, and D. K. Y. Wong, Square wave voltammetry versus electrochemical impedance spectroscopy as a rapid detection technique at electrochemical immunosensors. *Biosens. Bioelectron.* **2010**,25 (6), 1467

[59] A. Romani, M. Minunni, N. Mulinacci, P. Pinelli, F. F. Vincieri, M. Del Carlo, and M. Mascini, Comparison among Differential Pulse Voltammetry, Amperometric Biosensor, and HPLC/DAD Analysis for Polyphenol Determination. *J. Agric. Food. Chem.* **2000**,48 (4), 1197

[60] X. Wu, S. Mao, J. Chen, and J. Huang, Strategies for Improving the Performance of Sensors Based on Organic Field-Effect Transistors. *Adv. Mater.* **2018**,30 (17), e1705642

[61] A.-M. Pappa, O. Parlak, G. Scheiblin, P. Mailley, A. Salleo, and R. M. Owens, Organic Electronics for Point-of-Care Metabolite Monitoring. *Trends Biotechnol.* **2017**,36 (1), 45

[62] S. H. Kim, K. Hong, W. Xie, K. H. Lee, S. Zhang, T. P. Lodge, and C. D.

Frisbie, Electrolyte-Gated Transistors for Organic and Printed Electronics. *Adv. Mater.* **2013**,25 (13), 1822

[63] M. Berggren and A. Richter-Dahlfors, Organic Bioelectronics. *Adv. Mater.* **2007**,19 (20), 3201

[64] C. Wang, H. Dong, W. Hu, Y. Liu, and D. Zhu, Semiconducting π-Conjugated Systems in Field-Effect Transistors: A Material Odyssey of Organic Electronics. *Chem. Rev.* **2012**,112 (4), 2208

[65] G. Horowitz, Organic Field-Effect Transistors. *Adv. Mater.* **1998**,10 (5), 365

[66] T. P. Brody, The thin film transistor—A late flowering bloom. *IEEE Transactions on Electron Devices* **1984**,31 (11), 1614

[67] O. S. Kwon, S. J. Park, J.-Y. Hong, A. R. Han, J. S. Lee, J. S. Lee, J. H. Oh, and J. Jang, Flexible FET-Type VEGF Aptasensor Based on Nitrogen-Doped Graphene Converted from Conducting Polymer. *ACS Nano* **2012**,6 (2), 1486

[68] S. J. Park, O. S. Kwon, S. H. Lee, H. S. Song, T. H. Park, and J. Jang, Ultrasensitive Flexible Graphene Based Field-Effect Transistor (FET)-Type Bioelectronic Nose. *Nano Lett.* **2012**,12 (10), 5082

[69] W. Lee, D. Kim, J. Rivnay, N. Matsuhisa, T. Lonjaret, T. Yokota, H. Yawo, M. Sekino, G. G. Malliaras, and T. Someya, Integration of Organic Electrochemical and Field-Effect Transistors for Ultraflexible, High Temporal Resolution Electrophysiology Arrays. *Adv. Mater.* **2016**,28 (44), 9722

[70] O. Parlak, S. T. Keene, A. Marais, V. F. Curto, and A. Salleo, Molecularly selective nanoporous membrane-based wearable organic electrochemical device for noninvasive cortisol sensing. *Sci. Adv.* **2018**,4 (7), eaar2904

[71] Q. Liu, Y. Liu, F. Wu, X. Cao, Z. Li, M. Alharbi, A. N. Abbas, M. R. Amer, and C. Zhou, Highly Sensitive and Wearable In2O3 Nanoribbon Transistor Biosensors with Integrated On-Chip Gate for Glucose Monitoring in Body Fluids. *ACS Nano* **2018**,12 (2), 1170

[72] M. Esashi and T. Matsuo, Integrated Micro Multi Ion Sensor Using Field Effect of Semiconductor. *IEEE Trans. Biomed. Eng.* **1978**,BME-25 (2), 184

[73] F. Yan, M. Zhang, and J. Li, Solution-gated graphene transistors for chemical and biological sensors. *Adv. Healthc. Mater.* **2014**,3 (3), 313

[74] Z. Gao, H. Xia, J. Zauberman, M. Tomaiuolo, J. Ping, Q. Zhang, P. Ducos, H. Ye, S. Wang, X. Yang, F. Lubna, Z. T. Luo, L. Ren, and A. T. C. Johnson, Detection of Sub-fM DNA with Target Recycling and Self-Assembly Amplification on Graphene Field Effect Biosensors. *Nano Lett.* **2018**,18 (6), 3509

[75] C. Wang, X. Cui, Y. Li, H. Li, L. Huang, J. Bi, J. Luo, L. Q. Ma, W. Zhou, Y. Cao, B. Wang, and F. Miao, A label-free and portable graphene FET aptasensor for children blood lead detection. *Sci. Rep.* **2016**,6, 21711

[76] X. Du, I. Skachko, A. Barker, and E. Y. Andrei, Approaching ballistic transport in suspended graphene. *Nat. Nanotechnol.* **2008**,3, 491

[77] Y. H. Kwak, D. S. Choi, Y. N. Kim, H. Kim, D. H. Yoon, S.-S. Ahn, J.-W. Yang, W. S. Yang, and S. Seo, Flexible glucose sensor using CVD-grown graphene-based field effect transistor. *Biosens. Bioelectron.* **2012**,37 (1), 82

[78] Y. Yang, X. Yang, X. Zou, S. Wu, D. Wan, A. Cao, L. Liao, Q. Yuan, and X. Duan, Ultrafine Graphene Nanomesh with Large On/Off Ratio for High-Performance Flexible Biosensors. *Adv. Funct. Mater.* **2017**,27 (19), 1604096

[79] K. S. Bhat, R. Ahmad, J.-Y. Yoo, and Y.-B. Hahn, Nozzle-jet printed flexible field-effect transistor biosensor for high performance glucose detection. *J. Colloid Interface Sci.* **2017**,506, 188

[80] D. Sarkar, W. Liu, X. Xie, A. C. Anselmo, S. Mitragotri, and K. Banerjee, MoS2 Field-Effect Transistor for Next-Generation Label-Free Biosensors. *ACS Nano* **2014**,8 (4), 3992

[81] H. S. White, G. P. Kittlesen, and M. S. Wrighton, Chemical derivatization of an array of three gold microelectrodes with polypyrrole: fabrication of a molecule-based transistor. *J. Am. Chem. Soc.* **1984**,106 (18), 5375

[82] D. A. Bernards, D. J. Macaya, M. Nikolou, J. A. DeFranco, S. Takamatsu, and G. G. Malliaras, Enzymatic sensing with organic electrochemical transistors. *J. Mater. Chem.* **2008**,18 (1), 116

[83] A. N. Yang, Y. Z. Li, C. X. Yang, Y. Fu, N. X. Wang, L. Li, and F. Yan, Fabric Organic Electrochemical Transistors for Biosensors. *Adv. Mater.* **2018**,30, 201800051

[84] L. Zhang and T. Andrew, Vapor-Coated Monofilament Fibers for Embroidered Electrochemical Transistor Arrays on Fabrics. *Adv. Electron. Mater.* **2018**,4 (9), 1800271

[85] C. Liao, C. Mak, M. Zhang, H. L. Chan, and F. Yan, Flexible organic electrochemical transistors for highly selective enzyme biosensors and used for saliva testing. *Adv. Mater.* **2015**,27 (4), 676

[86] P. Lin, X. Luo, I. M. Hsing, and F. Yan, Organic electrochemical transistors integrated in flexible microfluidic systems and used for label-free DNA sensing. *Adv. Mater.* **2011**,23 (35), 4035

[87] R. G. Sosnowski, E. Tu, W. F. Butler, J. P. O'Connell, and M. J. Heller, Rapid determination of single base mismatch mutations in DNA hybrids by direct electric field control. *Proc. Nat. Acad. Sc.* **1997**,94 (4), 1119

[88] L. Chen, Y. Fu, N. Wang, A. Yang, Y. Li, J. Wu, H. Ju, and F. Yan, Organic Electrochemical Transistors for the Detection of Cell Surface Glycans. *ACS Appl. Mater. Inter.* **2018**,10 (22), 18470

[89] Y. Fu, N. Wang, A. Yang, H. K. w. Law, L. Li, and F. Yan, Highly Sensitive Detection of Protein Biomarkers with Organic Electrochemical Transistors. *Adv. Mater.* **2017**,29 (41), 1703787

[90] X. Guo, J. Liu, F. Liu, F. She, Q. Zheng, H. Tang, M. Ma, and S. Yao, Label-free and sensitive sialic acid biosensor based on organic electrochemical transistors. *Sens. Actuators B Chem.* **2017**,240, 1075

[91] I. Gualandi, M. Marzocchi, A. Achilli, D. Cavedale, A. Bonfiglio, and B. Fraboni, Textile Organic Electrochemical Transistors as a Platform for Wearable Biosensors. *Sci. Rep.* **2016**,6, 33637

[92] R. Faddoul, R. Coppard, and T. Berthelot, presented at the SENSORS, IEEE, Valencia, 2014, 1088.

[93] S. Zhang, E. Hubis, G. Tomasello, G. Soliveri, P. Kumar, and F. Cicoira, Patterning of Stretchable Organic Electrochemical Transistors. *Chem. Mater.* **2017**,29 (7), 3126

[94] W. Lee, D. Kim, N. Matsuhisa, M. Nagase, M. Sekino, G. G. Malliaras, T. Yokota, and T. Someya, Transparent, conformable, active multielectrode array using organic electrochemical transistors. *Proc. Nat. Acad. Sc.* **2017**,114 (40), 10554

[95] A. Campana, T. Cramer, D. T. Simon, M. Berggren, and F. Biscarini, Electrocardiographic Recording with Conformable Organic Electrochemical Transistor Fabricated on Resorbable Bioscaffold. *Adv. Mater.* **2014**,26 (23), 3874

[96] A. Williamson, M. Ferro, P. Leleux, E. Ismailova, A. Kaszas, T. Doublet, P. Quilichini, J. Rivnay, B. Rozsa, G. Katona, C. Bernard, and G. G. Malliaras, Localized Neuron Stimulation with Organic Electrochemical Transistors on Delaminating Depth Probes. *Adv. Mater.* **2015**,27 (30), 4405

[97] D. Khodagholy, T. Doublet, P. Quilichini, M. Gurfinkel, P. Leleux, A. Ghestem, E. Ismailova, T. Hervé, S. Sanaur, C. Bernard, and G. G. Malliaras, In vivo recordings of brain activity using organic transistors. *Nat. Commun.* **2013**,4, 1575

[98] J. Y. Oh, S. Rondeau-Gagne, Y. C. Chiu, A. Chortos, F. Lissel, G. N. Wang, B. C. Schroeder, T. Kurosawa, J. Lopez, T. Katsumata, J. Xu, C. Zhu, X. Gu, W. G. Bae, Y. Kim, L. Jin, J. W. Chung, J. B. Tok, and Z. Bao, Intrinsically stretchable and healable semiconducting polymer for organic transistors. *Nature* **2016**,539 (7629), 411

[99] K.-I. Jang, K. Li, H. U. Chung, S. Xu, H. N. Jung, Y. Yang, J. W. Kwak, H. H. Jung, J. Song, C. Yang, A. Wang, Z. Liu, J. Y. Lee, B. H. Kim, J.-H. Kim, J. Lee, Y. Yu, B. J. Kim, H. Jang, K. J. Yu, J. Kim, J. W. Lee, J.-W. Jeong, Y. M. Song, Y. Huang, Y. Zhang, and J. A. Rogers, Self-assembled three dimensional network designs for soft electronics. *Nat. Commun.* **2017**,8, 15894

[100] L. Qiu, J. Deng, X. Lu, Z. Yang, and H. Peng, Integrating perovskite solar cells into a flexible fiber. *Angew. Chem. Int. Ed. Engl.* **2014**,53 (39), 10425

[101] Y. Fu, X. Cai, H. Wu, Z. Lv, S. Hou, M. Peng, X. Yu, and D. Zou, Fiber supercapacitors utilizing pen ink for flexible/wearable energy storage. *Adv. Mater.* **2012**,24 (42), 5713

[102] C. Müller, M. Hamedi, R. Karlsson, R. Jansson, R. Marcilla, M. Hedhammar, and O. Inganäs, Woven Electrochemical Transistors on Silk Fibers. *Adv. Mater.* **2011**,23 (7), 898

[103] H. M. Kim, H. W. Kang, D. K. Hwang, H. S. Lim, B.-K. Ju, and J. A. Lim, Metal–Insulator–Semiconductor Coaxial Microfibers Based on Self-Organization of Organic Semiconductor:Polymer Blend for Weavable, Fibriform Organic Field-Effect Transistors. *Adv. Funct. Mater.* **2016**,26 (16), 2706

[104] M. Hamedi, R. Forchheimer, and O. Inganas, Towards woven logic from organic electronic fibres. *Nat Mater* **2007**,6 (5), 357

[105] Z. Yang, J. Deng, X. Sun, H. Li, and H. Peng, Stretchable, Wearable Dye-Sensitized Solar Cells. *Adv. Mater.* **2014**,26 (17), 2643

[106] L. Torsi, M. Magliulo, K. Manoli, and G. Palazzo, Organic field-effect transistor sensors: a tutorial review. *Chem. Soc. Rev.* **2013**,42 (22), 8612

[107] L. Kergoat, B. Piro, D. T. Simon, M.-C. Pham, V. Noël, and M. Berggren, Detection of Glutamate and Acetylcholine with Organic Electrochemical Transistors Based on Conducting Polymer/Platinum Nanoparticle Composites. *Adv. Mater.* **2014**,26 (32), 5658

[108] C. Liao and F. Yan, Organic Semiconductors in Organic Thin-Film Transistor-Based Chemical and Biological Sensors. *Polymer Reviews* **2013**,53 (3), 352

[109] P. Lin, F. Yan, and H. L. Chan, Ion-sensitive properties of organic electrochemical transistors. *ACS Appl Mater Interfaces* **2010**,2 (6), 1637

[110] H. Tang, F. Yan, P. Lin, J. Xu, and H. L. W. Chan, Highly Sensitive Glucose Biosensors Based on Organic Electrochemical Transistors Using Platinum Gate Electrodes Modified with Enzyme and Nanomaterials. *Adv. Funct. Mater.* **2011**,21 (12), 2264

[111] C. Liao, M. Zhang, L. Niu, Z. Zheng, and F. Yan, Highly selective and sensitive glucose sensors based on organic electrochemical transistors with graphene-modified gate electrodes. *J. Mater. Chem. B* **2013**,1 (31), 3820

[112] C. Liao, M. Zhang, L. Niu, Z. Zheng, and F. Yan, Organic electrochemical transistors with graphene-modified gate electrodes for highly sensitive and selective dopamine sensors. *J. Mater. Chem. B* **2014**,2 (2), 191

[113] H. Tang, P. Lin, H. L. Chan, and F. Yan, Highly sensitive dopamine biosensors based on organic electrochemical transistors. *Biosens. Bioelectron.* **2011**,26 (11), 4559

[114] R.-X. He, M. Zhang, F. Tan, P. H. M. Leung, X.-Z. Zhao, H. L. W. Chan, M. Yang, and F. Yan, Detection of bacteria with organic electrochemical transistors. *J. Mater. Chem.* **2012**,22 (41), 22072

[115] P. Lin, F. Yan, J. Yu, H. L. Chan, and M. Yang, The application of organic electrochemical transistors in cell-based biosensors. *Adv. Mater.* **2010**,22 (33), 3655

[116] L. H. Jimison, S. A. Tria, D. Khodagholy, M. Gurfinkel, E. Lanzarini, A. Hama, G. G. Malliaras, and R. M. Owens, Measurement of barrier tissue integrity with an organic electrochemical transistor. *Advnced Materials* **2012**,24 (44), 5919

[117] G. Tarabella, M. Villani, D. Calestani, R. Mosca, S. Iannotta, A. Zappettini, and N. Coppedè, A single cotton fiber organic electrochemical transistor for liquid electrolyte saline sensing. *J. Mater. Chem.* **2012**,22 (45), 23830

[118] Y. Wang, X. Qing, Q. Zhou, Y. Zhang, Q. Liu, K. Liu, W. Wang, M. Li, Z. Lu, Y. Chen, and D. Wang, The woven fiber organic electrochemical transistors based on polypyrrole nanowires/reduced graphene oxide composites for glucose sensing. *Biosens. Bioelectron.* **2017**,95, 138

[119] Z. Liu, S. P. Lau, and F. Yan, Functionalized graphene and other two-dimensional materials for photovoltaic devices: device design and processing. *Chem. Soc. Rev.* **2015**,44 (15), 5638

[120] S. Chutipongtanate and V. Thongboonkerd, Systematic comparisons of artificial urine formulas for in vitro cellular study. *Anal. Biochem.* **2010**,402 (1), 110

[121] K. G. Christmas, L. B. Gower, S. R. Khan, and H. El-Shall, Aggregation and Dispersion Characteristics of Calcium Oxalate Monohydrate: Effect of Urinary Species. *J. Colloid Interface Sci.* **2002**,256 (1), 168

[122] S. L. Cowart and M. E. Stachura, in *Clinical Methods: The History, Physical, and Laboratory Examinations*, edited by H. K. Walker, W. D. Hall, and J. W. Hurst (Butterworths, Boston, 1990).

[123] V. Vitart, I. Rudan, C. Hayward, N. K. Gray, J. Floyd, C. N. Palmer, S. A.

Knott, I. Kolcic, O. Polasek, J. Graessler, J. F. Wilson, A. Marinaki, P. L. Riches, X. Shu, B. Janicijevic, N. Smolej-Narancic, B. Gorgoni, J. Morgan, S. Campbell, Z. Biloglav, L. Barac-Lauc, M. Pericic, I. M. Klaric, L. Zgaga, T. Skaric-Juric, S. H. Wild, W. A. Richardson, P. Hohenstein, C. H. Kimber, A. Tenesa, L. A. Donnelly, L. D. Fairbanks, M. Aringer, P. M. McKeigue, S. H. Ralston, A. D. Morris, P. Rudan, N. D. Hastie, H. Campbell, and A. F. Wright, SLC2A9 is a newly identified urate transporter influencing serum urate concentration, urate excretion and gout. *Nature genetics* **2008**,40 (4), 437

[124] Y. Wang, C. Zhu, R. Pfattner, H. Yan, L. Jin, S. Chen, F. Molina-Lopez, F. Lissel, J. Liu, N. I. Rabiah, Z. Chen, J. W. Chung, C. Linder, M. F. Toney, B. Murmann, and Z. Bao, A highly stretchable, transparent, and conductive polymer. *Sci. Adv.* **2017**,3 (3), e1602076

[125] R. A. Serway and J. W. Jewett, *Principles of physics*. (Saunders College Pub. Fort Worth, TX, 1998).

[126] N. Wang, Y. Liu, Y. Fu, and F. Yan, AC Measurements Using Organic Electrochemical Transistors for Accurate Sensing. *ACS Appl. Mater. Inter.* **2017**,10 (31), 25834

[127] K.-I. Jang, S. Y. Han, S. Xu, K. E. Mathewson, Y. Zhang, J.-W. Jeong, G.-T. Kim, R. C. Webb, J. W. Lee, T. J. Dawidczyk, R. H. Kim, Y. M. Song, W.-H. Yeo, S. Kim, H. Cheng, S. I. Rhee, J. Chung, B. Kim, H. U. Chung, D. Lee, Y. Yang, M. Cho, J. G. Gaspar, R. Carbonari, M. Fabiani, G. Gratton, Y. Huang, and J. A. Rogers, Rugged and breathable forms of stretchable electronics with adherent composite substrates for transcutaneous monitoring. *Nat. Commun.* **2014**,5, 4779

[128] M. L. Hammock, A. Chortos, B. C.-K. Tee, J. B.-H. Tok, and Z. Bao, 25th Anniversary Article: The Evolution of Electronic Skin (E-Skin): A Brief History, Design Considerations, and Recent Progress. *Adv. Mater.* **2013**,25

(42), 5997

[129] T. Someya, T. Sekitani, S. Iba, Y. Kato, H. Kawaguchi, and T. Sakurai, A large-area, flexible pressure sensor matrix with organic field-effect transistors for artificial skin applications. *Proceedings of the National Academy of Sciences of the United States of America* **2004**,101 (27), 9966

[130] K. H. Gilchrist, L. Giovangrandi, R. H. Whittington, and G. T. A. Kovacs, Sensitivity of cell-based biosensors to environmental variables. *Biosens. Bioelectron.* **2005**,20 (7), 1397

[131] A. N. Naimushin, S. D. Soelberg, D. U. Bartholomew, J. L. Elkind, and C. E. Furlong, A portable surface plasmon resonance (SPR) sensor system with temperature regulation. *Sens. Actuators B Chem.* **2003**,96 (1), 253

[132] A. Vaz, A. Ubarretxena, I. Zalbide, D. Pardo, H. Solar, A. Garcia-Alonso, and R. Berenguer, Full Passive UHF Tag With a Temperature Sensor Suitable for Human Body Temperature Monitoring. *IEEE Transactions on Circuits and Systems II: Express Briefs* **2010**,57 (2), 95

[133] D. A. Bernards and G. G. Malliaras, Steady-State and Transient Behavior of Organic Electrochemical Transistors. *Adv. Funct. Mater.* **2007**,17 (17), 3538

[134] M. Rinaudo, Chitin and chitosan: Properties and applications. *Prog. Polym. Sci.* **2006**,31 (7), 603

[135] J. Rivnay, P. Leleux, M. Ferro, M. Sessolo, A. Williamson, D. A. Koutsouras, D. Khodagholy, M. Ramuz, X. Strakosas, R. M. Owens, C. Benar, J.-M. Badier, C. Bernard, and G. G. Malliaras, High-performance transistors for bioelectronics through tuning of channel thickness. *Sci. Adv.* **2015**,1 (4), e1400251

[136] R. X. He, P. Lin, Z. K. Liu, H. W. Zhu, X. Z. Zhao, H. L. Chan, and F. Yan, Solution-gated graphene field effect transistors integrated in microfluidic systems and used for flow velocity detection. *Nano Lett.* **2012**,12 (3), 1404

[137] H. Lee, E. Kim, Y. Lee, H. Kim, J. Lee, M. Kim, H.-J. Yoo, and S. Yoo, Toward all-day wearable health monitoring: An ultralow-power, reflective organic pulse oximetry sensing patch. *Sci. Adv.* **2018**,4 (11), eaas9530

[138] T. R. Ray, J. Choi, A. J. Bandodkar, S. Krishnan, P. Gutruf, L. Tian, R. Ghaffari, and J. A. Rogers, Bio-Integrated Wearable Systems: A Comprehensive Review. *Chem. Rev.* **2019**,119 (8), 5461

[139] J. Song, P. Lin, Y.-F. Ruan, W.-W. Zhao, W. Wei, J. Hu, S. Ke, X. Zeng, J.-J. Xu, H.-Y. Chen, W. Ren, and F. Yan, Organic Photo-Electrochemical Transistor-Based Biosensor: A Proof-of-Concept Study toward Highly Sensitive DNA Detection. *Adv. Healthc. Mater.* **2018**,0 (0), 1800536

[140] A.-M. Pappa, S. Inal, K. Roy, Y. Zhang, C. Pitsalidis, A. Hama, J. Pas, G. G. Malliaras, and R. M. Owens, Polyelectrolyte Layer-by-Layer Assembly on Organic Electrochemical Transistors. *ACS Appl. Mater. Inter.* **2017**,9 (12), 10427

[141] N. Wang, A. Yang, Y. Fu, Y. Li, and F. Yan, Functionalized Organic Thin Film Transistors for Biosensing. *Acc. Chem. Res.* **2019**,52 (2), 277

[142] H. Lee, Y. J. Hong, S. Baik, T. Hyeon, and D. H. Kim, Enzyme-Based Glucose Sensor: From Invasive to Wearable Device. *Adv. Healthc. Mater.* **2018**,7 (8), e1701150

[143] D. Nilsson, M. Chen, T. Kugler, T. Remonen, M. Armgarth, and M. Berggren, Bi-stable and Dynamic Current Modulation in Electrochemical Organic Transistors. *Adv. Mater.* **2002**,14 (1), 51

[144] H. U. Chung, B. H. Kim, J. Y. Lee, J. Lee, Z. Xie, E. M. Ibler, K. Lee, A. Banks, J. Y. Jeong, J. Kim, C. Ogle, D. Grande, Y. Yu, H. Jang, P. Assem, D. Ryu, J. W. Kwak, M. Namkoong, J. B. Park, Y. Lee, D. H. Kim, A. Ryu, J. Jeong, K. You, B. Ji, Z. Liu, Q. Huo, X. Feng, Y. Deng, Y. Xu, K.-I. Jang, J. Kim, Y. Zhang, R. Ghaffari, C. M. Rand, M. Schau, A. Hamvas, D. E. Weese-Mayer, Y. Huang, S.

M. Lee, C. H. Lee, N. R. Shanbhag, A. S. Paller, S. Xu, and J. A. Rogers, Binodal, wireless epidermal electronic systems with in-sensor analytics for neonatal intensive care. *Science* **2019**,363 (6430), eaau0780

[145] S. Park, S. W. Heo, W. Lee, D. Inoue, Z. Jiang, K. Yu, H. Jinno, D. Hashizume, M. Sekino, T. Yokota, K. Fukuda, K. Tajima, and T. Someya, Self-powered ultra-flexible electronics via nano-grating-patterned organic photovoltaics. *Nature* **2018**,561 (7724), 516

[146] W. Lee, S. Kobayashi, M. Nagase, Y. Jimbo, I. Saito, Y. Inoue, T. Yambe, M. Sekino, G. G. Malliaras, T. Yokota, M. Tanaka, and T. Someya, Nonthrombogenic, stretchable, active multielectrode array for electroanatomical mapping. *Sci. Adv.* **2018**,4, eaau2426

[147] E. B. Fortescue, C. I. Berul, F. Cecchin, E. P. Walsh, J. K. Triedman, and M. E. Alexander, Patient, procedural, and hardware factors associated with pacemaker lead failures in pediatrics and congenital heart disease. *Heart Rhythm* **2004**,1 (2), 150

[148] Y. Yamamoto, D. Yamamoto, M. Takada, H. Naito, T. Arie, S. Akita, and K. Takei, Efficient Skin Temperature Sensor and Stable Gel-Less Sticky ECG Sensor for a Wearable Flexible Healthcare Patch. *Adv. Healthc. Mater.* **2017**,6 (17), 1700495

[149] M. Isik, T. Lonjaret, H. Sardon, R. Marcilla, T. Herve, G. G. Malliaras, E. Ismailova, and D. Mecerreyes, Cholinium-based ion gels as solid electrolytes for long-term cutaneous electrophysiology. *Journal of Materials Chemistry C* **2015**,3 (34), 8942

[150] M. Ganji, E. Kaestner, J. Hermiz, N. Rogers, A. Tanaka, D. Cleary, S. H. Lee, J. Snider, M. Halgren, G. R. Cosgrove, B. S. Carter, D. Barba, I. Uguz, G. G. Malliaras, S. S. Cash, V. Gilja, E. Halgren, and S. A. Dayeh, Development and Translation of PEDOT:PSS Microelectrodes for Intraoperative Monitoring.

Adv. Funct. Mater. **2017**, 1700232

[151] V. Vishak, F. J. T., G. Alexander, M. I. P., M. Iain, M. R. R., and R. Jonathan, Subthreshold Operation of Organic Electrochemical Transistors for Biosignal Amplification. *Advanced Science* **2018**,0 (0), 1800453

[152] G. D. Spyropoulos, J. N. Gelinas, and D. Khodagholy, Internal ion-gated organic electrochemical transistor: A building block for integrated bioelectronics. *Sci. Adv.* **2019**,5 (2), eaau7378

[153] E. Bihar, T. Roberts, M. Saadaoui, T. Hervé, J. B. De Graaf, and G. G. Malliaras, Inkjet-Printed PEDOT:PSS Electrodes on Paper for Electrocardiography. *Adv. Healthc. Mater.* **2017**, 1601167

[154] E. Bihar, T. Roberts, E. Ismailova, M. Saadaoui, M. Isik, A. Sanchez-Sanchez, D. Mecerreyes, T. Hervé, J. B. De Graaf, and G. G. Malliaras, Fully Printed Electrodes on Stretchable Textiles for Long-Term Electrophysiology. *Advanced Materials Technologies* **2017**, 1600251

[155] P. Leleux, J. Rivnay, T. Lonjaret, J.-M. Badier, C. Bénar, T. Hervé, P. Chauvel, and G. G. Malliaras, Organic Electrochemical Transistors for Clinical Applications. *Adv. Healthc. Mater.* **2015**,4 (1), 142

[156] M. Braendlein, T. Lonjaret, P. Leleux, J.-M. Badier, and G. G. Malliaras, Voltage Amplifier Based on Organic Electrochemical Transistor. *Advanced Science* **2016**, 1600247

[157] C. Yao, Q. Li, J. Guo, F. Yan, and I. M. Hsing, Rigid and flexible organic electrochemical transistor arrays for monitoring action potentials from electrogenic cells. *Adv. Healthc. Mater.* **2015**,4 (4), 528

[158] X. Gu, C. Yao, Y. Liu, and I. M. Hsing, 16-Channel Organic Electrochemical Transistor Array for In Vitro Conduction Mapping of Cardiac Action Potential. *Adv. Healthc. Mater.* **2016**,5 (18), 2345

[159] L. Q. Flagg, R. Giridharagopal, J. Guo, and D. S. Ginger, Anion-Dependent

Doping and Charge Transport in Organic Electrochemical Transistors. *Chem. Mater.* **2018**,30 (15), 5380

[160] X. Wu, A. Surendran, J. Ko, O. Filonik, E. M. Herzig, P. Müller-Buschbaum, and W. L. Leong, Ionic-Liquid Doping Enables High Transconductance, Fast Response Time, and High Ion Sensitivity in Organic Electrochemical Transistors. *Adv. Mater.* **2018**,0 (0), 1805544

[161] M. S. SPACH, R. C. BARR, J. W. HAVSTAD, and E. C. LONG, Skin-Electrode Impedance and Its Effect on Recording Cardiac Potentials. *Circulation* **1966**,34 (4), 649

[162] X.-L. Yang, G.-Z. Liu, Y.-H. Tong, H. Yan, Z. Xu, Q. Chen, X. Liu, H.-H. Zhang, H.-B. Wang, and S.-H. Tan, The history, hotspots, and trends of electrocardiogram. *J Geriatr Cardiol* **2015**,12 (4), 448